

AD-782 178

POLARIZED EMITTANCE. VOLUME I:
POLARIZED BIDIRECTIONAL REFLECTANCE
WITH LAMBERTIAN OR NON-LAMBERTIAN
DIFFUSE COMPONENTS

J. R. Maxwell, et al

Environmental Research Institute of Michigan

Prepared for:

Ballistic Research Laboratories

May 1974

DISTRIBUTED BY:



National Technical Information Service
U. S. DEPARTMENT OF COMMERCE
5285 Port Royal Road, Springfield Va. 22151

UNCLASSIFIED

SECURITY CLASSIFICATION OF THIS PAGE (When Data Entered)

REPORT DOCUMENTATION PAGE		READ INSTRUCTIONS BEFORE COMPLETING FORM
1. REPORT NUMBER CONTRACT REPORT NO. 154	2. GOVT ACCESSION NO.	3. RECIPIENT'S CATALOG NUMBER AD-782178
4. TITLE (and Subtitle) POLARIZED EMITTANCE (VOL.I): POLARIZED BIDIRECTIONAL REFLECTANCE WITH LAMBERTIAN OR NON-LAMBERTIAN DIFFUSE COMPONENTS		5. TYPE OF REPORT & PERIOD COVERED Final 10 April - 31 Dec 72
7. AUTHOR(s) Dr. J. R. Maxwell Mr. S. F. Weiner		6. PERFORMING ORG. REPORT NUMBER 192500-1-T(1) (Vol. I)
9. PERFORMING ORGANIZATION NAME AND ADDRESS Environmental Institute of Michigan P. O. Box 618 Ann Arbor, Michigan 48107		8. CONTRACT OR GRANT NUMBER(s) DAAD05-72-C-0246
11. CONTROLLING OFFICE NAME AND ADDRESS USA Ballistic Research Laboratories Aberdeen Proving Ground, Maryland 21005		10. PROGRAM ELEMENT, PROJECT, TASK AREA & WORK UNIT NUMBERS 6.11.02B RDT&E 1T061102B11A
14. MONITORING AGENCY NAME & ADDRESS (if different from Controlling Office)		12. REPORT DATE MAY 1974
		13. NUMBER OF PAGES 126
16. DISTRIBUTION STATEMENT (of this Report)		15. SECURITY CLASS. (of this report) UNCLASSIFIED
		15a. DECLASSIFICATION/DOWNGRADING SCHEDULE
17. DISTRIBUTION STATEMENT (of the abstract entered in Block 20, if different from Report)		
18. SUPPLEMENTARY NOTES		
19. KEY WORDS (Continue on reverse side if necessary and identify by block number) Bidirectional Reflectance Surface Model Shadowing Polarization Parameters Obscuration Source-Receiver Lambertian Reflectance Fixed-Bistatic Data Non-Lambertian Reflectance		
20. ABSTRACT (Continue on reverse side if necessary and identify by block number) Volume I of this report provides the Ballistic Research Laboratories with a discussion of the algorithms upon which the bidirectional reflectance model is based in particular the non-Lambertian volume model which was constructed under this contract. The report provides a validation of the model with respect to the materials supplied by BRL. It includes a listing of appropriate model parameters with a description of how to use the model, and a listing of the computer program with its subroutines.		

DD FORM 1473 EDITION OF 1 NOV 65 IS OBSOLETE

UNCLASSIFIED

~~REF ID: A6512~~ ~~CLASSIFIED~~ SECURITY CLASSIFICATION OF THIS PAGE (Refer Data Entered)

UNCLASSIFIED

SECURITY CLASSIFICATION OF THIS PAGE(When Data Entered)

Block 20. Abstract

The model makes it possible to calculate bidirectional reflectance data from a very small amount of measured data. Accuracy demonstrated indicates that the model is very effective, although improvement can still be obtained at large receiver zenith angles.

ia

UNCLASSIFIED

SECURITY CLASSIFICATION OF THIS PAGE(When Data Entered)

FOREWORD

The work reported herein, covering the period 10 April 1972 to 31 December 1972, was carried out by the Infrared and Optics Division of the Environmental Research Institute of Michigan (formerly the Willow Run Laboratories of The University of Michigan), Ann Arbor, Michigan. The work, which was performed under Contract DAAD05-72-C-0246 for the Army Ballistic Research Laboratories, was done in three parts, each of which represents one volume.

The three volumes comprising the present series on polarized radiance are:

I - Polarized Bidirectional Reflectance with Lambertian or Non-Lambertian Diffuse Components

II - Polarized Spectral Emittance from 4 to 14 μm

III - Wavelength Dependence of Polarized Bidirectional Reflectance

The ERIM number for Volume I of this report is 192500-1-T(I).

PREFACE

Under contract commitments with the Air Force Avionics Laboratory (Contract F33615-70-C-1123), a bidirectional reflectance model was developed to predict reflectance from rough surfaces as a function of the zenith and azimuth angles of source and receiver, given a set of input parameters derived from limited measurements. It was observed, however, that the model required further extension to account for anomalies in the comparison of measured data with calculated model predictions. Specifically, it was determined that the model would be more accurate if it could account for a non-Lambertian, non-specular component of the reflectance which was assumed to result from scattering within the target material. Extension of the model to take the non-Lambertian angular dependence into account was carried out under this BRL contract, as well as coding the model in Fortran IV and validating it.

This extension of the bidirectional reflectance model plus other extensions performed under the AFAL contract have considerably improved the fit between model predictions and measured data.

The work done under this contract with BRL has been combined with the work done under the Air Force contract to form a unified model. Therefore, for completeness, the AF-sponsored part of the model is included in this report.

CONTENTS

1.	Introduction	1
2.	Bidirectional Reflectance	3
3.	Background Information	6
4.	Surface Model	8
4.1.	Available Area	8
4.2.	Fresnel Coefficients	8
4.3.	Shadowing and Obscuration	10
5.	Volume Models	12
5.1.	Lambertian	12
5.2.	Non-Lambertian	12
6.	Model Validation	17
6.1.	Reflectance for Sample Material A02018-001	18
6.2.	Reflectance for Sample Material A02018-002	26
6.3.	Polarization Angle for Sample Materials A02018-001 and A02018-002	26
6.4.	Percent Polarization for Sample Materials A02018-001	48
6.5.	Reflectance for Sample Material A02100	48
7.	Model Parameters	66
7.1.	Source Polarization Parameters	66
7.2.	Surface Model Parameters	67
7.3.	Lambertian Volume Model Parameters	68
7.4.	Non-Lambertian Volume Model Parameters	68
Appendix I:	Documentation of Bidirectional Reflectance Program (RHOPRIME)	73
Appendix II:	Instructions for Use of Program with Sample Computer Output	89
Appendix III:	Rhoprime Program Listing	95
References		118
Distribution List		119

1

FIGURES

1. Bidirectional Reflectance Geometry and Parameters	4
2. Example of Reflectance ρ' for A02018-001. θ_r Scanned in Plane	7
3. Volume Scattering Geometry and Parameters	13
4. Fixed Bistatic ρ' for A02018-001. Polarizations $\perp\perp, \perp 45, \perp\parallel$	19
5. Measured ρ' for A02018-001. $\phi_r = 0, 180^\circ$; Polarizations $\perp\perp, \perp 45, \perp\parallel$	21
6. Calculated ρ' for A02018-001 Using Lambertian Volume Model and Non-Lambertian Volume Model With and Without Shadowing and Obscuration Factor, $\theta_i = 40^\circ; \phi_i = 0^\circ, 180^\circ; \phi_r = 0^\circ, 180^\circ$; Polarizations $\perp\perp, \perp\parallel$	22
7. Measured ρ' for A02018-001. $\phi_r = 90^\circ, 270^\circ$; Polarizations $\perp\perp, \perp 45, \perp\parallel$	24
8. Calculated ρ' for A02018-001 Using Lambertian Volume Model and Non-Lambertian Volume Model With and Without Shadowing and Obscuration Factor, $\theta_i = 40^\circ, \phi_i = 180^\circ; \phi_r = 90^\circ, 270^\circ$; Polarizations $\perp\perp, \perp\parallel$	25
9. Measured ρ' for A02018-001. $\phi_r = 30^\circ, 210^\circ$; Polarizations $\perp\perp, \perp 45, \perp\parallel$	27
10. Calculated ρ' for A02018-001 Using Non-Lambertian Volume Model With Shadowing and Obscuration Factor. $\phi_r = 30^\circ, 210^\circ$; Polarizations $\perp\perp, \perp\parallel$	28
11. Measured ρ' for A02018-001. $\phi_r = 60^\circ, 240^\circ$; Polarizations $\perp\perp, \perp 45, \perp\parallel$	29
12. Calculated ρ' for A02018-001 Using Non-Lambertian Volume Model With Shadowing and Obscuration Factor. $\phi_r = 60^\circ, 240^\circ$; Polarizations $\perp\perp, \perp\parallel$	30
13. Measured ρ' for A02018-001. $\phi_r = 0^\circ, 180^\circ$; Polarizations $-45\perp, -45-45, -45\parallel$	31
14. Calculated ρ' for A02018-001 Using Non-Lambertian Volume Model With Shadowing and Obscuration Factor. $\phi_r = 0^\circ, 180^\circ$; Polarizations $-45\perp, -45\parallel$	32
15. Measured ρ' for A02018-001. $\phi_r = 90^\circ, 270^\circ$; Polarization $\parallel\perp, \parallel-45, \parallel\parallel$	33
16. Calculated ρ' for A02018-001 Using Non-Lambertian Volume Model With Shadowing and Obscuration Factor. $\phi_r = 90^\circ, 270^\circ$; Polarizations $\parallel\perp, \parallel\parallel$	34
17. Measured ρ' for A02018-001. $\phi_r = 30^\circ, 210^\circ$; Polarizations $\parallel\perp, \parallel-45, \parallel\parallel$	35
18. Calculated ρ' for A02018-001 Using Non-Lambertian Volume Model With Shadowing and Obscuration Factor. $\phi_r = 30^\circ, 210^\circ$; Polarizations $\parallel\perp, \parallel\parallel$	36

V_i'

19. Measured ρ' for A02018-001. $\phi_r = 60^\circ, 240^\circ$; Polarizations $\parallel\perp, \parallel-45, \parallel\parallel$	37
20. Calculated ρ' for A02018-001 Using Non-Lambertian Volume Model With Shadowing and Obscuration Factor. $\phi_r = 60^\circ, 240^\circ$; Polarizations $\parallel\perp, \parallel\parallel$	38
21. Fixed Bistatic ρ' for A02018-002. Polarizations $\perp\perp, \perp 45, \perp\parallel$	39
22. Measured ρ' for A02018-002. $\phi_r = 0^\circ, 180^\circ$; Polarizations $\perp\perp, \perp-45, \perp\parallel$	40
23. Calculated ρ' for A02018-002 Using Lambertian Volume Model. $\phi_r = 0^\circ, 180^\circ$; Polarizations $\perp\perp, \perp\parallel$	41
24. Measured ρ' for A02018-002. $\phi_r = 90^\circ, 270^\circ$; Polarizations $\perp\perp, \perp-45, \perp\parallel$	42
25. Calculated ρ' for A02018-002 Using Lambertian Volume Model. $\phi_r = 90^\circ, 270^\circ$; Polarizations $\perp\perp, \perp\parallel$	43
26. Measured ρ' for A02018-002. $\phi_r = 0^\circ, 180^\circ$; Polarizations $\parallel\perp, \parallel-45, \parallel\parallel$	44
27. Calculated ρ' for A02018-002 Using Lambertian Volume Model. $\phi_r = 0^\circ, 180^\circ$; Polarizations $\parallel\perp, \parallel\parallel$	45
28. Measured ρ' for A02018-002. $\phi_r = 90^\circ, 270^\circ$; Polarizations $\parallel\perp, \parallel-45, \parallel\parallel$	46
29. Calculated ρ' for A02018-002 Using Lambertian Volume Model. $\phi_r = 90^\circ, 270^\circ$; Polarizations $\parallel\perp, \parallel\parallel$	47
30. Variation of Polarization Angle of Reflected Radiance as Function of Source-Receiver Position. $\phi_r = 0^\circ, 180^\circ$	50
31. Variation of Polarization Angle of Reflected Radiance as Function of Source-Receiver Position. $\phi_r = 30^\circ, 210^\circ$	51
32. Variation of Polarization Angle of Reflected Radiance as Function of Source-Receiver Position. $\phi_r = 60^\circ, 240^\circ$	52
33. Variation of Polarization Angle of Reflected Radiance as Function of Source-Receiver Position. $\phi_r = 90^\circ, 270^\circ$	53
34. Percent Polarization Variation for A02018-002 as Function of Source-Receiver Position. $\phi_r = 0^\circ, 180^\circ$; Perpendicular Source	54
35. Percent Polarization Variation for A02018-002 as Function of Source-Receiver Position. $\phi_r = 0^\circ, 180^\circ$; Parallel Source	54
36. Percent Polarization Variation for A02018-001 as Function of Source-Receiver Position. $\phi_r = 0^\circ, 180^\circ$; Perpendicular Source	54
37. Percent Polarization Variation for A02018-001 as Function of Source-Receiver Position. $\phi_r = 90^\circ, 270^\circ$; Perpendicular Source	55
38. Percent Polarization Variation for A02018-001 as Function of Source-Receiver Position. $\phi_r = 90^\circ, 270^\circ$; Parallel Source	55

39. Fixed Bistatic ρ' for A02100. Polarizations $\perp\perp$, $\perp-45^\circ$, $\perp\parallel$	56
40. Measured ρ' for A02100. $\theta_i = 0^\circ$, $\phi_i = 0^\circ$, $\phi_r = 0^\circ, 180^\circ$; Polarizations $\perp\perp$, $\perp-45^\circ$, $\perp\parallel$	57
41. Calculated ρ' for A02100 Using Non-Lambertian Volume Model. $\theta_i = 0^\circ$, $\phi_i = 180^\circ$, $\phi_r = 0^\circ, 180^\circ$; Polarization $\perp\parallel$	58
42. Calculated ρ' for A02100 Using Lambertian Volume Model. $\theta_i = 0^\circ$, $\phi_i = 180^\circ$, $\phi_r = 0^\circ, 180^\circ$; Polarization $\perp\parallel$	59
43. Measured ρ' for A02100. $\theta_i = 20^\circ$, $\phi_i = 180^\circ$, $\phi_r = 0^\circ, 180^\circ$; Polarizations $\perp\perp$, $\perp-45^\circ$, $\perp\parallel$	60
44. Calculated ρ' for A02100 Using Non-Lambertian Volume Model. $\theta_i = 20^\circ$, $\phi_i = 180^\circ$, $\phi_r = 0^\circ, 180^\circ$; Polarization $\perp\parallel$	61
45. Calculated ρ' for A02100 Using Lambertian Volume Model. $\theta_i = 20^\circ$, $\phi_i = 180^\circ$, $\phi_r = 0^\circ, 180^\circ$; Polarization $\perp\parallel$	62
46. Measured ρ' for A02100. $\theta_i = 40^\circ$, $\phi_i = 180^\circ$, $\phi_r = 0^\circ, 180^\circ$; Polarizations $\perp\perp$, $\perp-45^\circ$, $\perp\parallel$	63
47. Calculated ρ' for A02100 Using Non-Lambertian Volume Model. $\theta_i = 40^\circ$, $\phi_i = 180^\circ$, $\phi_r = 0^\circ, 180^\circ$; Polarization $\perp\parallel$	64
48. Calculated ρ' for A02100 Using Lambertian Volume Model. $\theta_i = 40^\circ$, $\phi_i = 180^\circ$, $\phi_r = 0^\circ, 180^\circ$; Polarization $\perp\parallel$	65
49. Bidirectional Reflectance Geometry	75

TABLES

I. Model Parameters for Sample Paints	18
II. True Source Polarization Angles	18
III. $\rho'(\theta_n, \phi_n; \theta_n, \phi_n) \cos^2 \theta_n$ Values for A02017-001	69
IV. $\rho'(\theta_n, \phi_n; \theta_n, \phi_n) \cos^2 \theta_n$ Values for A02018-001	70
V. $\rho'(\theta_n, \phi_n; \theta_n, \phi_n) \cos^2 \theta_n$ Values for A02018-002	71
VI. $\rho'(\theta_n, \phi_n; \theta_n, \phi_n) \cos^2 \theta_n$ Values for A02100	72
VII. RHOPRIME Input Listing	92
VIII. Long Form Output	93
IX. Short Form Output	94

POLARIZED RADIANCE

Volume I

Polarized Bidirectional Reflectance with Lambertian
or Non-Lambertian Diffuse Components

10 April Through 31 December 1972

1

INTRODUCTION

A model for predicting the radiance at a remote sensor must include the spatial, spectral, and polarization characteristics of the bidirectional reflectance and directional emittance with respect to target and background surfaces. In principle, the directional reflectance and directional emittance properties of materials must be known for all source and receiver angles, polarizations, and wavelengths. A Lambertian assumption may be valid for some types of backgrounds, but for most man-made targets is scarcely adequate. Measurement of all spatial, polarization, and spectral characteristics of the bidirectional reflectance and directional emittance for a large number of material samples is impractical. Even if such measurement were performed, the data could not all be stored efficiently enough to make it accessible for digital computations. Clearly, an empirical model is required to approximate the bidirectional reflectance and directional emittance properties from a limited number of measurements.

The bidirectional reflectance model first developed by the Environmental Research Institute of Michigan (ERIM) for the Air Force [1, 2] is described in this report. The model accounts for effects that produce both specular and diffuse components. In particular, a surface model relates bidirectional reflectance for all source-receiver angles and polarizations to fixed bistatic measurements and a Brewster angle measurement. The model has been extended under this contract to enable calculation of either a Lambertian diffuse component or a non-Lambertian diffuse component. The latter component accounts for angular and depolarization properties arising from internal scattering effects. Our extension of the bidirectional reflectance model has considerably improved the fit between model predictions and measured data, as will be shown in Section 6.

As it now stands, the model permits generation of an enormous amount of bidirectional reflectance data from a very small amount of measured data. The accuracy shown in Section 6 on Model Validation indicates that the model is very effective, although it can still be improved, particularly at large receiver zenith angles. With the ability to account for elliptical (particularly circular) polarization now built in, the model is available for use with circularly polarized sources, if these sources prove useful in the future.

In this report, we compare measured data with results computed from both the initial model and from the extended model, and then evaluate the relative performance of the two. We

establish a domain of validity for each, based on material properties. Since the modeling is empirical, only a limited amount of measured data are required as input parameters. In this case, the parameters are the fixed bistatic data.

All modeling described in Volume I of this report was performed with respect to one wavelength, $\lambda = 1.06 \mu\text{m}$.

2 BIDIRECTIONAL REFLECTANCE

One physical property which can be measured directly from a sample of material is bidirectional reflectance. The physical definition is

$$\rho'(\theta_i, \phi_i; \theta_r, \phi_r) = \frac{\delta L_r(\theta_r, \phi_r)}{\delta E_i(\theta_i, \phi_i)} \quad (1a)$$

where $\delta E_i(\theta_i, \phi_i)$ is the incremental irradiance (power per unit area) impinging on the surface of a material from the direction (θ_i, ϕ_i) , and $L_r(\theta_r, \phi_r)$ is the resulting increment of radiance (power per unit projected area per unit solid angle) scattered from that surface in the direction (θ_r, ϕ_r) . Figure 1 illustrates the situation. The bistatic angle, 2β , is that angle between the vectors which point to the source and the receiver respectively.

Equation (1a) can be rewritten in terms of directly-accessible experimental parameters as

$$\rho'(\theta_i, \phi_i; \theta_r, \phi_r) = \frac{\frac{\delta P_r}{\delta A \cos \theta_r \delta \Omega_r}}{\frac{\delta P_i}{\delta A}} \quad (1b)$$

where δP_i is the power, in watts, incident from the direction (θ_i, ϕ_i) on the small area δA , and δP_r is the resulting power scattered into the small solid angle $\delta \Omega_r$ in the direction (θ_r, ϕ_r) .

When polarization dependence is to be shown, subscripts are appended to the ρ' term. Thus when we write $\rho'_{\alpha_i \alpha_r}$, the leading subscript, α_i , describes the source polarization while the trailing subscript, α_r , describes the receiver polarization. The source polarization, always referred to the plane of incidence, describes the polarization state of the electric field vector. The appended subscript symbols \parallel and \perp indicate whether the source electric vector polarization is parallel to or perpendicular to the incidence plane. The reflected electric field polarization state is specified by the same symbols, but here the reference plane is that reflectance plane defined by the sample normal and the direction to the receiver. (For example, $\rho'_{\perp \parallel}$ represents reflectance measured when source polarization is perpendicular to the incidence plane and receiver polarization is parallel to the reflectance plane.) Notice that when either the source or the receiver, or both, are scanned in angle over the sample, the incidence and reflectance planes change orientation with relation both to the sample and to each other.

Bidirectional reflectance depends on the physical properties of the material as well as on the geometric state of its surface. Different surface states result in different reflectances. Hence, a complete collection of bidirectional reflectance data for any single material would require measurements of a large number of samples of the material, each with a different surface state. Each sample would have to be measured with several source-receiver polarization combinations. Consequently a very large number of source and receiver positions would be

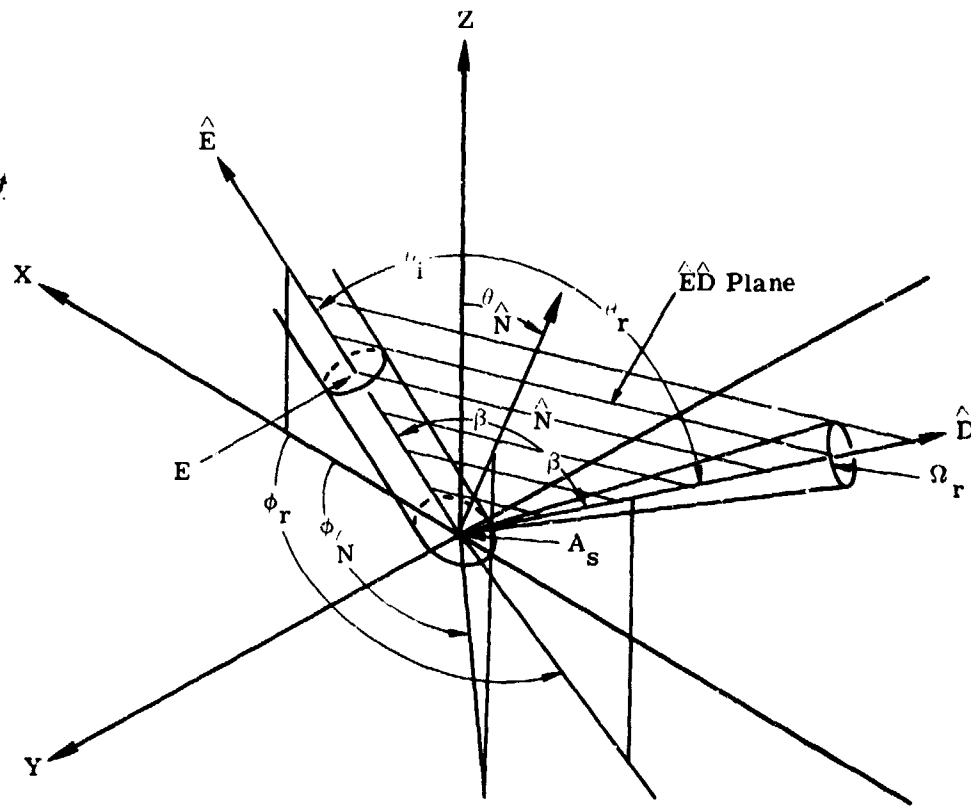


FIGURE 1. BIDIRECTIONAL REFLECTANCE GEOMETRY AND PARAMETERS

required for each set of polarization states. Finally, the entire procedure would have to be repeated at many different wavelengths. The purpose of modeling is to predict reflectance data from only a limited number of measurements and hence eliminate the need for an otherwise unwieldy measurement program.

3
BACKGROUND INFORMATION

The bidirectional reflectance model is based on observations of polarized bidirectional data from rough, painted surfaces which exhibit a Brewster angle (Fresnel-like behavior in relation to the specular geometry). The degree of depolarization appears slight, and on that basis for the initial modeling work in this program single specular reflection from the rough front surface was assumed to be the dominant reflection mechanism. Multiple front-surface reflections and internal scatterings were observed to be smaller and were initially incorporated into a Lambertian "volume" model to account for the diffuse component.

The assumption that the diffuse component is Lambertian, however, makes it difficult to account for certain anomalies that occur when measured data are compared with the model's output. For example, Fig. 2 is a bidirectional reflectance curve showing the reflectances at the receiver as the receiver scans over zenith angles from 0° to 90° in the $\phi_r = 0^\circ$ and $\phi_r = 180^\circ$ half planes. The source remains fixed at $\theta_i = 40^\circ$ and $\phi_i = 180^\circ$. The upper curve shows reflectances when source and receiver are both linearly polarized at the same polarization angle with respect to the target-incidence and target-receiver planes. (In this case, both are perpendicular-polarized.) The lower curve shows reflectances when source and receiver are cross-polarized with respect to one another. (Source is perpendicular-polarized; receiver is parallel-polarized.) Note the marked angular dependence in the lower curve. If the nonspecular component were truly Lambertian, no such angular dependence would be present.

Also, although radiation sources in this work are all linearly polarized, future work may well involve more general cases. Therefore, the model should account for the most general type of polarization —namely, elliptical.

For the above reasons, and in order to obtain a closer overall correspondence between model prediction and measured data, the model has been extended to account for the following:

- (1) possible non-Lambertian angular dependence of depolarized component
- (2) shadowing and obscuration produced by the roughness of the surface
- (3) elliptical polarization

The model —a phenomenological one in that its use requires a limited number of measurements —is described in the next two sections. Section 4 includes a discussion of specular reflectance from the surface, effects caused by shadowing and obscuration resulting from surface roughness, and polarization effects. Section 5 describes the volume model.

A02018 001

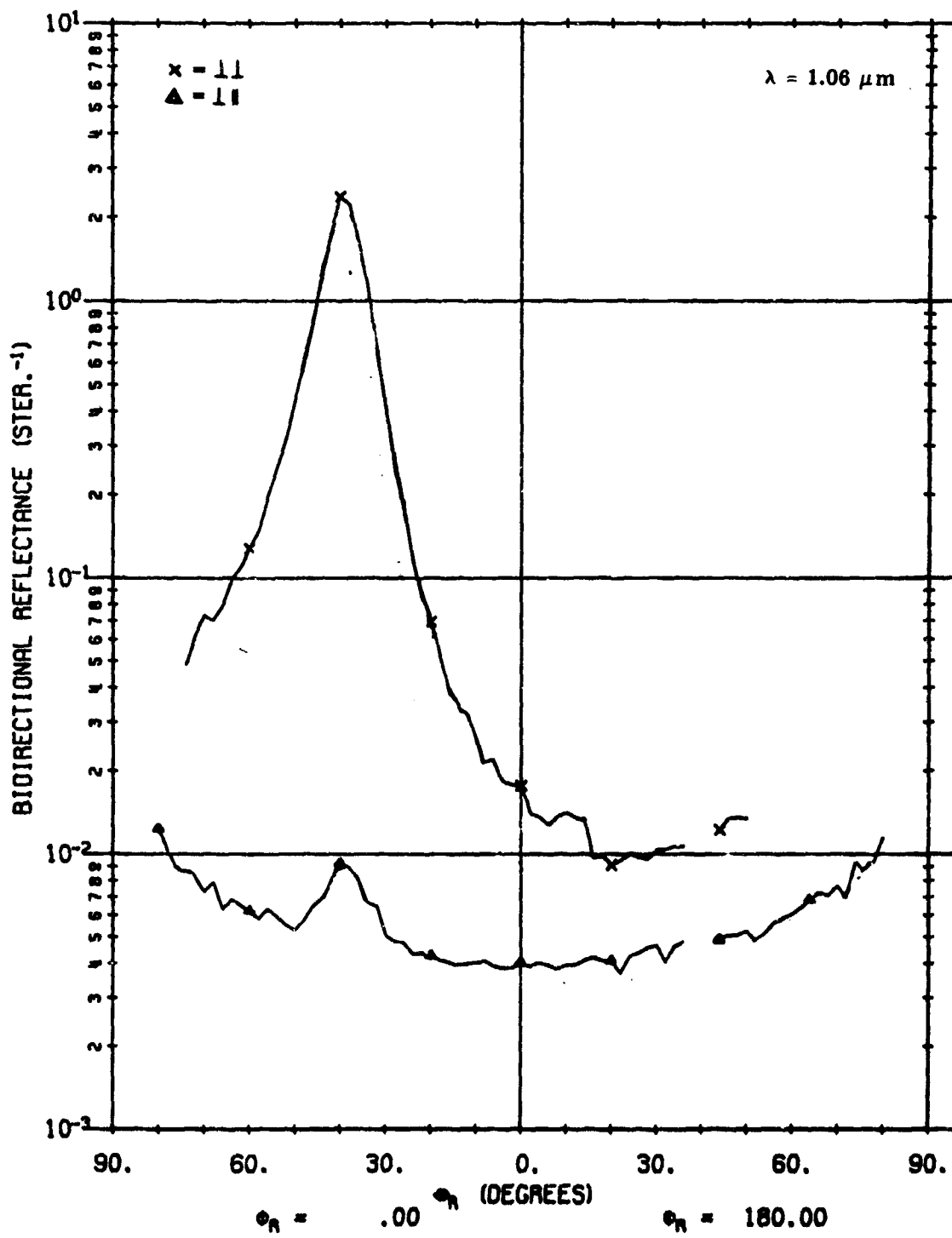


FIGURE 2. EXAMPLE OF ρ' FOR A02018-001. $\theta_i = 40^\circ$, θ_r scanned in plane.

4 SURFACE MODEL

In this section, we review the surface model and also discuss the interference effects that necessitated model modification.

4.1. AVAILABLE AREA

If the rough surface is considered to be made up of small sequins having a distribution of orientations, there will be some specular reflectance at any receiver angle and the extent of that reflectance will be determined in part by the amount of surface oriented for specular reflection at that receiver angle. (The area available for such reflection will also depend on how some sequins shadow or obscure others.) Since measurements do, in fact, show a reflectance distribution over the hemisphere, we assume that the above description is valid and that there is, indeed, a distribution of surface areas which have normals pointing in different directions. Therefore, to establish the distribution of available surface area, we define a density function $\Xi(\theta, \phi)$ which describes the relative density of local surface normals (per steradian) pointing in the direction (θ, ϕ) .

The effect of the distribution of surface normals is measured by a zero bistatic measurement in which $\theta_i = \theta_r$ and $\phi_i = \phi_r$. (Note that we really use a fixed bistatic scan with a small bistatic angle. A true zero bistatic scan would be very difficult to obtain since source and receiver obviously cannot occupy the same position.)

4.2. FRESNEL COEFFICIENTS

Fresnel reflectance coefficients describe the reflectance and polarization of specularly reflected radiation as functions of source and detector positions and of the complex index of refraction. However, since we are trying to find reflectance as a function of source and detector positions only, we must know—or be able to determine—the index of refraction. (As discussed later in this section, we can determine the index by measuring the Brewster angle.) Since, in the surface model, we consider only single, local specular reflections, the Fresnel equations automatically account for polarization.

If the receiver subtends the solid angle $\delta\Omega_r$ from the sample (see Fig. 1) the solid angle $\delta\Omega_{\hat{n}}$ in which local surface normals must lie to permit collection of the local specularly reflected radiation by the receiver is given by:

$$\delta\Omega_{\hat{n}} = \frac{\delta\Omega_r}{4} \cos \beta \quad (2)$$

This solid angle is centered about the direction $(\theta_{\hat{n}}, \phi_{\hat{n}})$.

Let δP_i be power incident on area δA . The fraction of surface area, $\delta A(\hat{\theta}, \hat{\phi})$, which reflects radiation into the receiver is given by

$$\delta A(\hat{\theta}, \hat{\phi}) = \Xi(\hat{\theta}, \hat{\phi}) \delta A \frac{\delta \Omega}{\delta A} \quad (3)$$

The power incident on $\delta A(\hat{\theta}, \hat{\phi})$ is

$$\delta P_i \frac{\delta A(\hat{\theta}, \hat{\phi})}{\delta A} \frac{\cos \beta}{\cos \theta_i} \quad (4)$$

Since the Fresnel reflectance, $R(\beta)$, is just the ratio of reflected power to incident power, then

$$\delta P_r = R(\beta) \delta P_i - \frac{\delta A(\hat{\theta}, \hat{\phi})}{\delta A} \frac{\cos \beta}{\cos \theta_i} \quad (5)$$

Recall that in Eq. (1b): $\rho'(\theta_i, \phi_i; \theta_r, \phi_r) = \frac{\delta P_r}{\delta P_i}$. Substituting Eqs. (5), (3) and (2):

$$\rho'(\theta_i, \phi_i; \theta_r, \phi_r) = \frac{R(\beta) \Xi(\hat{\theta}, \hat{\phi})}{4 \cos \theta_i \cos \theta_r} \quad (6)$$

By considering the case when source and receiver are in the same position, i.e., a zero bistatic ($\beta = 0$) case, $\Xi(\hat{\theta}, \hat{\phi})$ can be determined. In this situation

$$\rho'(\hat{\theta}, \hat{\phi}; \hat{\theta}, \hat{\phi}) = \frac{R(0) \Xi(\hat{\theta}, \hat{\phi})}{4 \cos^2 \theta} \quad (7)$$

and

$$\Xi(\theta, \phi) = \frac{4 \rho'(\hat{\theta}, \hat{\phi}; \hat{\theta}, \hat{\phi}) \cos^2 \theta}{R(0)} \quad (8)$$

Now substitute back into Eq. (6) and

$$\rho'(\theta_i, \phi_i; \theta_r, \phi_r) = \frac{R(\beta)}{R(0)} \frac{\rho'(\hat{\theta}, \hat{\phi}; \hat{\theta}, \hat{\phi}) \cos^2 \theta}{\cos \theta_i \cos \theta_r} \quad (9)$$

Equation (9) is an expression for the bidirectional reflectance given in terms of measured data and Fresnel reflectance coefficients. However, to evaluate the Fresnel coefficients so they can be used in Eq. (9) takes a little work. For example, $R(\beta)$ is a function of the real and imaginary parts of the complex index of refraction, $n' = n - ik$ (see Ref. 3 or Appendix III). Therefore, n and k must be found before $R(\beta)$ can be determined.

Moreover, k is taken to be very small* so that n can be determined experimentally by measuring the Brewster angle, θ_B , and then using $n = \tan \theta_B$ to solve for n .

4.3. SHADOWING AND OBSCURATION

Referring to Eq. (9), we can derive a zero bistatic curve, $\rho'(\theta_{\hat{n}}, \phi_{\hat{n}}; \theta_{\hat{n}}, \phi_{\hat{n}})$, from a $\rho'(\theta_i, \phi_i, \theta_r, \phi_r)$ curve with θ_i, ϕ_i fixed and θ_r variable by inverting the equation so that

$$\rho'(\theta_{\hat{n}}, \phi_{\hat{n}}, \theta_{\hat{n}}, \phi_{\hat{n}}) = \frac{R(0)}{R(\beta)} \frac{\rho'(\theta_i, \phi_i, \theta_r, \phi_r) \cos \theta_i \cos \theta_r}{\cos^2 \theta_{\hat{n}}} \quad (10)$$

after doing this for a variety of θ_i 's, we found that the curves obtained differed systematically from those obtained from a fixed bistatic measurement. Apparently, because of surface roughness, some sequins shadow or obscure others; this reduces reflectance everywhere except at a purely back-scattered position. The model must therefore be modified to correct for such interference.

Torrance and Sparrow [4] have developed an analytical function that helps correct the situation; however, we have constructed our own function using empirical considerations only. Our function results in better agreement between measured and derived fixed bistatic curves than does the analytical function of Torrance and Sparrow. The empirical function (SO) is defined as:

$$SO = \frac{1 + \frac{\theta_{\hat{n}}}{\Omega} e^{-2\beta/\tau}}{1 + \frac{\theta_{\hat{n}}}{\Omega}} \left(\frac{1}{1 + \frac{\phi_n \theta_i}{\Omega}} \right) \quad (11)$$

where Ω and τ are parameters, and ϕ_n is a factor calculated from the geometry, which adjusts the fall-off rate of the shadowing and obscuration function in the forward-scattered direction.

*For the calculations in this study, results of past measurement programs [1] were used to establish the refractive indices. In those programs, it was determined that the magnitude of the total index of refraction was close to 1.65; that the imaginary part of the index of refraction could be neglected, compared to the real part; and that the index of refraction, for the wavelengths of incident radiation under consideration (1 to 4 μm), did not vary appreciably.

We now modify Eq. (9):

$$\rho'(\theta_i, \phi_i; \theta_r, \phi_r) = \frac{R(\beta)}{R(0)} \frac{\rho'(\theta_i, \phi_i; \theta_r, \phi_r) \cos^2 \theta_r}{\cos \theta_i \cos \theta_r} \text{ (SO)} \quad (12)$$

Equation (10) becomes

$$\rho'(\theta_i, \phi_i; \theta_r, \phi_r) = \frac{R(0)}{R(\beta)} \frac{\rho'(\theta_i, \phi_i; \theta_r, \phi_r) \cos \theta_i \cos \theta_r}{(\cos^2 \theta_i) \text{ (SO)}} \quad (13)$$

5
VOLUME MODELS

The following discussion outlines the reasoning behind the extended portion of the bidirectional reflectance model. (The extended portion is referred to as the "volume" model.)

Different materials with varying degrees of surface roughness and different optical properties show differences in nonspecular reflectance behavior. These differences show up in the extent to which the nonspecular reflectance is dependent upon angular position of the receiver.

To make provision for materials that do exhibit such angular dependence and for those that do not, two volume models are used. The following discussion describes, first, a Lambertian volume model which has no angular dependence, and then a non-Lambertian volume model in which angular dependence is important.

5.1. LAMBERTIAN

In addition to Fresnel reflection from a surface, other effects such as might take place beneath the surface can produce a nonspecular reflectance component everywhere in the hemisphere. If the surface roughness as well as the absorption properties of the surface are right, this volume reflectance may be completely diffuse and uniform over the hemisphere. Moreover, the reflected radiation will be totally depolarized, regardless of the polarization of the source. Thus, if the receiver is polarized in the orthogonal direction to the source polarization, an in-plane measurement will represent the volume component only. However, only half the volume component is actually represented, since there should be an equal diffuse contribution polarized in the same direction as the source.

The Lambertian volume component is one of the input parameters for the model when a target material with Lambertian reflectance properties is considered. A method whereby values for this parameter may be extracted is described in Section 6.

5.2. NON-LAMBERTIAN

On the basis of the Lambertian diffuse model described above, no angular dependence would be expected for the diffuse component. However, for some materials, actual measurements show that there is an angular dependence. To provide for the angular dependence of the diffuse component, the model has been extended by including scattering that takes place beneath the surface.

Assuming an exponential scattering function as the radiation first enters and then leaves the surface, and making reference to Fig. 3, we construct an expression for the volume scattering component of the bidirectional reflectance as follows:

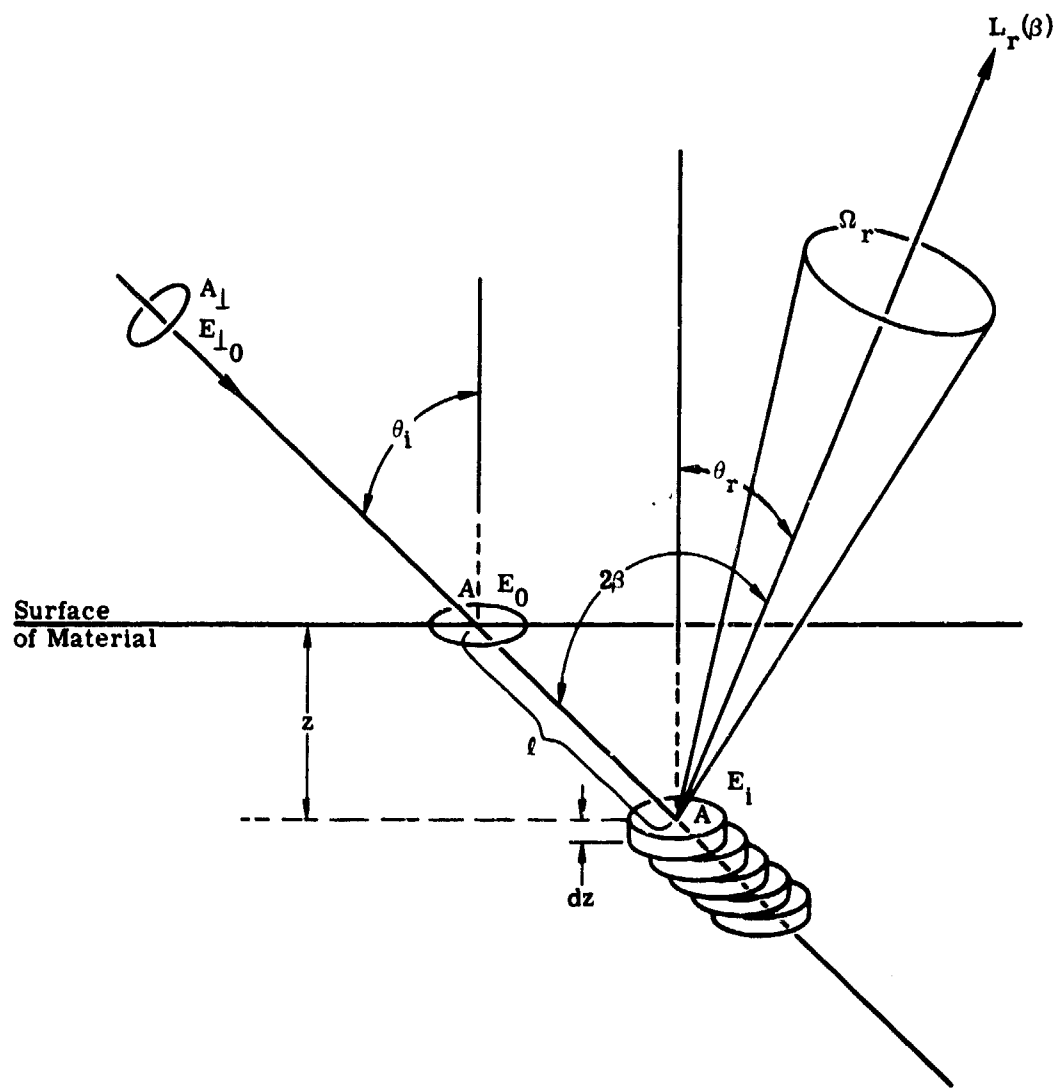


FIGURE 3. VOLUME SCATTERING GEOMETRY AND PARAMETERS

- E_{10} = irradiance at surface of area A_{\perp} , where A_{\perp} is the area of cross section of the collimated beam and is normal to the beam
 E_0 = irradiance on surface element of area A
 E_i = irradiance on surface of slab or area A at distance z beneath surface
 $L_r(\beta)$ = radiance scattered from primary beam through 2β in direction of receiver
 β = half of angle between target-to-source and target-to-receiver vectors
 σ = total scattering cross section (ignoring absorption)
 $\sigma(\beta)$ = differential scattering cross section with respect to β , i.e., $\int \sigma(\beta) d\Omega = \int d\sigma/d\Omega d\Omega = \sigma$
 Ω = solid angle subtended at target by receiver, assuming a point target
 θ_i = angle of incident beam relative to fixed z axis
 θ_r = angle of reflected beam relative to fixed z axis

The objective of the following calculation is to determine that portion of the primary beam scattered from distance z beneath the surface through an angle 2β toward a receiver which subtends solid angle Ω .

First, the bidirectional reflectance defined in Eq. (1) is now $\rho' = L_r/E_0$ with respect to the slab (see Fig. 3). To determine E_0 :

$$A_{\perp} = A \cos \theta_i \quad (14)$$

$$E_0 = \frac{P}{A} = \frac{P}{A_{\perp}/\cos \theta_i} = \frac{P \cos \theta_i}{A_{\perp}} = E_{10} \cos \theta_i \quad (15)$$

where P is the power at surface of area A.

The irradiance incident on the slab at distance z beneath its surface is:

$$E_i = E_0 e^{-\sigma t} = E_0 e^{-\sigma z / \cos \theta_i} \quad (16)$$

where $t = z / \cos \theta_i$. Hence

$$E_i = E_{10} \cos \theta_i e^{-\sigma z / \cos \theta_i} \quad (17)$$

and

$$dE_i = -E_{10} \sigma e^{-\sigma z / \cos \theta_i} dz \quad (18)$$

where dE_i is the amount by which irradiance decreases in going from distance z to distance $z + dz$ beneath surface. Note also that $e^{-\sigma z / \cos \theta_i}$ and $e^{-\sigma z / \cos \theta_r}$ represent the scattering loss from the beam on the way in and on the way out of the material, respectively. To determine L_r ,

$$P_r = L_r A \Omega_r \cos \theta_r = \text{power at the receiver} \quad (19)$$

dL_r = radiance scattered, in direction of receiver, from one small slab
of thickness dz

Radiance from slab in direction θ_r (or β) can be written:

$$dL_r = -dE_i \sigma(\beta) \quad (21)$$

since $\sigma(\beta)$ is, by definition the fraction of beam scattered into 2β . Note that (since we are ignoring absorption) irradiance lost from the incident beam is the radiance of the scattered beam; therefore a minus sign precedes dE_i . Hence, if there is no further power loss

$$dP_r = -A \Omega_r dE_i \sigma(\beta) \quad (22)$$

However, power loss caused by beam scattering occurs on the way out as well as the way in; the loss is represented by $\left(e^{-\sigma z / \cos \theta_r}\right)$ on the way out.

Therefore

$$dP_r = \left(-A \Omega_r \sigma(\beta) e^{-\sigma z / \cos \theta_r} dE_i \right) = -\frac{A_\perp}{\cos \theta_i} \Omega_r \sigma(\beta) e^{-\sigma z / \cos \theta_r} dE_i \quad (23)$$

Substituting the expression for dE_i , Eq. (18), into Eq. (23), we obtain:

$$dP_r = E_{\perp 0} \sigma e^{-\sigma z / \cos \theta_i} \left(\frac{A_\perp \sigma(\beta) e^{-\sigma z / \cos \theta_r}}{\cos \theta_i} \right) \Omega_r dz \quad (24)$$

$$P_r = \int_0^\infty dP_r = \frac{E_{\perp 0} A_\perp \Omega_r}{\cos \theta_i} \cdot \frac{\sigma(\beta)}{\left(\frac{1}{\cos \theta_i} + \frac{1}{\cos \theta_r} \right)} \quad (25)$$

where the integration from 0 to ∞ assumes no transmission of power through the material, i.e., the material has effectively an infinite thickness with respect to transmission. Therefore

$$L_r = \frac{P_r}{A \cos \theta_r \Omega_r} = \frac{E_{\perp 0} \sigma(\beta)}{\cos \theta_r \left(\frac{1}{\cos \theta_i} + \frac{1}{\cos \theta_r} \right)} \quad (26)$$

and

$$\rho' = \frac{L_r}{E_{\perp 0}} = \frac{\sigma(\beta)}{\cos \theta_i \cos \theta_r \left(\frac{1}{\cos \theta_i} + \frac{1}{\cos \theta_r} \right)} = \frac{\sigma(\beta)}{\left(\cos \theta_i + \cos \theta_r \right)} \quad (27)$$

In ignoring the finite thickness of the layer of material, we have also ignored the possible specular reflectance of the bottom surface. To account for the possibility of specular reflection from the bottom layer, it may be useful to provide a parameter function peaked near $\theta_{\hat{n}} = 0$. Therefore, we include all β dependence in a function $f(\beta)$, and all $\theta_{\hat{n}}$ dependence in a function $g(\theta_{\hat{n}})$, and write

$$\rho' = 2 \frac{\rho_V f(\beta) g(\theta_{\hat{n}})}{\cos \theta_i + \cos \theta_r} \quad (28)$$

where $f(\beta)$ and $g(\theta_{\hat{n}})$ provide freedom for empirical adjustment. The constant, ρ_V , represents the value of ρ' when $\theta_i = \theta_r = 0$ and $f(\beta) = g(\theta_{\hat{n}}) = 1$.

6
MODEL VALIDATION

Use of the bidirectional reflectance model requires a limited amount of measured data (namely the zero bistatic measurement) from which complete sets of reflectances can be calculated. The results of these model-calculated bidirectional reflectances can then be compared to corresponding results of actual measurements. This was the procedure we followed to validate the model.

Model calculations and measured data were compared in terms of ρ' (the reflectance), α or ψ_r (the angle of polarization for the beam after reflection from the target), and P (the percentage of polarization of the reflected beam).

Measured data for materials of different properties (color and roughness) were used to demonstrate the model's performance. The materials are designated as A02018-001, A02018-002, and A02100. Material A02018-001 is a green paint and material A02018-002 is a tan paint. These materials were supplied by the Army Ballistic Research Laboratories for the purpose of developing the non-Lambertian diffuse component of the model.

Measured data for materials A02018-001 and A02018-002 were used for the fitting since it was felt that two surfaces of extremely different properties (color and roughness) would be necessary to demonstrate the performance of the model. Measurements on material A02017-001 show that the bidirectional reflectance very closely resembles that of material A02018-001. Therefore, sufficient information was developed in validating the model with material A02018-001 to permit assignment of parameters to material A02017-001 as well. Additional validation was performed with respect to A02100 (soil) and discussion is included. Model parameters are listed in Table I. (See Section 7 for definitions of model parameters.) The overall discussion of the model fitting is divided into five parts:

- (1) ρ' for A02018-001
- (2) ρ' for A02018-002
- (3) polarization angle (α or ψ_r) for A02018-001
- (4) percent polarization (P) for A02018-001 and A02018-002
- (5) ρ' for A02100

In what follows, the orientation of the source polarizer in the measurements of materials A02018-001 and A02018-002 was not actually perpendicular, parallel, nor at 45° to the plane of incidence but instead was offset by 5° in each case. Specifically, the appropriate correspondences, shown in Table II, should be recognized. These shifts were taken into account when the validation calculations were made on the computer; however, we continue to refer to "perpendicular," "parallel," and " 45° ."

TABLE I. MODEL PARAMETERS FOR SAMPLE PAINTS

Parameter	Material		
	A02017-001	A02018-001	A02018-002
n	1.65	1.65	1.65
k	0	0	0
$\rho_{\chi 1}$	---	---	0.044
$\rho_{\chi 2}$	---	---	0.044
ρ_v	.0064	0.007	0.05**
τ	15	15	15
Ω	40	40	40
$f(\beta)$	1	1	1
$g\left(\frac{\theta}{n}\right)$	1	1	1
$\rho' \left(\theta_{\hat{n}}, \theta_{\hat{n}}; \theta_{\hat{n}}, \theta_{\hat{n}} \right) \cos^2 \theta_{\hat{n}}$	---	---	---
λ	1.06 μm	1.06 μm	1.06 μm

*This material is run with the non-Lambertian volume model; therefore ρ_{χ} values are not necessary.

**Material 2018-002 was run with the Lambertian volume model; therefore ρ_v should not be used.

TABLE II. TRUE SOURCE POLARIZATION ANGLES

Receiver Azimuth Plane	Nominal Angles			
	$\perp (0^\circ)$	$\parallel (90^\circ)$	$+45^\circ$	-45°
$0^\circ - 180^\circ$				
$30^\circ - 210^\circ$	5°	-85°		-40°
$60^\circ - 240^\circ$				
$90^\circ - 270^\circ$	5°	+95°	+50°	
Fixed Bistatic	5°	+95°	+50°	

6.1. REFLECTANCE FOR SAMPLE MATERIAL A02018-001

Material A02018-001 is a green painted surface. The zero bistatic measurement with 5° polarization angle (i.e., almost perpendicular polarization) is shown in Fig. 4. (The zero bistatic data with parallel-polarized source, although not shown, have identical characteristics.) The zero bistatic plot is sharply peaked at 0°, falling off rapidly to a constant value at about

A02018 001

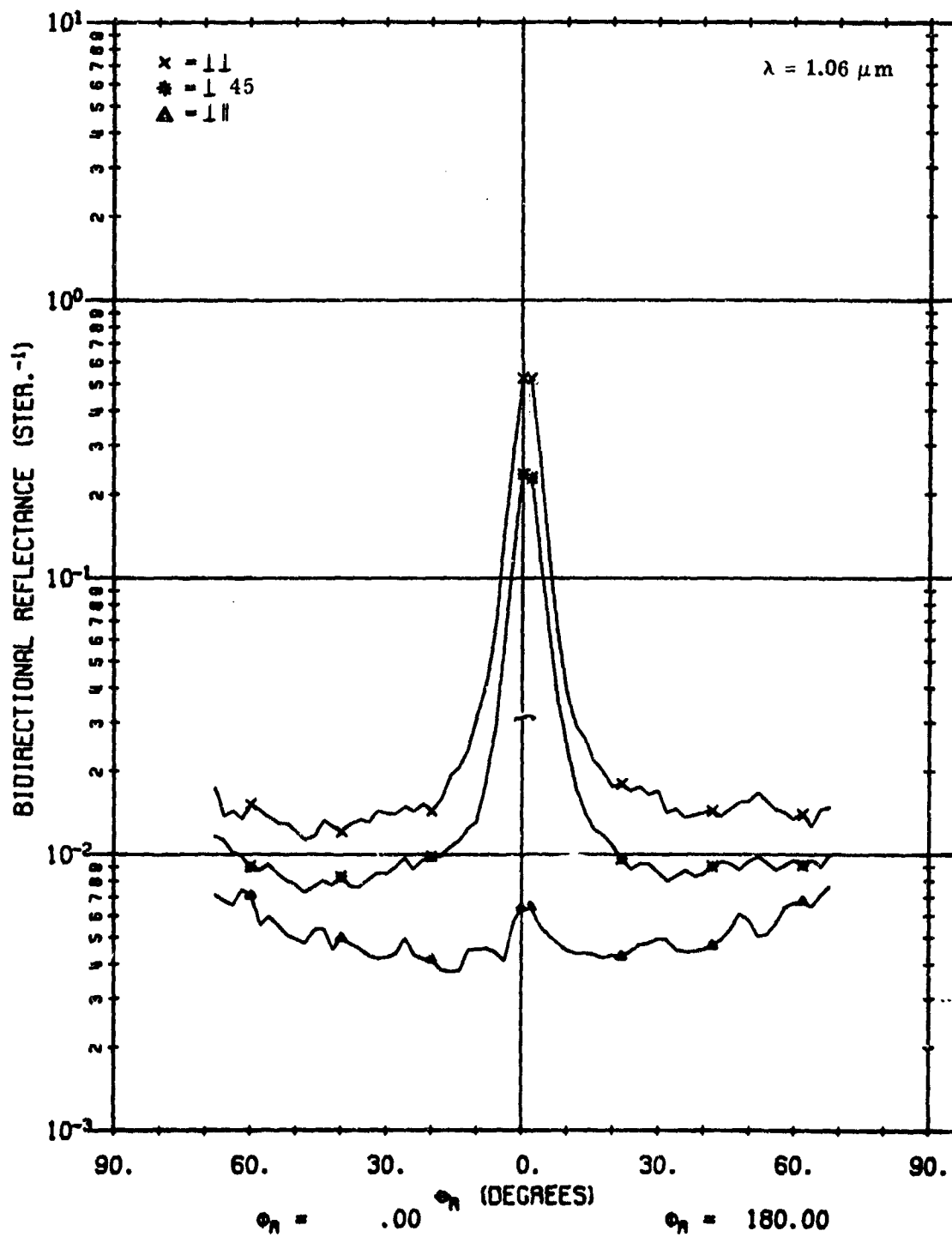


FIGURE 4. FIXED BISTATIC ρ' FOR A02018-001

20° . In all receiver polarizations, ρ' shows an angular dependence clearly departing from Lambertian behavior. The table of values for $\rho'(\hat{\theta}_i, \hat{\phi}_i; \hat{\theta}_r, \hat{\phi}_r) \cos^2 \theta_r$ used in the model was obtained from this measurement by reading off $\rho'_{\perp\perp}$ and $\rho'_{\perp\parallel}$ at each angle and then calculating $(\rho'_{\perp\perp} - \rho'_{\perp\parallel}) \cos^2 \theta_r$ where θ_r is the angle that the normal to the reflecting facet makes with the fixed z-axis. In zero bistatic scans, $\theta_i = \theta_r = \theta_n$ (see Fig. 1). (Physically the source and receiver were separated by 1.8° . Thus, both were 0.9° from the true θ_n . In the calculations, the axis was translated to bring the x-axis into correspondence with $\theta_n = 0$.) The subtraction, $\rho'_{\perp\perp} - \rho'_{\perp\parallel}$, eliminates the diffuse contribution which would distort the value for $\rho'(\hat{\theta}_i, \hat{\phi}_i; \hat{\theta}_r, \hat{\phi}_r)$ which is what must be measured (recall Eq. 9).

In Figs. 5, 7, 9 and 11,* plots of measured data are shown for $\theta_i = 40^{\circ}$, $\phi_i = 180^{\circ}$ and where θ_r is scanned in azimuth planes represented by $\phi_r = 0^{\circ}, 180^{\circ}; 90^{\circ}, 270^{\circ}; 30^{\circ}, 210^{\circ}; 60^{\circ}, 240^{\circ}$. Each measurement plot is followed by plots of data generated, respectively, by the Lambertian model with no shadowing and obscuration factor, by the non-Lambertian model with no shadowing and obscuration factor, and by the non-Lambertian model with the shadowing and obscuration factor. For example, Fig. 6 shows the calculated ρ' data for $\theta_i = 40^{\circ}$ and θ_r as scanned in the 0° and 180° azimuth planes for the above variations of the model. The simulated source is taken to have a "perpendicular" polarization angle. In these in-plane scans ($\phi_r = 0^{\circ}, 180^{\circ}$), the main peak is in the 0° azimuth plane which is the forward direction for the source angle of $\phi_i = +180^{\circ}$. Note the rise (in the plot of measured data) at large zenith angles for the cross-polarized component. This is a characteristic which suggests the need for the non-Lambertian volume model.

Surface Plus Lambertian Volume Model with No Shadowing and Obscuration Correction. Figure 6 plots (in solid lines) the model calculation using the surface model plus the Lambertian volume model with no correction for shadowing and obscuration. The following characteristics should be noted:

- (1) In the $\phi_r = 0$ (forward scattering) azimuth plane, the model fits the measured data very well between $\theta_r = 0$ and $\theta_r \approx 50^{\circ}$ for matched polarization of source and receiver. At $\theta_r = 60^{\circ}$, the calculated curve suddenly diverges. This is thought to be the result of the failure to account for shadowing and obscuration as discussed earlier. At $\theta_r = 0^{\circ}$ and on into the backscattered ($\phi_r = 180^{\circ}$) direction, the calculated values lie above the measured values and this, too, is believed to be the result of the lack of a shadowing and obscuration correction.
- (2) In the cross-polarization component ($\perp\parallel$), the model predicts a flat response except for a slight hump under the specular peak. The measured data, however, show a clear angular dependence on θ_r .

*Note: On all reprints of original computer plots, the symbols θ_r and ϕ_r are represented by Θ_R and Φ_R respectively.

A02018 001

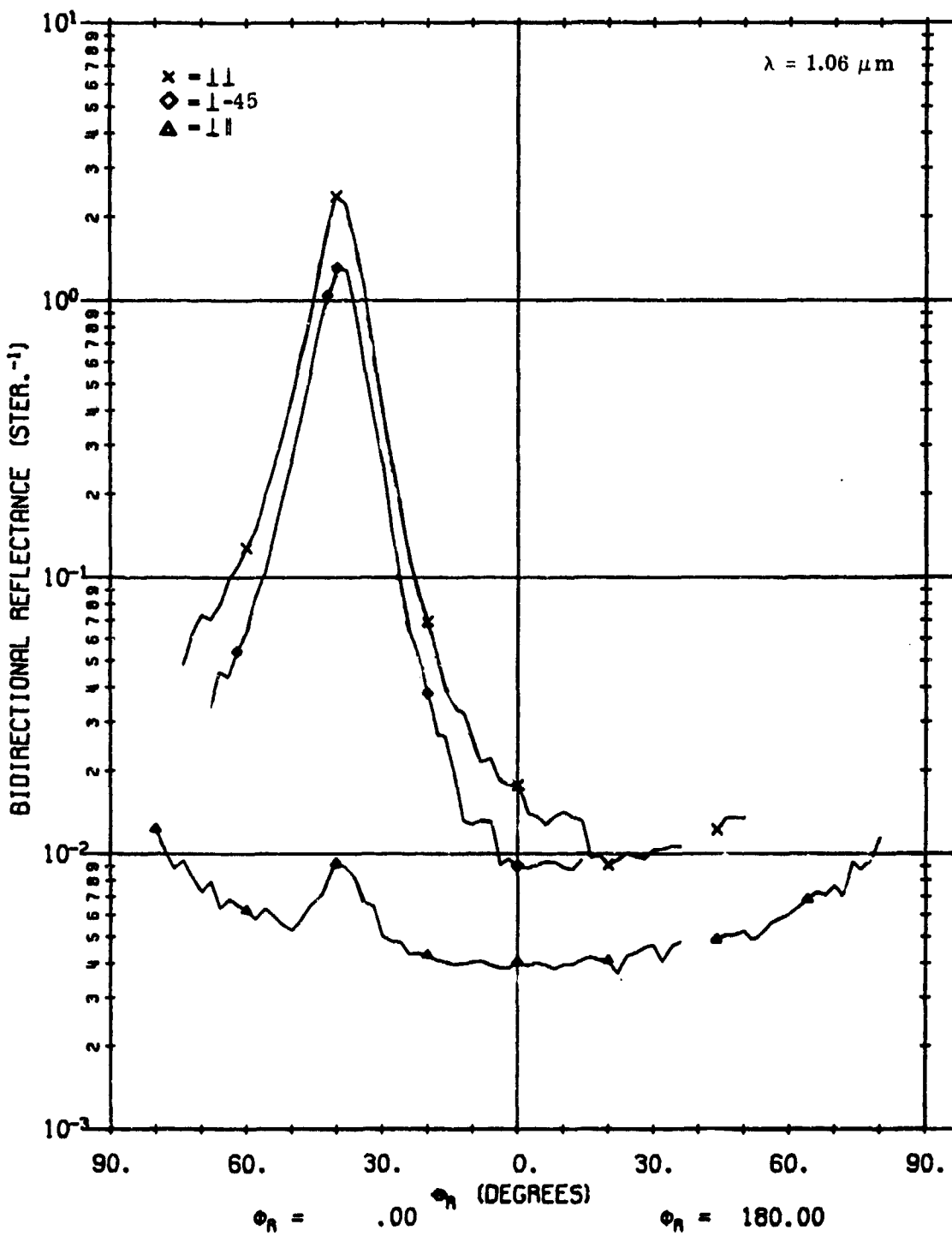


FIGURE 5. MEASURED ρ' FOR A02018-001. $\theta_i = 40^\circ$, $\phi_r = 0, 180^\circ$.

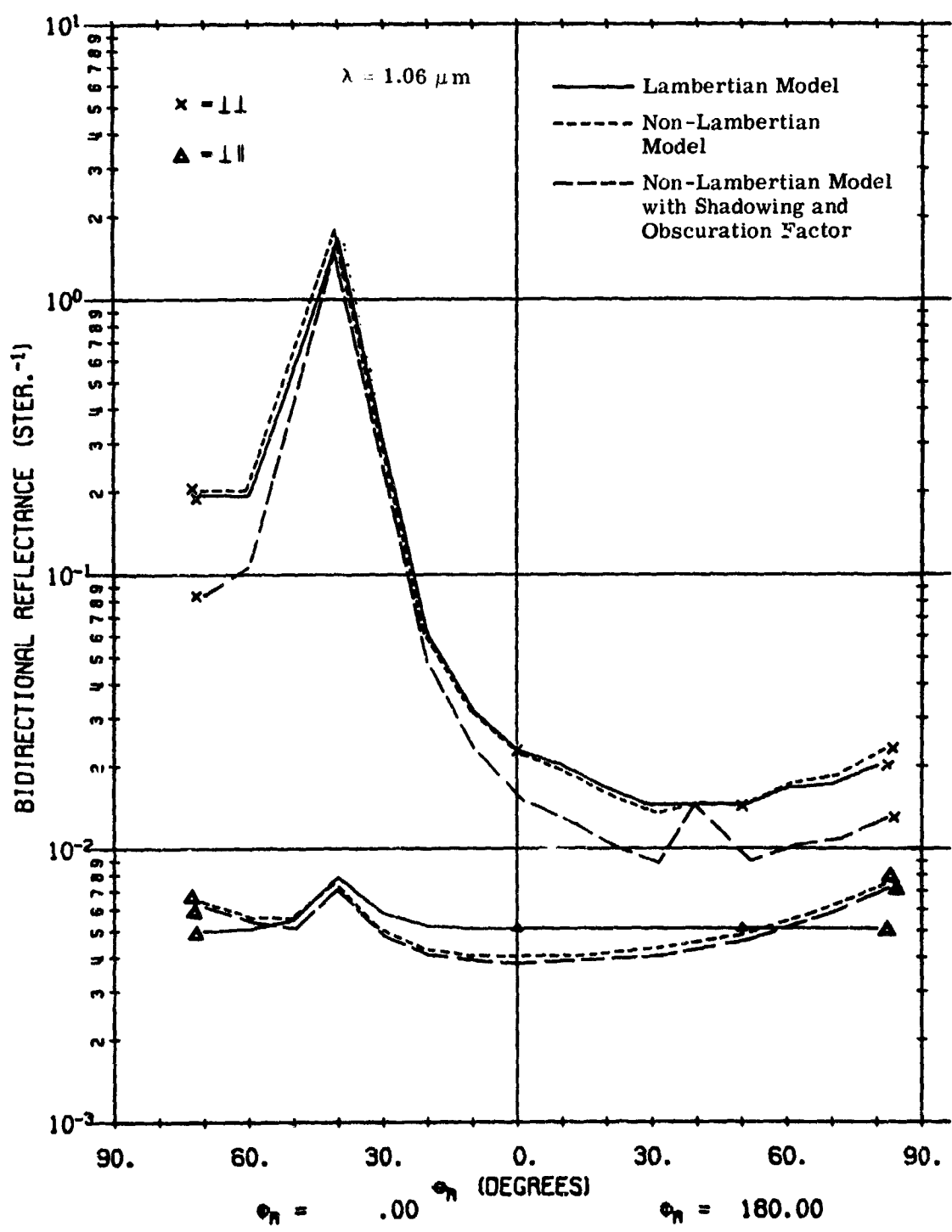


FIGURE 6. CALCULATED ρ' FOR A02018-001 USING LAMBERTIAN VOLUME MODEL AND NON-LAMBERTIAN MODEL WITH AND WITHOUT SHADOWING AND OBSCURATION FACTOR.

$$\theta_i = 40^\circ, \phi_r = 0^\circ, 180^\circ.$$

With the exception of these two characteristics, however, the surface plus Lambertian volume model with no shadowing and obscuration correction fits the measured data fairly well.

Non-Lambertian Volume Model with No Shadowing and Obscuration Correction. The dotted lines in Fig. 6 show a model plot using the same parameters, except that the non-Lambertian volume model is now used. Keep in mind that one may use the non-Lambertian volume scattering as a model by itself or in conjunction with a specular component. The latter is used here. In the like-polarized component, nothing has changed from the previous case. However, the cross-polarized component now fits the measured data much more closely. It rises steadily at large angles, both in the back-scattered and forward-scattered directions—a result of $1/(\cos \theta_i + \cos \theta_r)$ dependence shown in Eq. (28) for the volume model. However, the response for the like-polarized component does not drop sharply enough at either side of the peak, and at high angles in the forward-scattered direction, the awkward divergence still appears at 60° .

Thus, the non-Lambertian volume model improves the cross-polarized fit (with respect to material A02018-001) over that of the Lambertian volume model and, apart from anomalies at high angles and near 0° , provides a reasonable fit to the measurements.

Non-Lambertian Volume Model with Shadowing and Obscuration Correction. The dashed-line curves in Fig. 6 show results with the shadowing and obscuration correction applied to the non-Lambertian volume model calculation. The cross-polarized component is unaffected. The net effect on the match-polarized component is to reduce the reflectance everywhere except at the specular peak and at the direct backscattering peak (i.e., at $\beta = 0$). In particular, it lowers the forward-scatter contributions beyond 50° , bringing the model closer to measured data in this region. Overall, the fit obtained using the volume model with a shadowing and obscuration correction agrees closely with measurements.

The foregoing discussion applies to "in plane" receiver scans—those in the $\phi_r = 0$ and $\phi_r = 180^\circ$ azimuth planes. The azimuth plane perpendicular to the 0° , 180° plane is the 90° , 270° plane and is referred to as "out-of-plane". The plane we are in or out of is the plane of incident beam and target normal, or the target incidence plane. (See Fig. 1.)

In Fig. 7 we have the plot of measured data for the out-of-plane situation with perpendicular-polarized source again. In this case, however, the incidence plane is perpendicular to the reflection plane. At $\theta_i = 0$, therefore, $\rho'_{\perp\perp}$ in plane is the same as $\rho'_{\perp\parallel}$ out of plane. For this reason, the reflectances of match-polarized and cross-polarized components seem to exchange behaviors in the out-of-plane configuration, as is verified by the plotted measurements as well as by the model calculations. Figure 8 presents plots of a Lambertian model without the shadowing and obscuration factor, a surface plus non-Lambertian volume model without the shadowing and obscuration factor, and the surface plus non-Lambertian volume model with the shadowing and obscuration factor. As before, it is apparent that the use of the non-Lambertian volume model plus the shadowing and obscuration factor improves agreement between model and measurements so that, apart from a possible overall scale factor, the agreement is within measurement fluctuation.

A02018 001

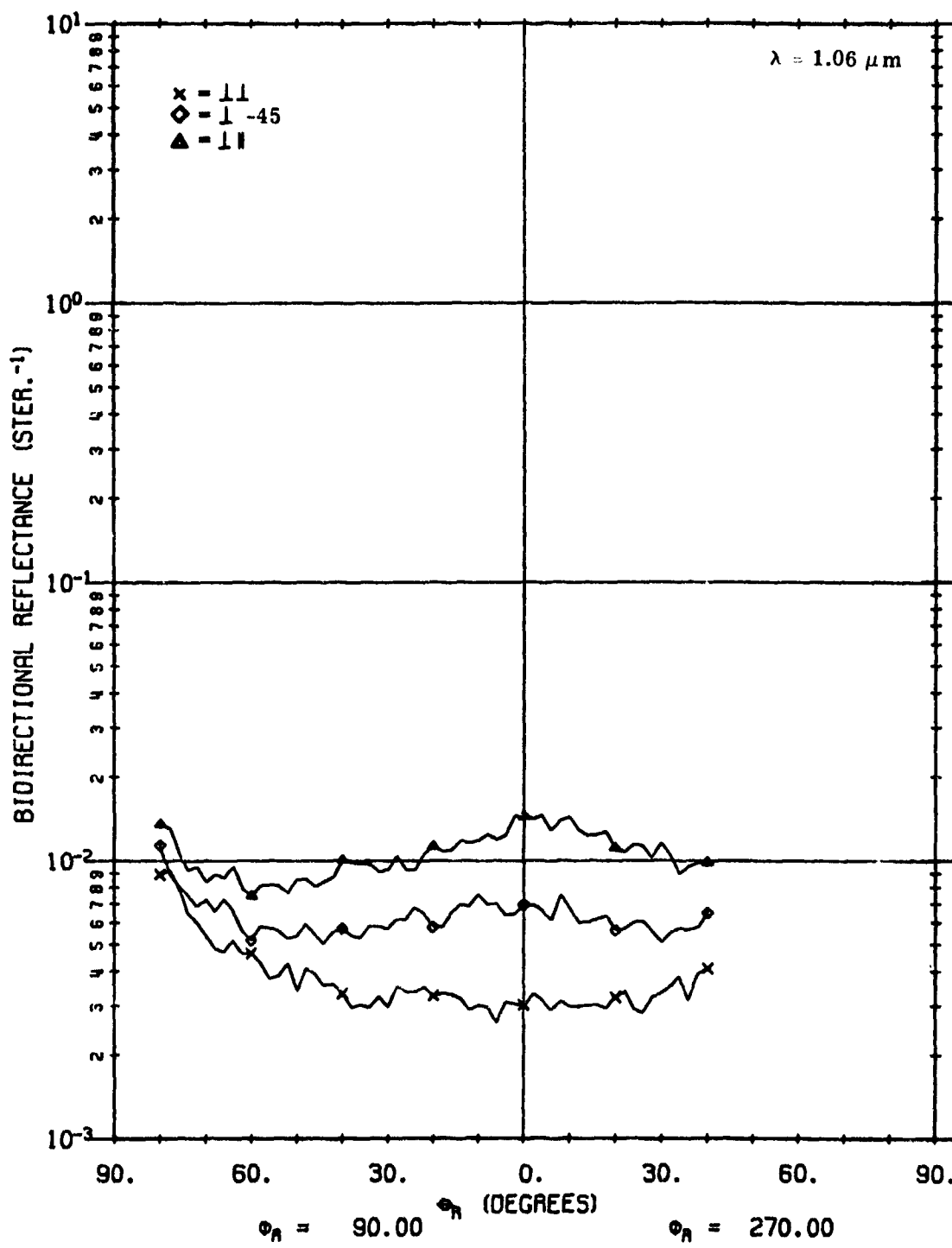


FIGURE 7. MEASURED ρ' FOR A02018-001. $\theta_i = 40^\circ$, $\phi_i = 180^\circ$, $\phi_r = 90^\circ$, 270° .

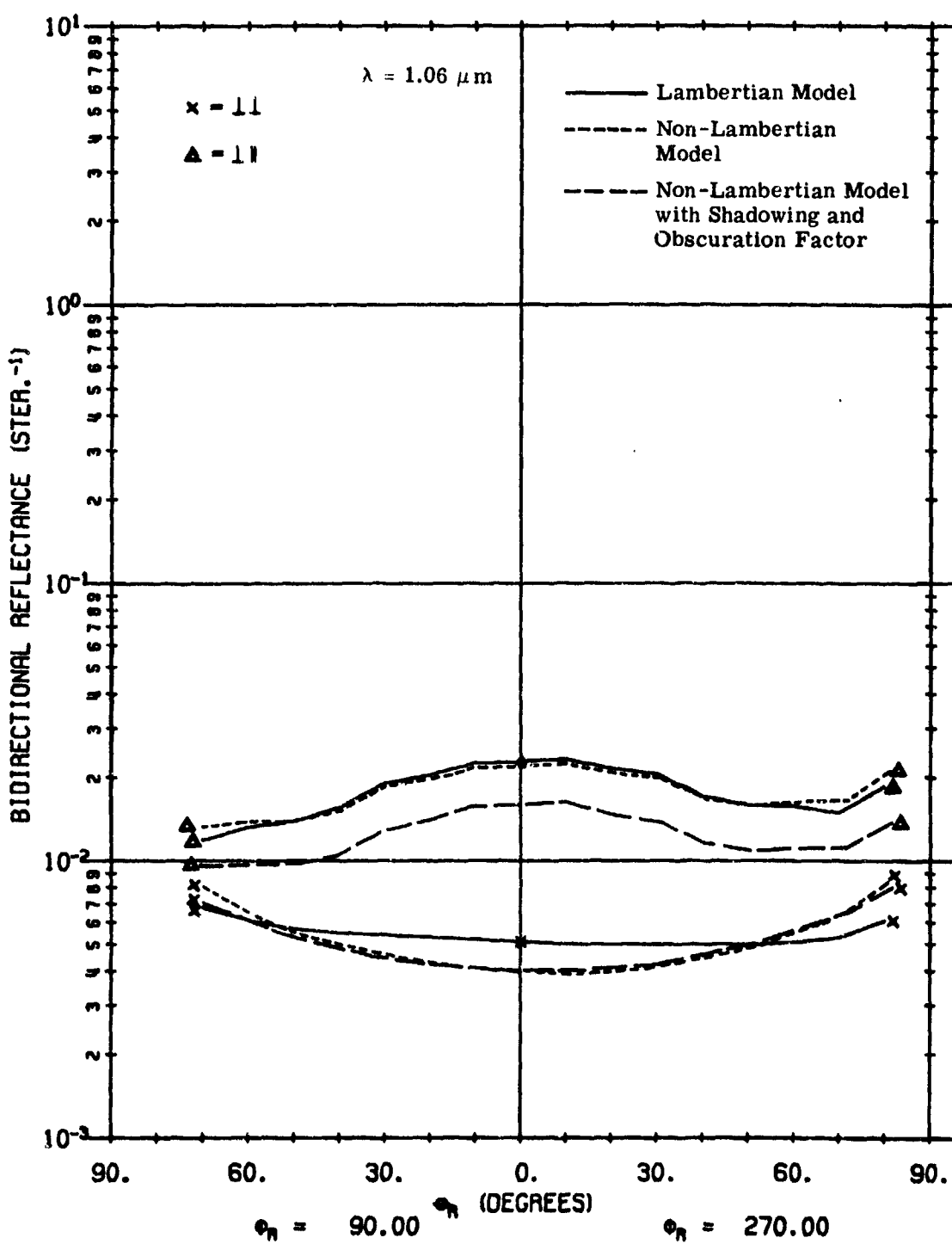


FIGURE 8. CALCULATED ρ' FOR A02018-001 USING LAMBERTIAN VOLUME MODEL AND NON-LAMBERTIAN VOLUME MODEL WITH AND WITHOUT SHADOWING AND OBSCURATION FACTOR. $\theta_i = 40^\circ$, $\phi_i = 180^\circ$; $\phi_r = 90^\circ, 270^\circ$.

For additional validation, plots are shown for the 30° , 210° azimuth planes (Figs. 9 and 10) and for the 60° , 240° azimuth planes (Figs. 11 and 12). The characteristics of calculated and measured curves, apart from a scale factor, are in excellent agreement. Figures 13 through 20 represent similar comparisons for the case when the source polarizer is set for -45° (in the 0° , 180° azimuth plane) and set parallel (in the 30° , 210° ; 60° , 240° ; and 90° , 270° planes). Measured plots are presented with the calculated plot to represent the surface plus non-Lambertian volume model and to include the shadowing and obscuration factor.

6.2. REFLECTANCE FOR SAMPLE MATERIAL A02018-002

Material A02018-002 consists of a tan painted surface.

Based on the zero bistatic scan, Fig. 21, material A02018-002 appears to be somewhat brighter than material A02018-001. Whereas the non-Lambertian volume model was clearly the best choice for material A02018-001, it is not in the case of A02018-002. In this latter case, the best choice is the Lambertian model.

The lack of angular dependence in the reflectance of the cross-polarized component could have a number of explanations. Multiple scattering increases for rougher surfaces. Since such scattering may not be angular dependent, it could become a large enough factor to swamp the angular dependence which is otherwise present. Moreover, the difference in color between the green and tan certainly alters the absorption and, consequently, can alter the angular dependence as well.

In any case, the appropriate model to use can be determined by looking at the cross-polarized component of the fixed bistatic scan. If a clear angular dependence is present, the non-Lambertian model should be used. But if there is little or no apparent angular dependence, as with material A02018-002, then the Lambertian model is more appropriate.

In Figs. 22 through 29, plots are provided for different azimuth planes, beginning with the plot for measured data, followed immediately by the corresponding plot from model calculations. In this group of illustrations, Figs. 22 through 25 represent perpendicular source polarization, while Figs. 26 through 29 represent a source parallel polarization for the 0° , 180° azimuth plane and for the 90° , 270° azimuth plane.

In all cases the fit appears to be excellent, except for occasional anomalies at large azimuth angles. Further modification of the shadowing and obscuration factor should decrease these present anomalies.

6.3. POLARIZATION ANGLE (ψ_p) FOR SAMPLE MATERIAL A02018-001

The reflectances of the perpendicular and parallel components of a linearly polarized beam vary as functions of the source-receiver angles and the index of refraction of the target material. (See, for example, the Fresnel equations, Ref. 3.) Based on observations, the index of refraction varies little over a wide range of paint surfaces. For the particular materials

A02018 001

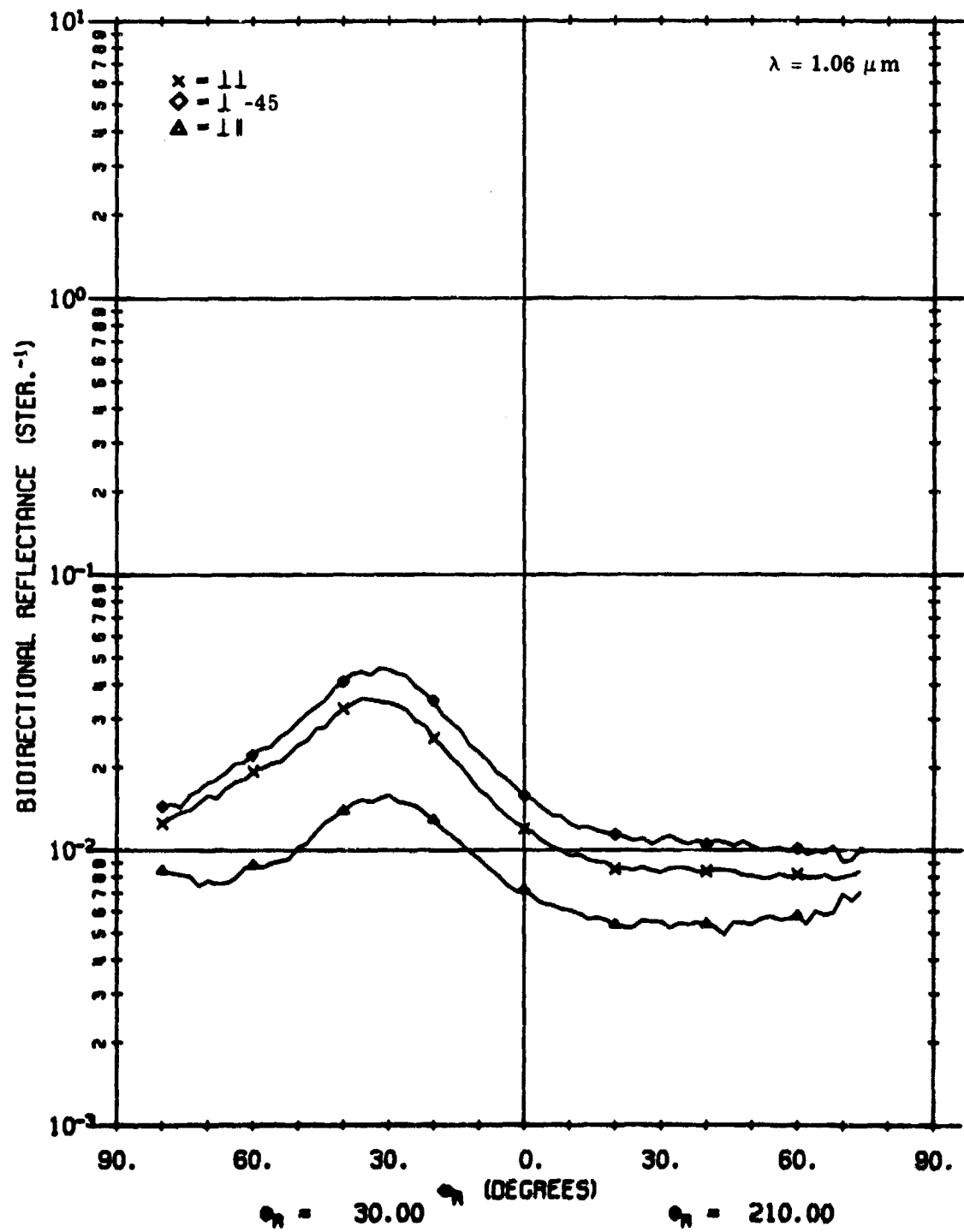


FIGURE 9. MEASURED ρ' FOR A02018-001. $\theta_i = 40^\circ$, $\phi_i = 180^\circ$, $\phi_r = 30^\circ, 210^\circ$.

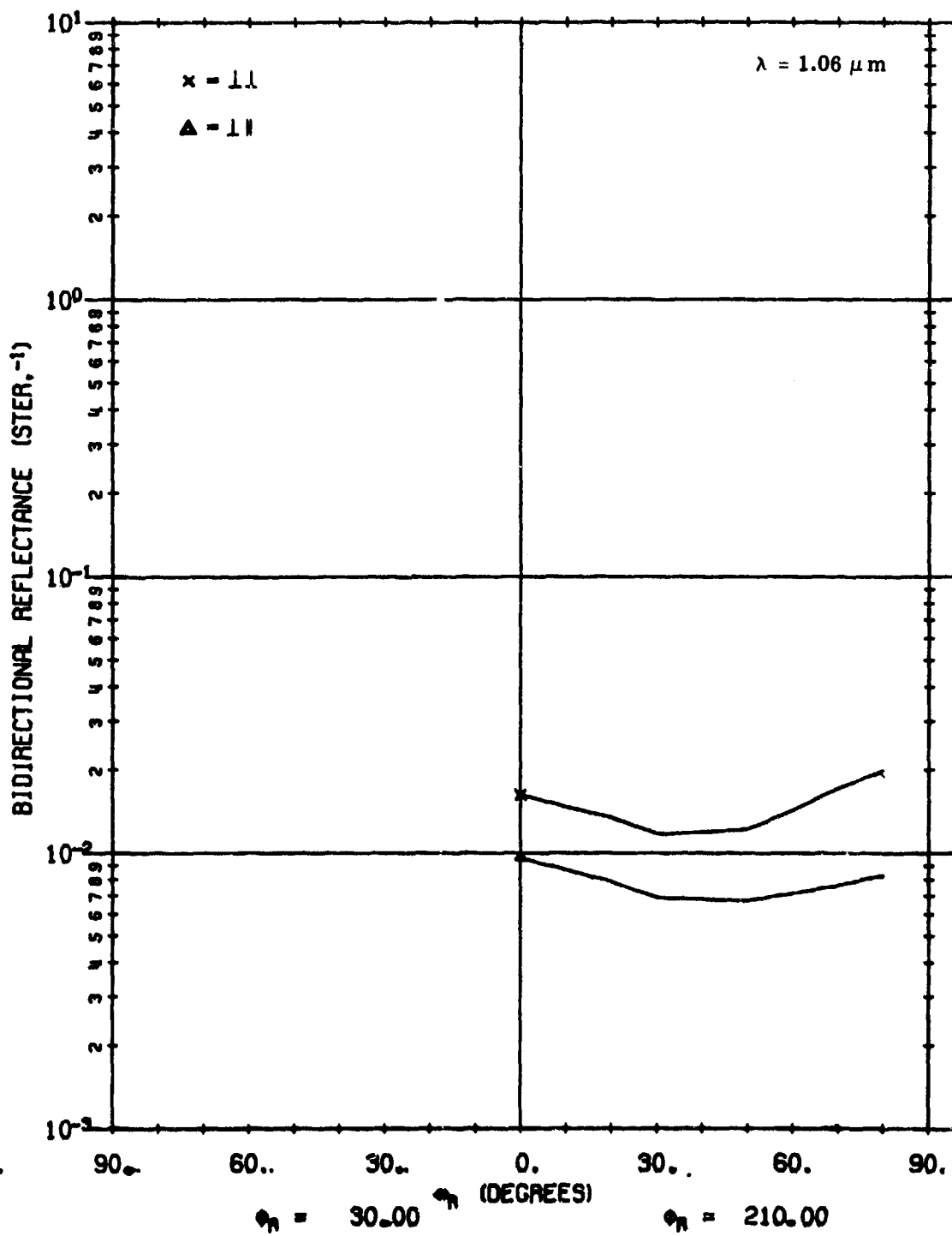


FIGURE 10. CALCULATED ρ' FOR A02018-001 USING NON-LAMBERTIAN VOLUME MODEL WITH SHADOWING AND OBSCURATION FACTOR. $\theta_i = 40^\circ$, $\phi_i = 180^\circ$, $\phi_r = 30^\circ, 210^\circ$.

A02018 001

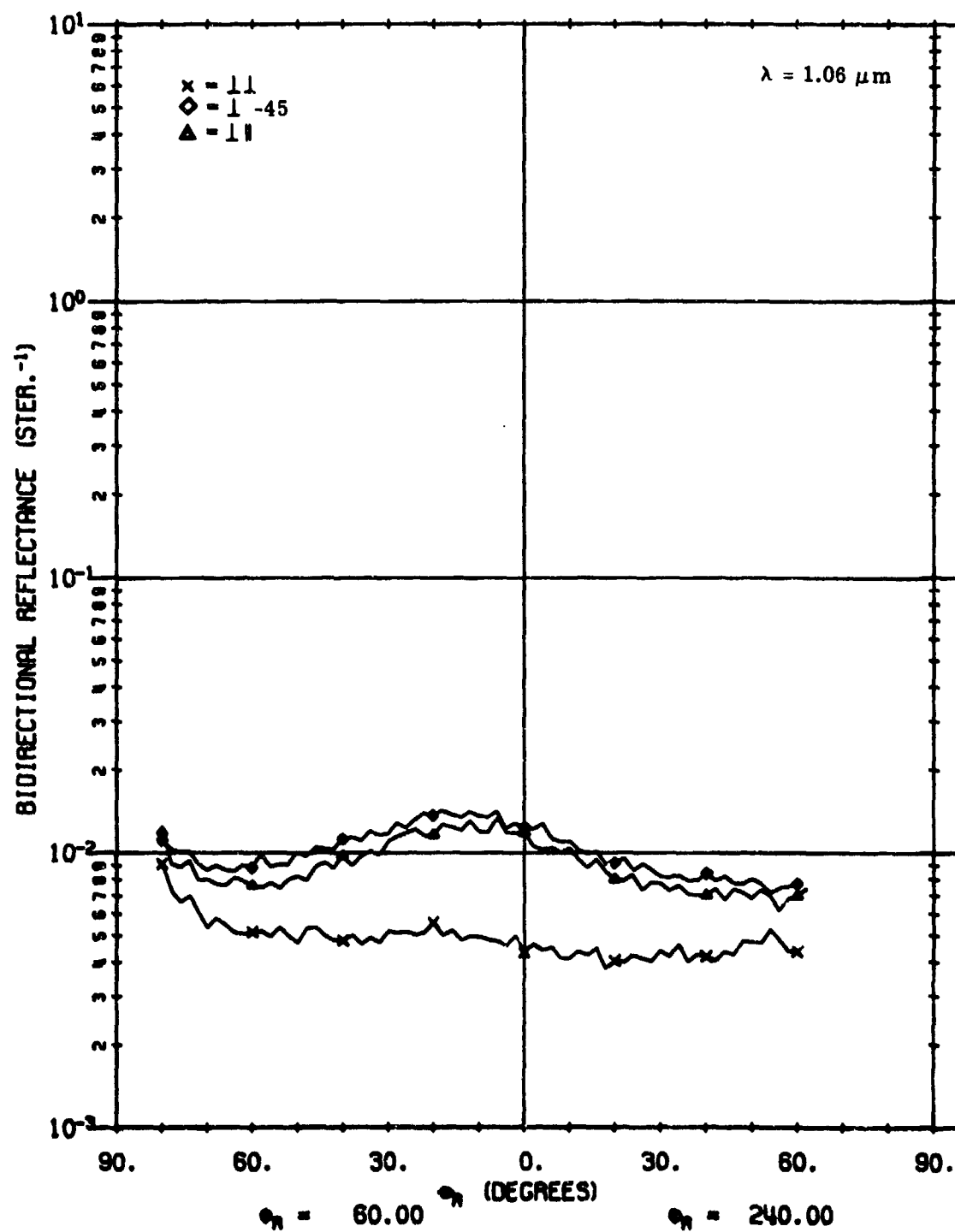


FIGURE 11. MEASURED ρ' FOR A02018-001. $\theta_i = 40^\circ$, $\phi_i = 180^\circ$, $\phi_r = 60^\circ, 240^\circ$.

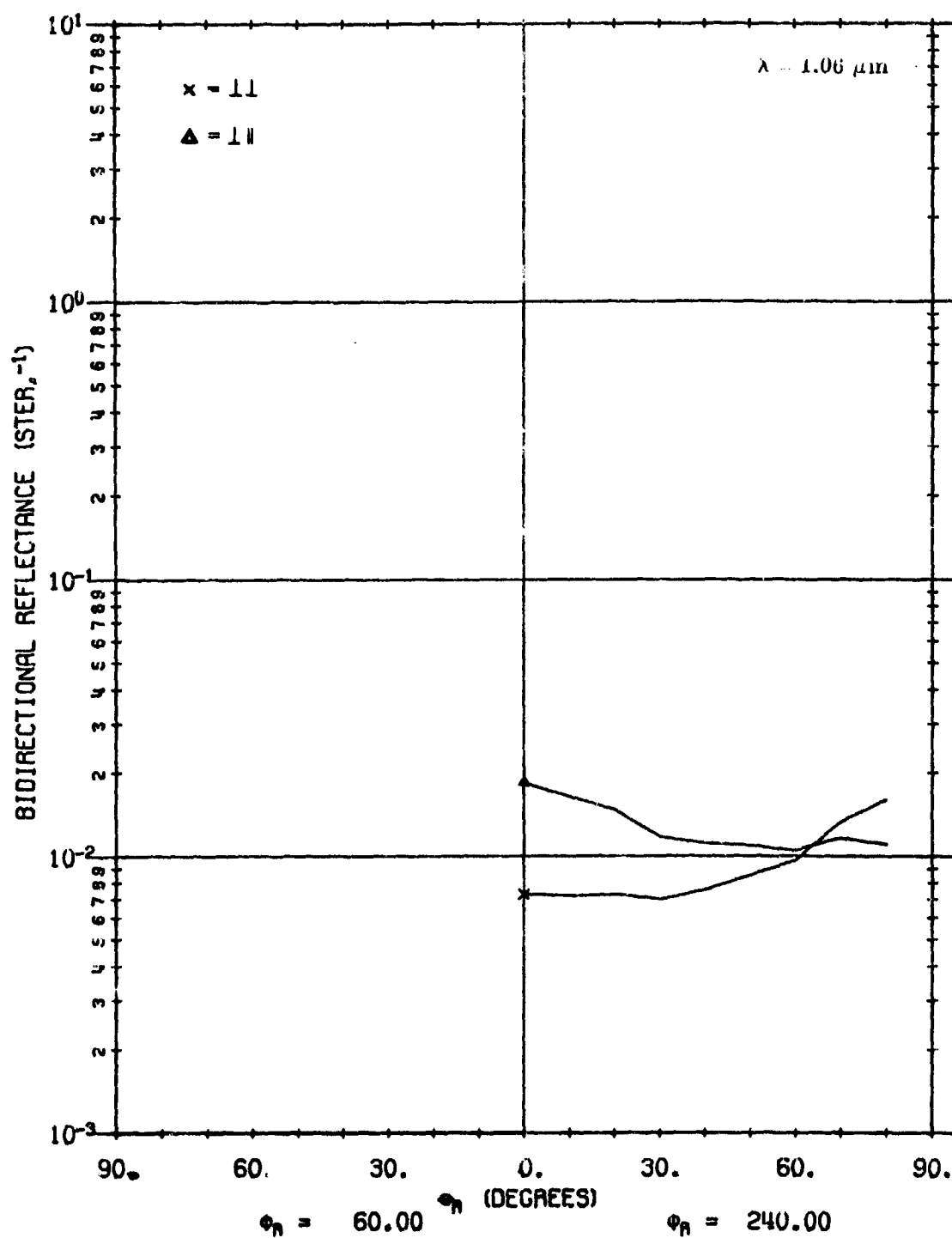


FIGURE 12. CALCULATED ρ' FOR A02018-001 USING NON-LAMBERTIAN VOLUME MODEL WITH SHADOWING AND OBSCURATION FACTOR. $\theta_i = 40^\circ$, $\phi_i = 180^\circ$, $\phi_r = 60^\circ, 240^\circ$.

A02018 001

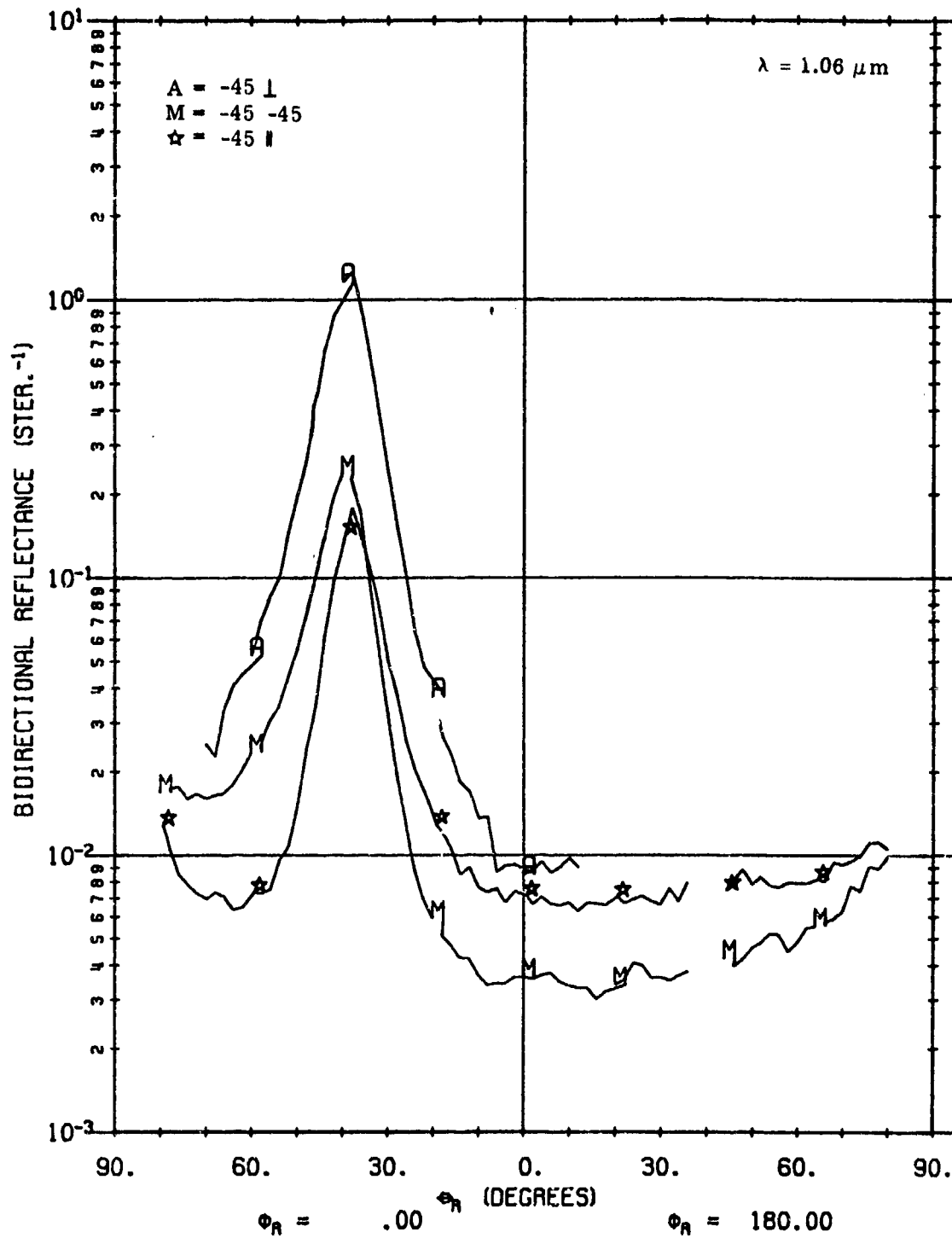


FIGURE 13. MEASURED ρ' FOR A02018-001. $\theta_i = 40^\circ$, $\phi_i = 180^\circ$, $\phi_r = 0^\circ, 180^\circ$.

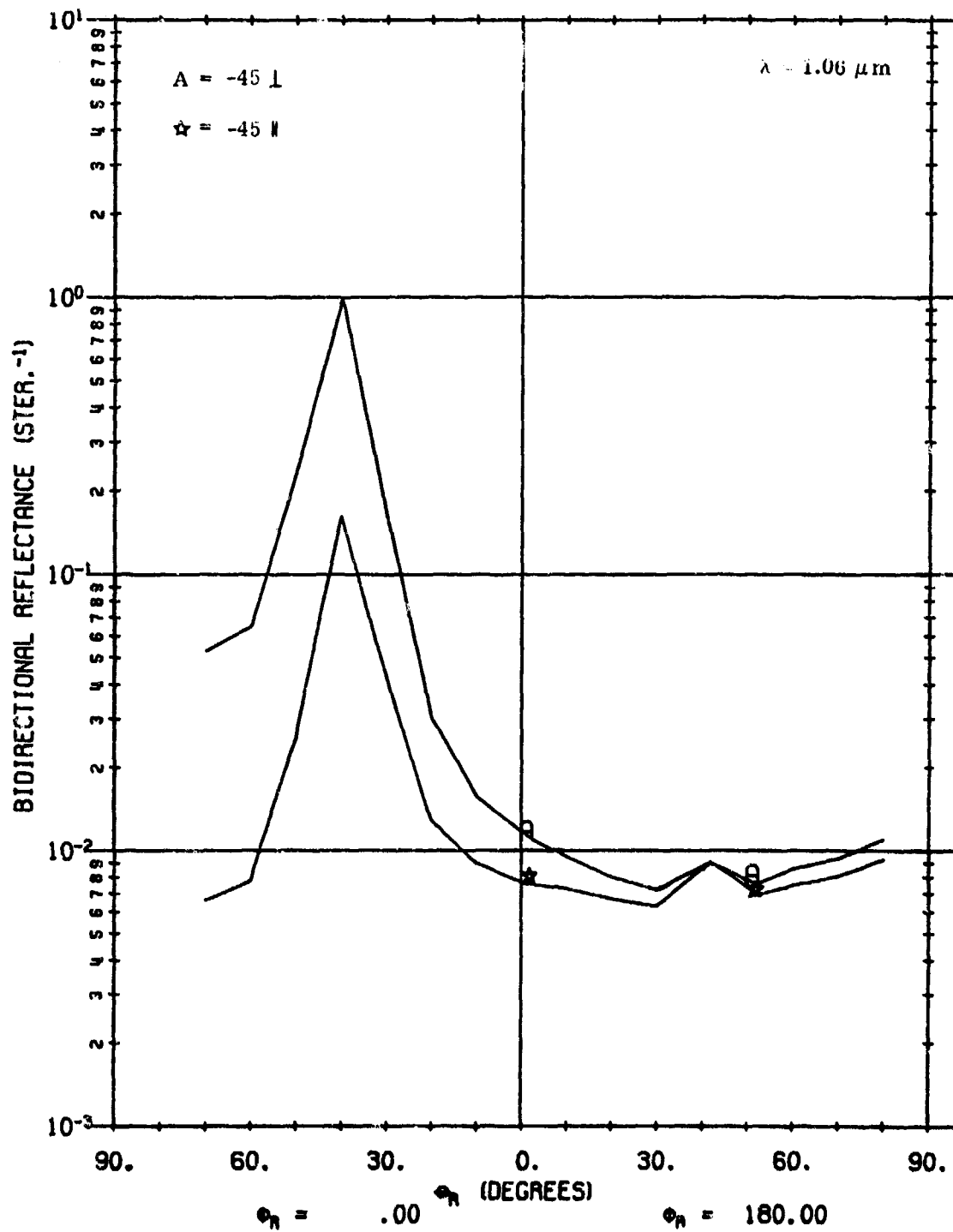


FIGURE 14. CALCULATED ρ' FOR A02018-001 USING NON-LAMBERTIAN VOLUME MODEL
 WITH SHADOWING AND OBSCURATION FACTOR. $\theta_i = 40^\circ$, $\phi_i = 180^\circ$, $\phi_r = 0^\circ, 180^\circ$.

A02018 001

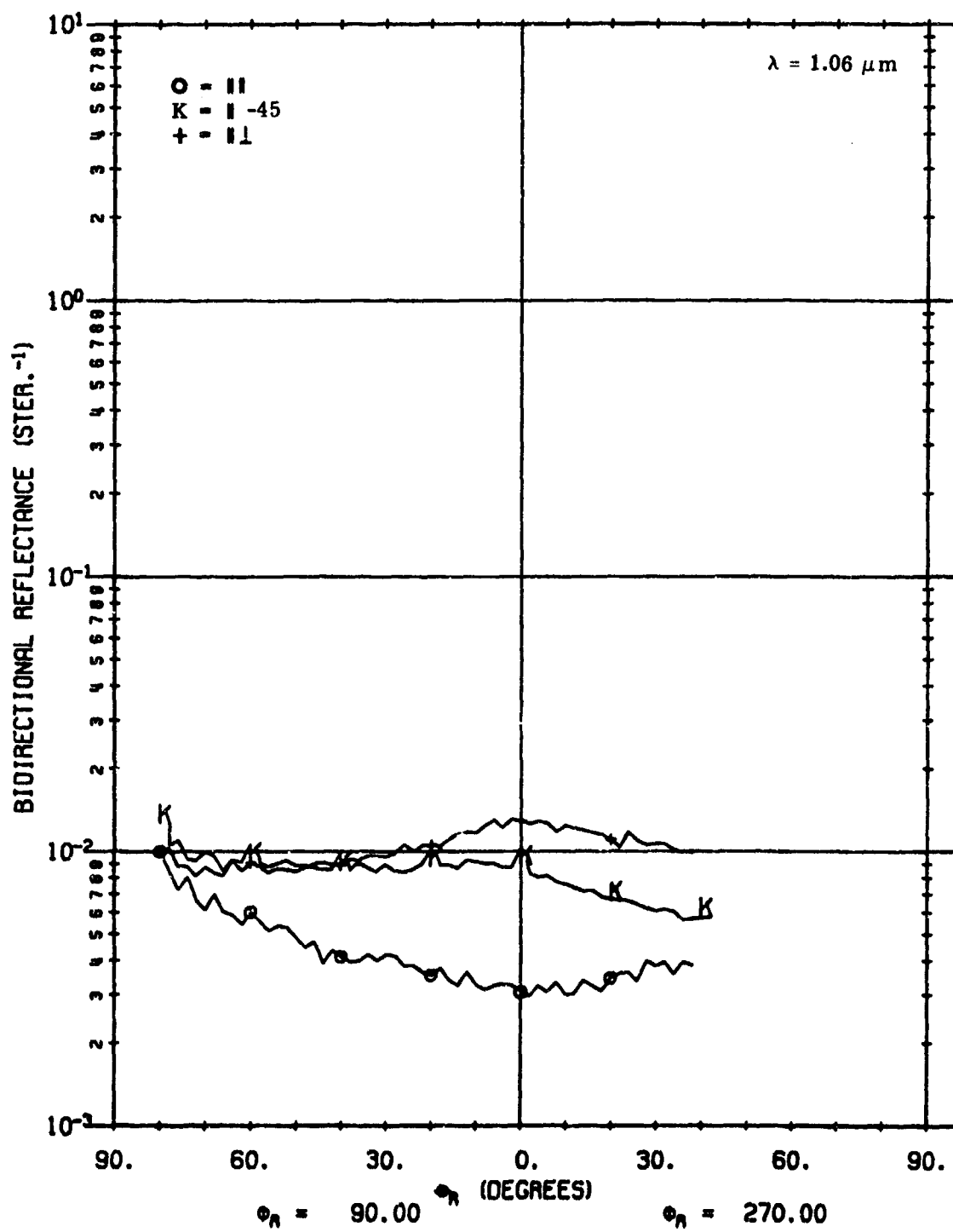


FIGURE 15. MEASURED ρ' FOR A02018-001. $\theta_i = 40^\circ$, $\phi_i = 180^\circ$, $\phi_r = 90^\circ, 270^\circ$.

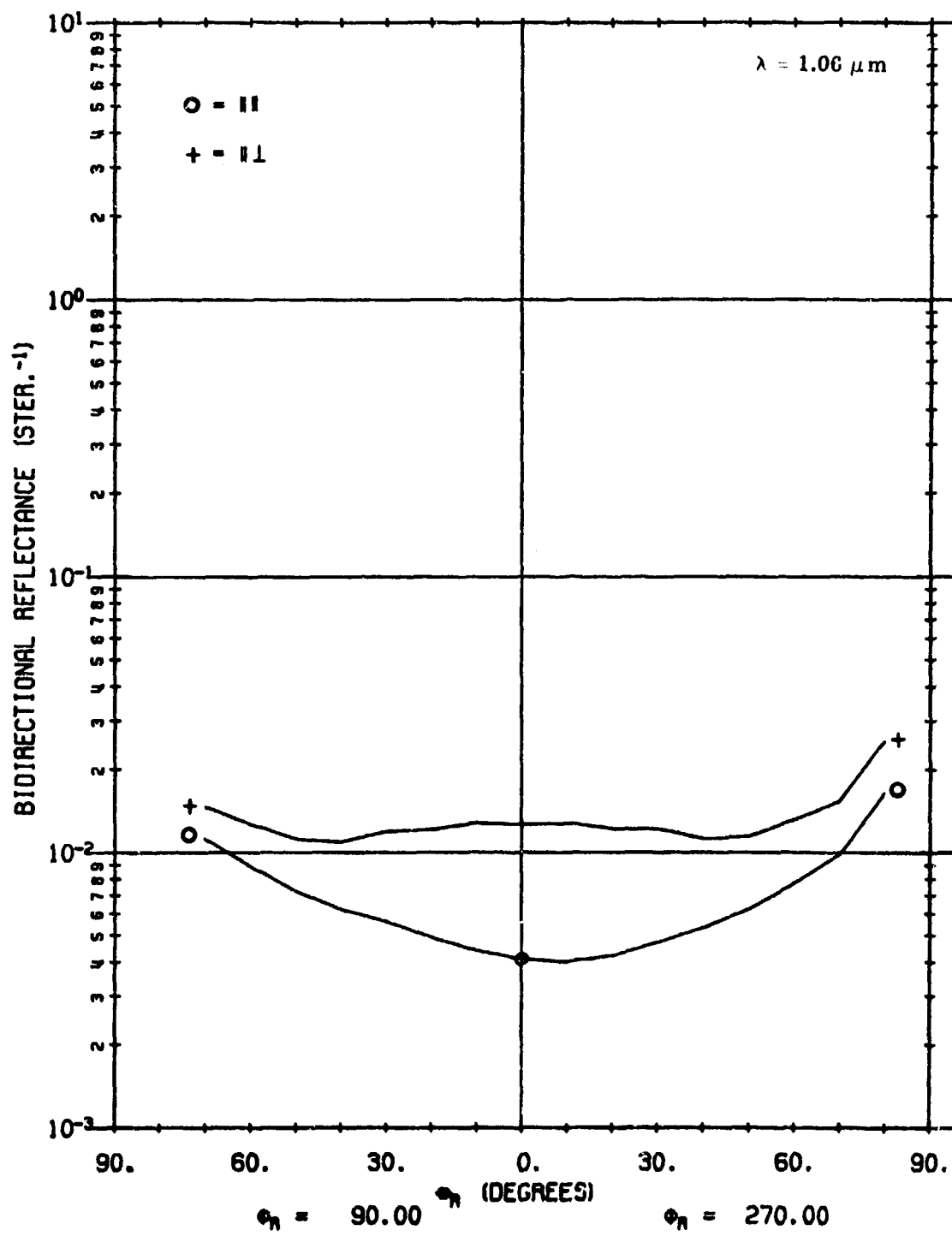


FIGURE 16. CALCULATED ρ' FOR A02018-001 USING NON-LAMBERTIAN VOLUME MODEL WITH SHADOWING AND OBSCURATION FACTOR. $\theta_i = 40^\circ$, $\phi_i = 180^\circ$, $\phi_r = 90^\circ, 270^\circ$.

A02018 001

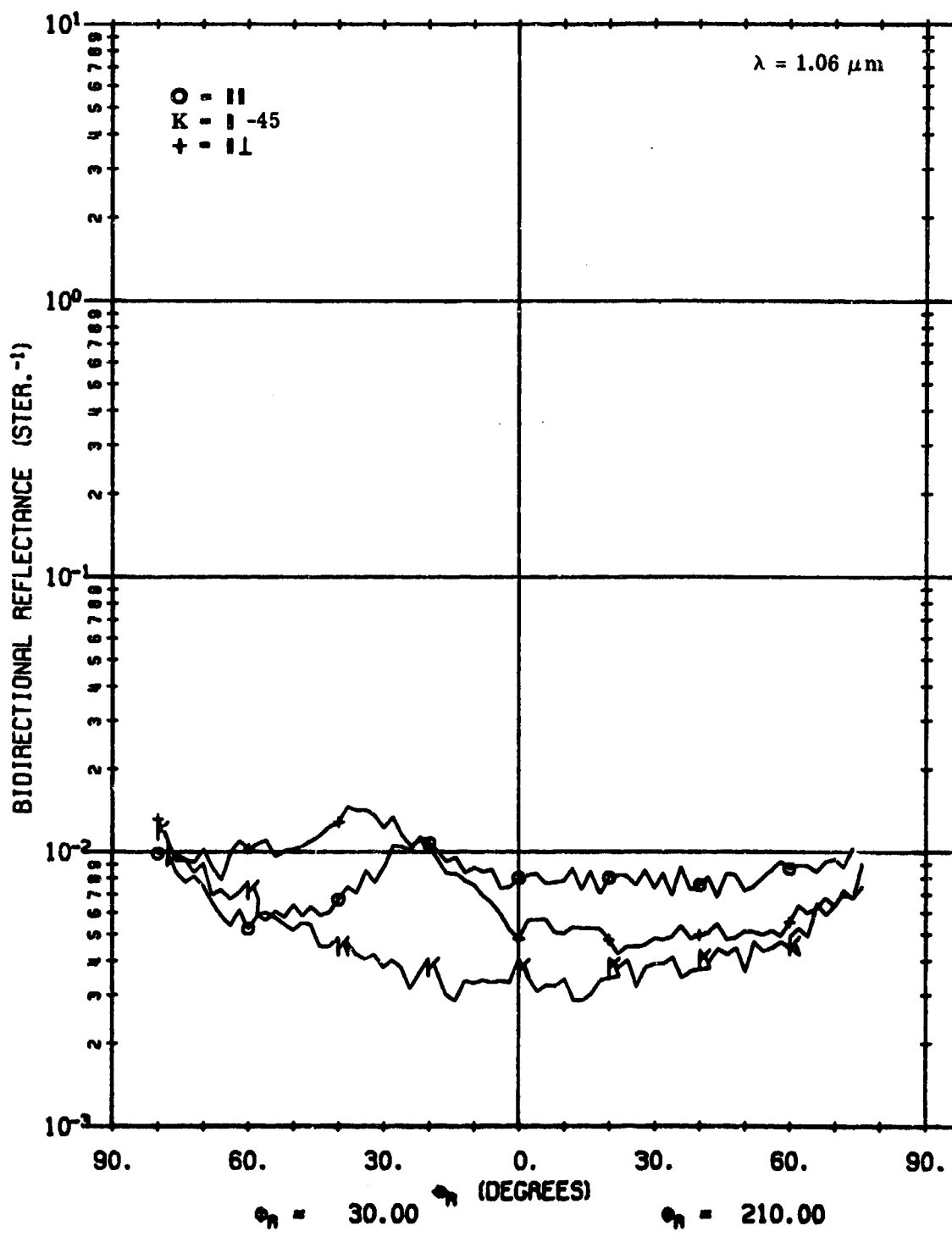


FIGURE 17. MEASURED ρ' FOR A02018-001. $\theta_i = 40^\circ$, $\phi_i = 180^\circ$, $\phi_r = 30, 210^\circ$.

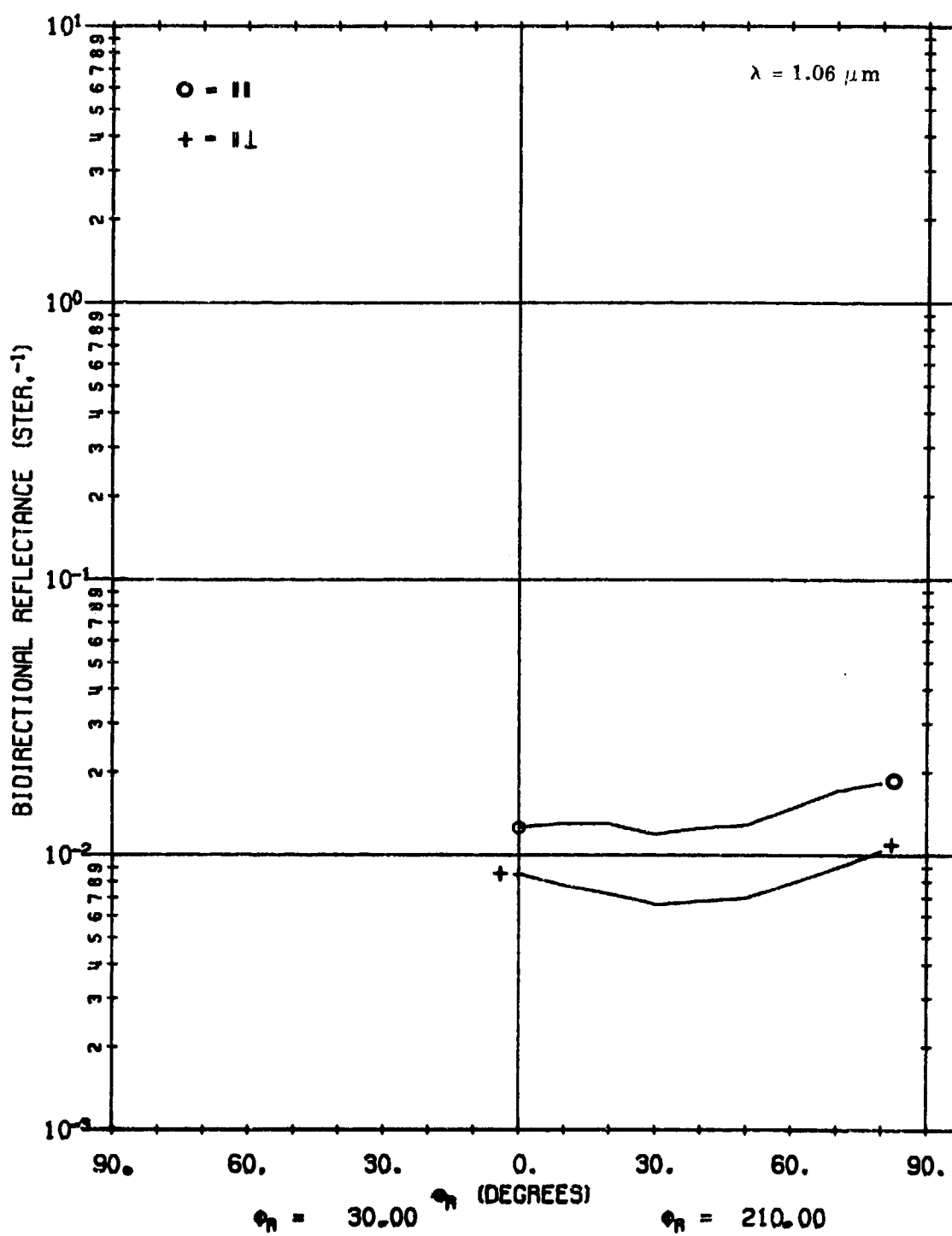


FIGURE 18. CALCULATED ρ' FOR A02018-001 USING NON-LAMBERTIAN VOLUME MODEL WITH SHADOWING AND OBSCURATION FACTOR. $\theta_i = 40^\circ$, $\phi_i = 180^\circ$, $\phi_r = 30^\circ, 210^\circ$.

A02018 001

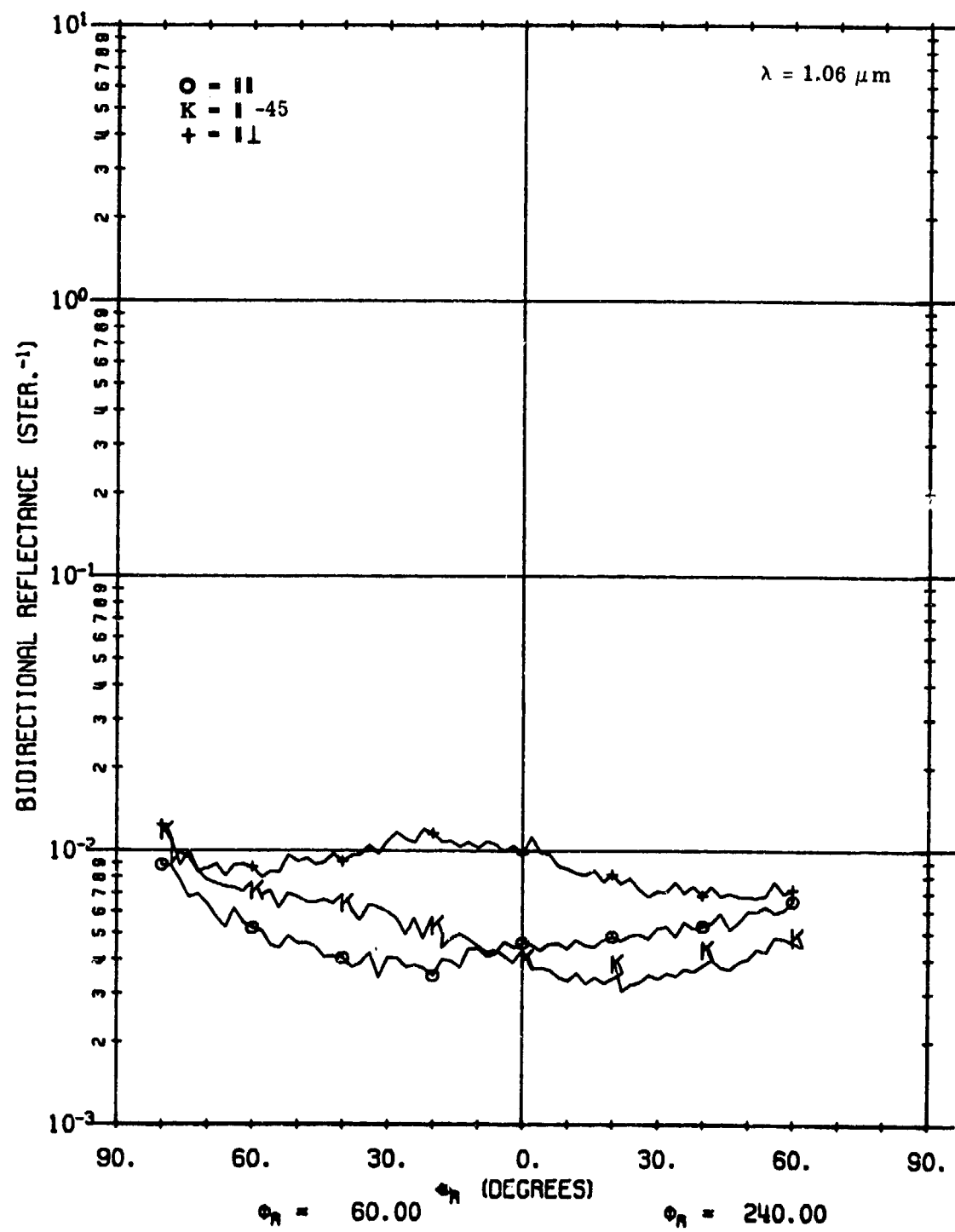


FIGURE 19. MEASURED ρ' FOR A02018-001. $\theta_1 = 40^\circ$, $\phi_1 = 180^\circ$, $\phi_r = 60^\circ, 240^\circ$.

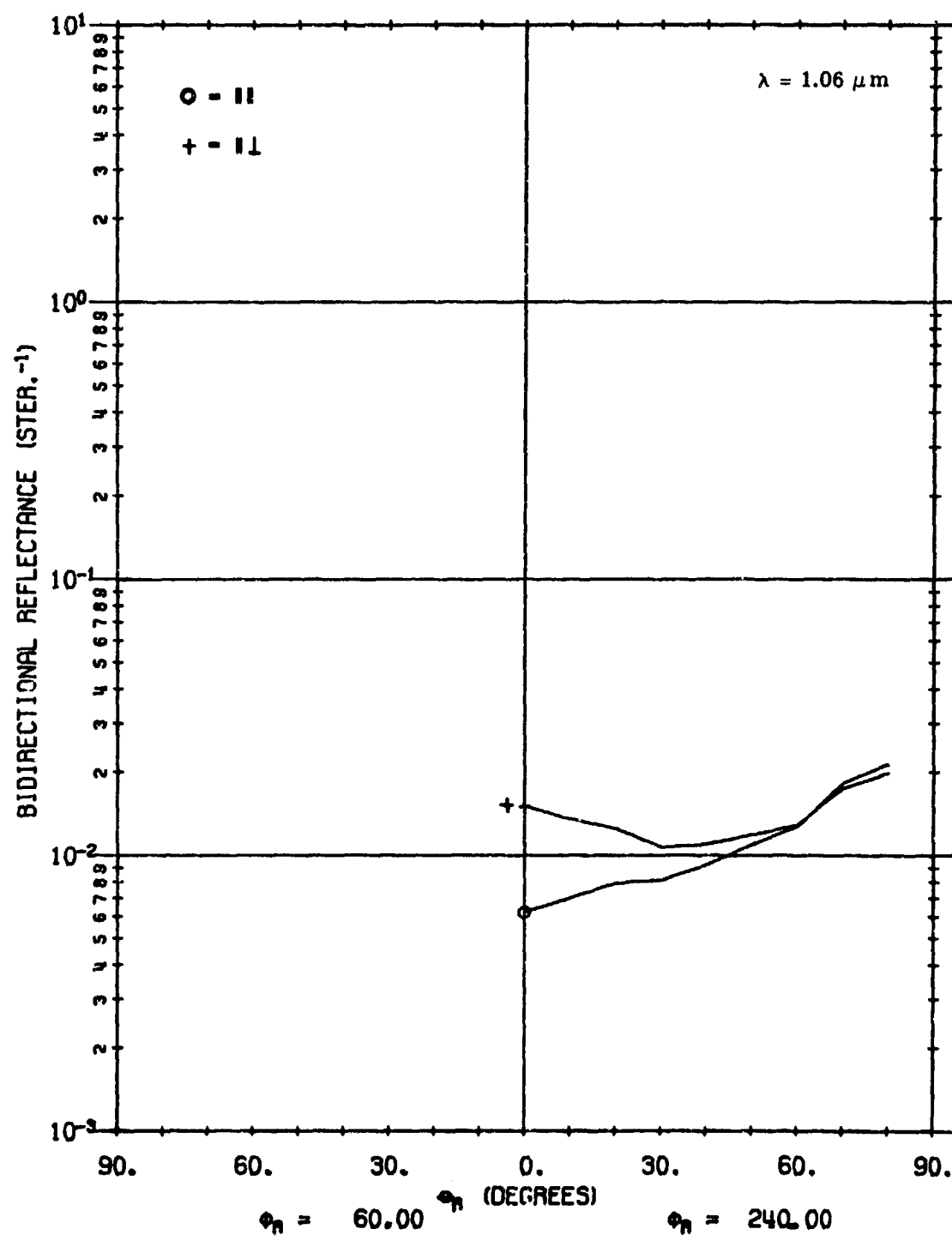


FIGURE 20. CALCULATED ρ' FOR A02018-001 USING NON-LAMBERTIAN VOLUME MODEL WITH SHADOWING AND OBSCURATION FACTOR. $\theta_i = 40^\circ$, $\phi_i = 180^\circ$, $\phi_r = 60^\circ, 240^\circ$.

A02018 002

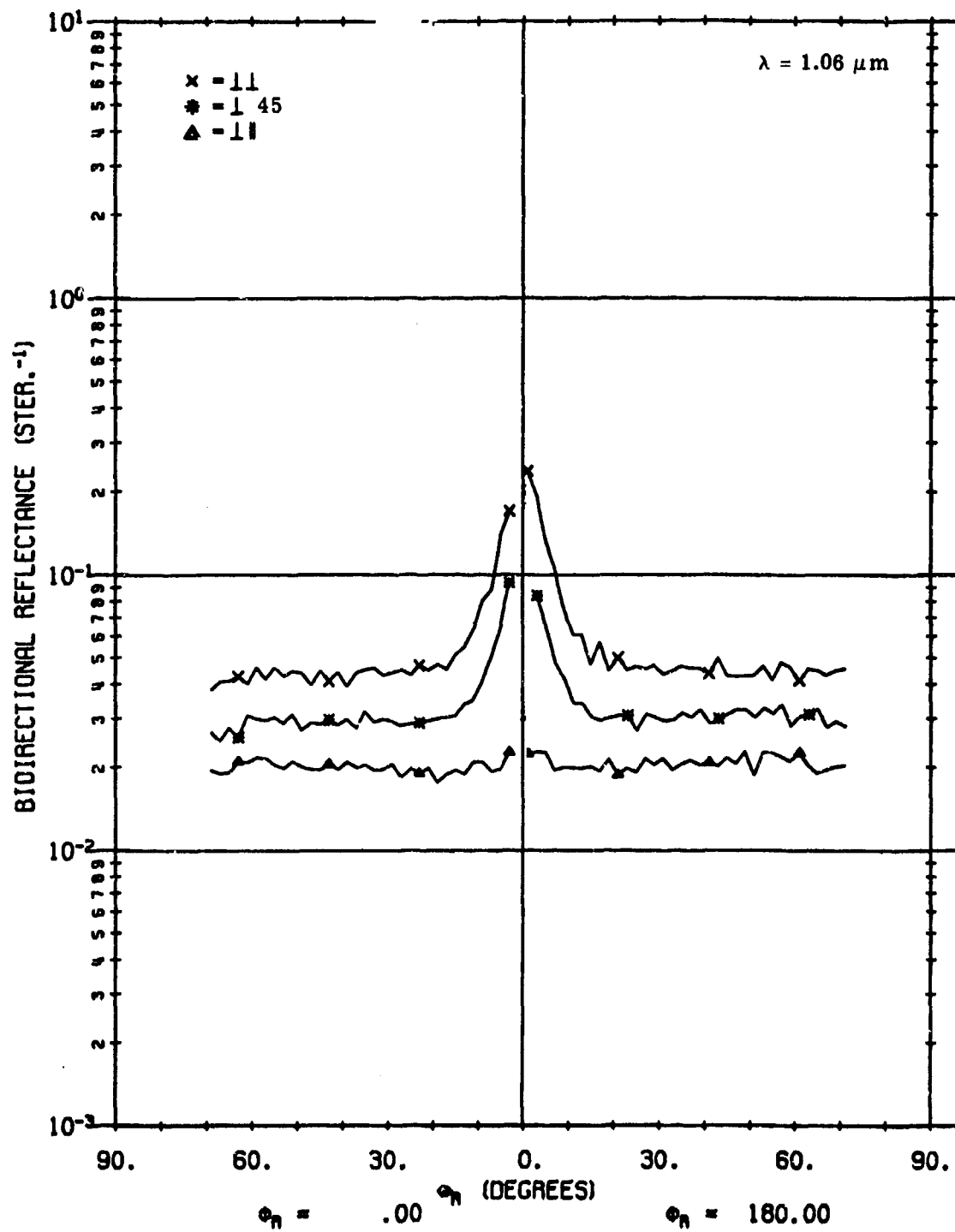


FIGURE 21. FIXED-BISTATIC ρ' FOR A02018-002

A02018 002

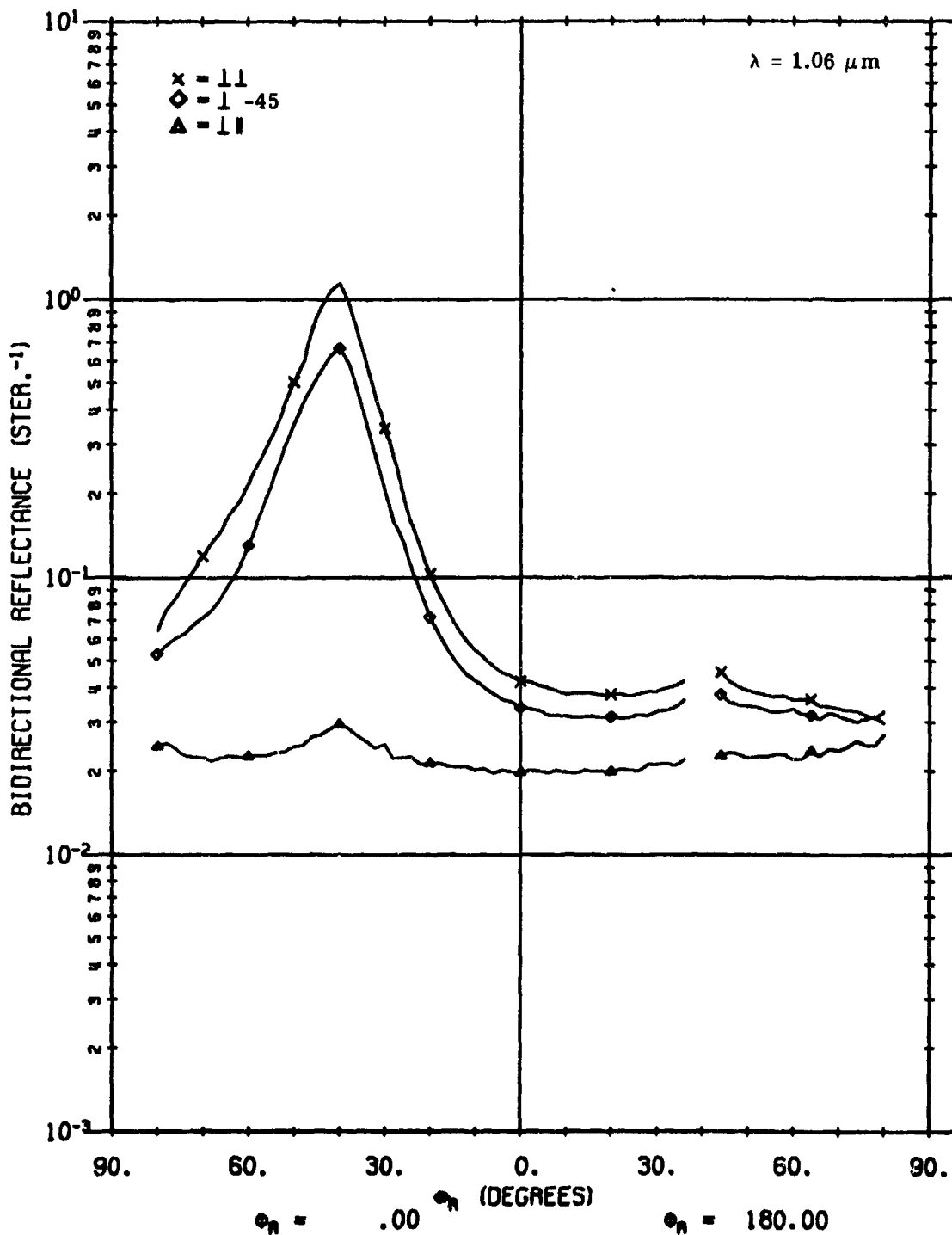


FIGURE 22. MEASURED ρ' FOR A02018-002. $\theta_i = 40^\circ$, $\phi_i = 180^\circ$, $\phi_r = 0^\circ, 180^\circ$.

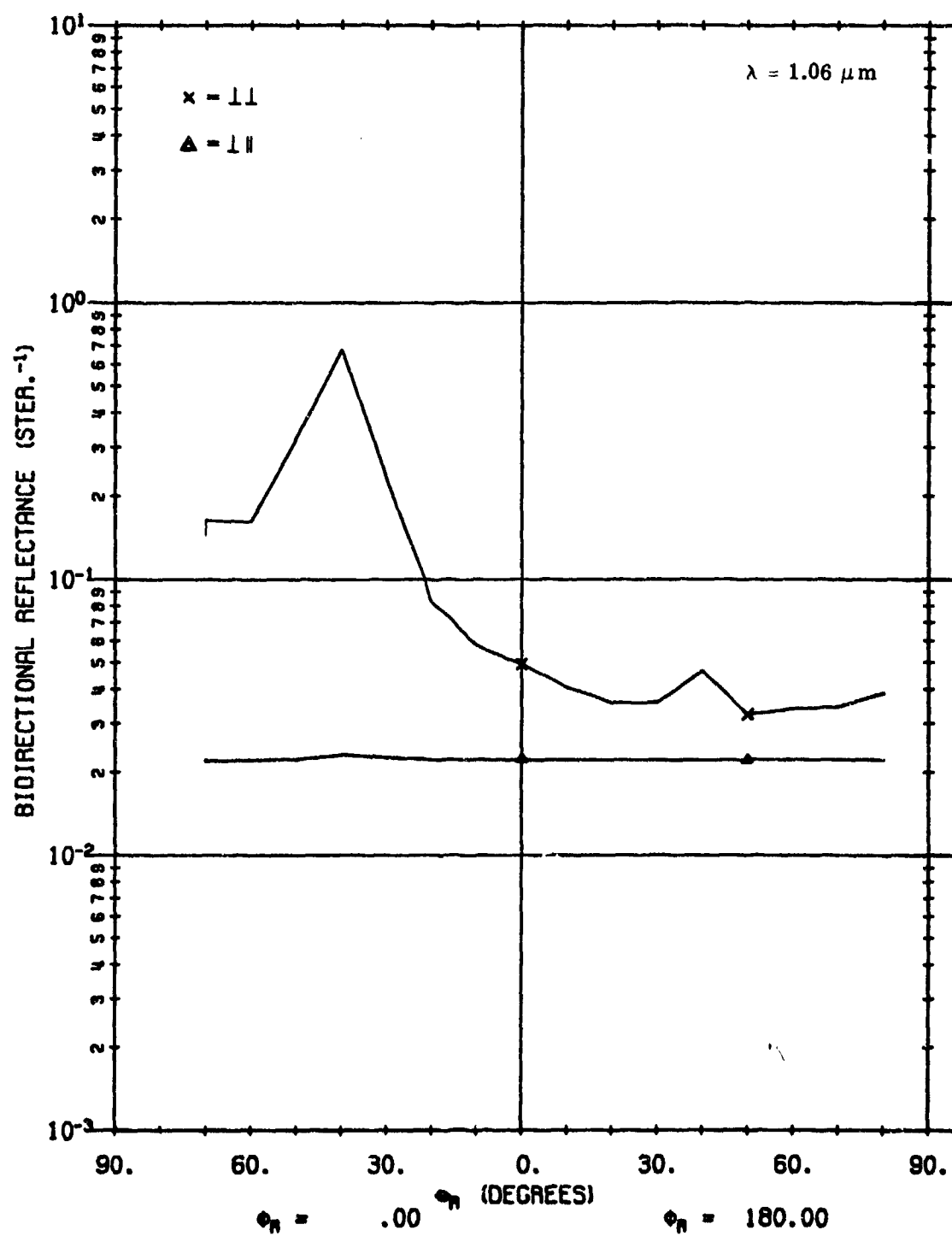


FIGURE 23. CALCULATED ρ' FOR A02018-002 USING LAMBERTIAN VOLUME MODEL.
 $\theta_i = 40^\circ, \phi_i = 180^\circ, \phi_r = 0^\circ, 180^\circ$.

A02018 002

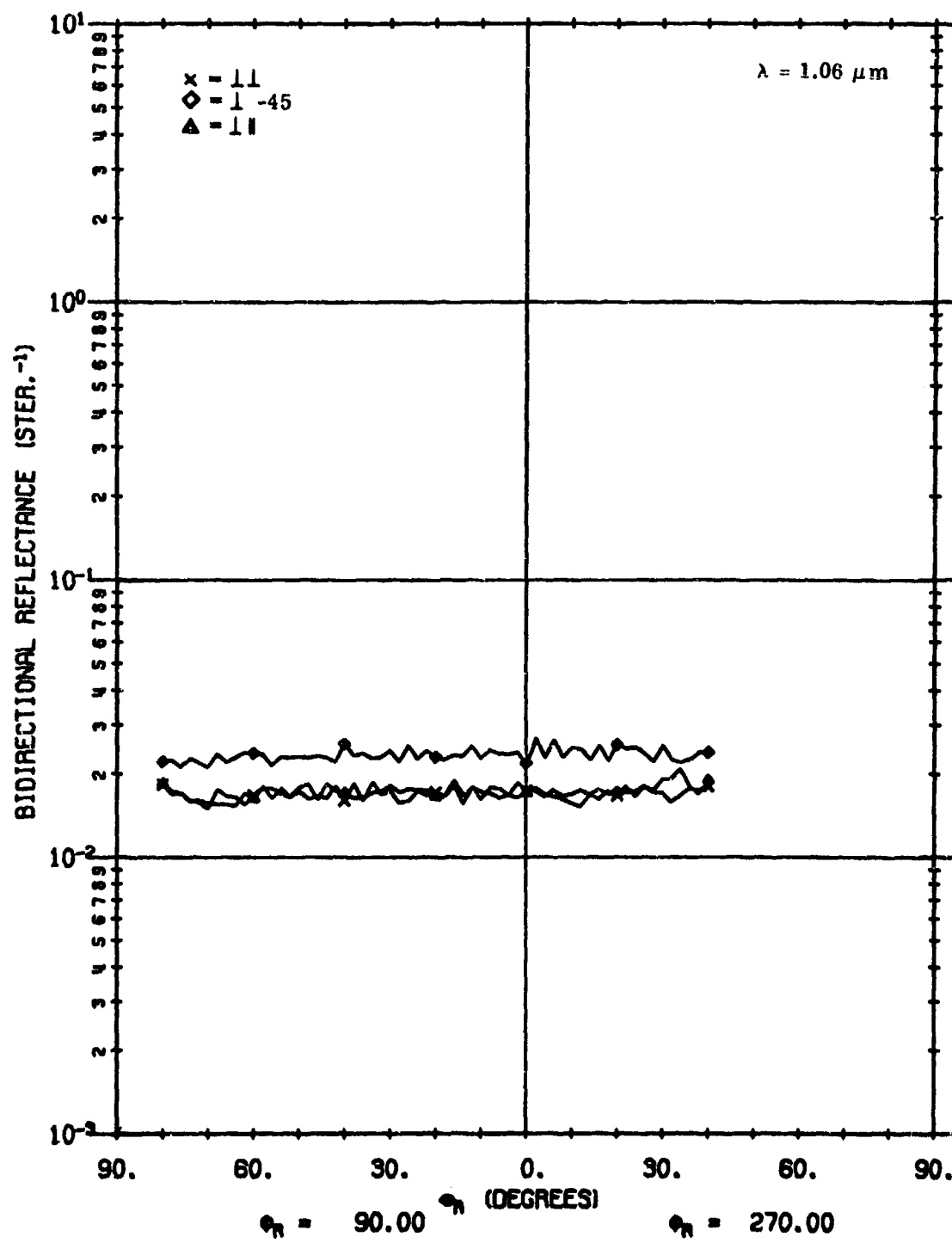


FIGURE 24. MEASURED ρ' FOR A02018-002. $\theta_i = 40^\circ$, $\phi_i = 180^\circ$, $\phi_r = 90^\circ, 270^\circ$.

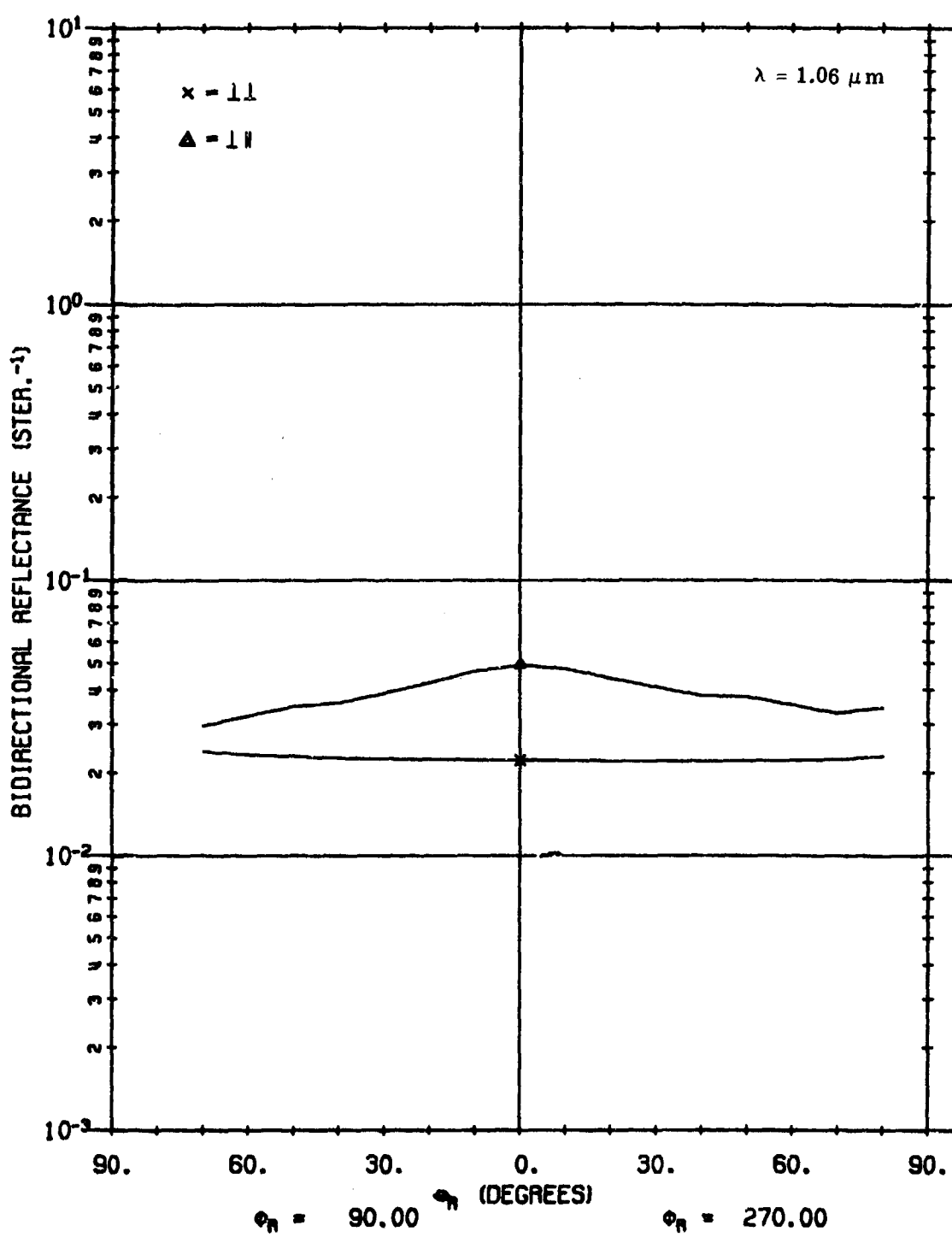


FIGURE 25. CALCULATED ρ' FOR A02018-002 USING LAMBERTIAN VOLUME MODEL.
 $\theta_i = 40^\circ$, $\phi_i = 180^\circ$, $\phi_r = 90^\circ$, 270° .

A02018 002

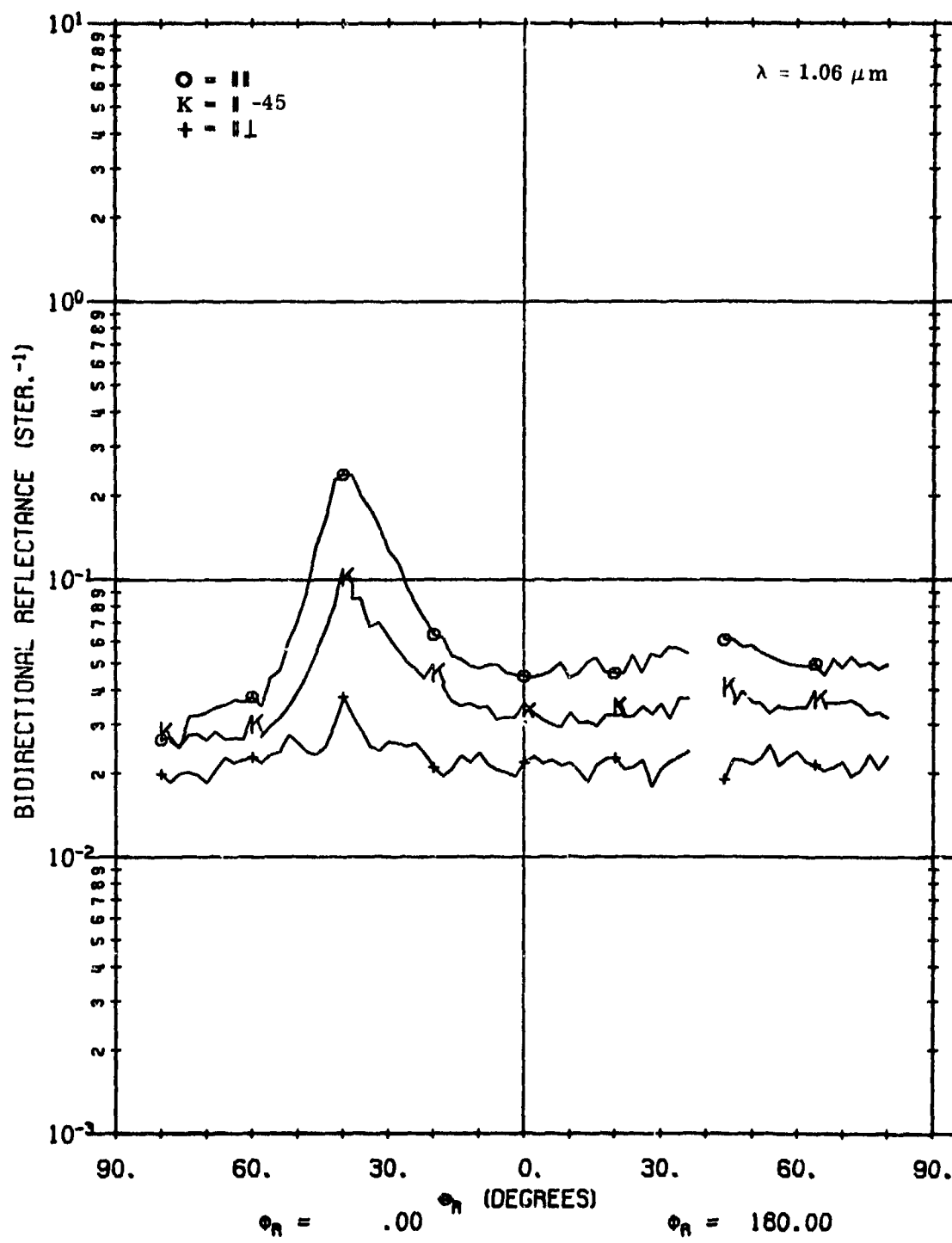


FIGURE 26. MEASURED ρ' FOR A02018-002. $\theta_i = 40^\circ$, $\phi_i = 180^\circ$, $\phi_r = 0^\circ, 180^\circ$.

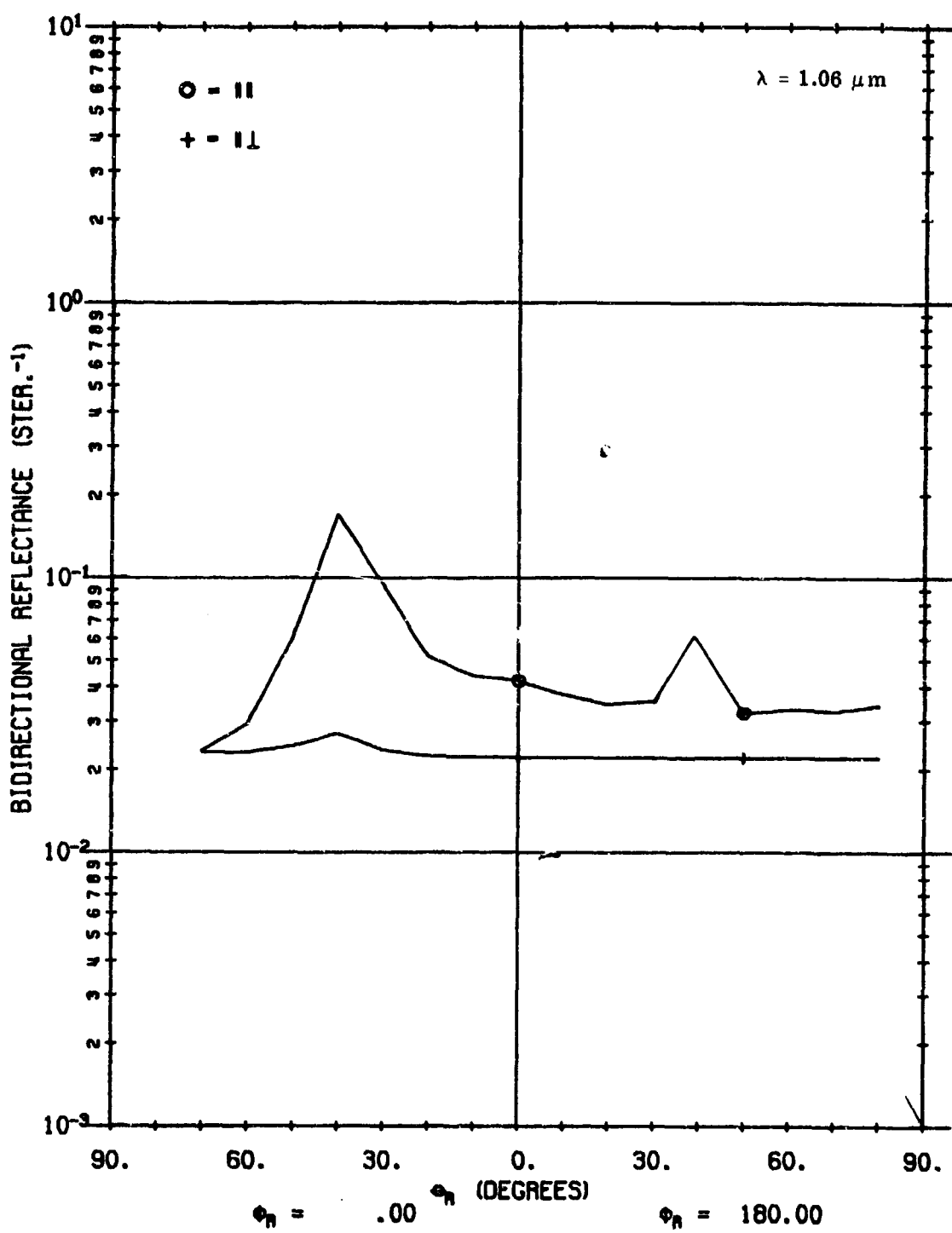


FIGURE 27. CALCULATED ρ' FOR A02018-002. $\theta_i = 40^\circ$, $\phi_i = 180^\circ$, $\phi_r = 0^\circ, 180^\circ$.

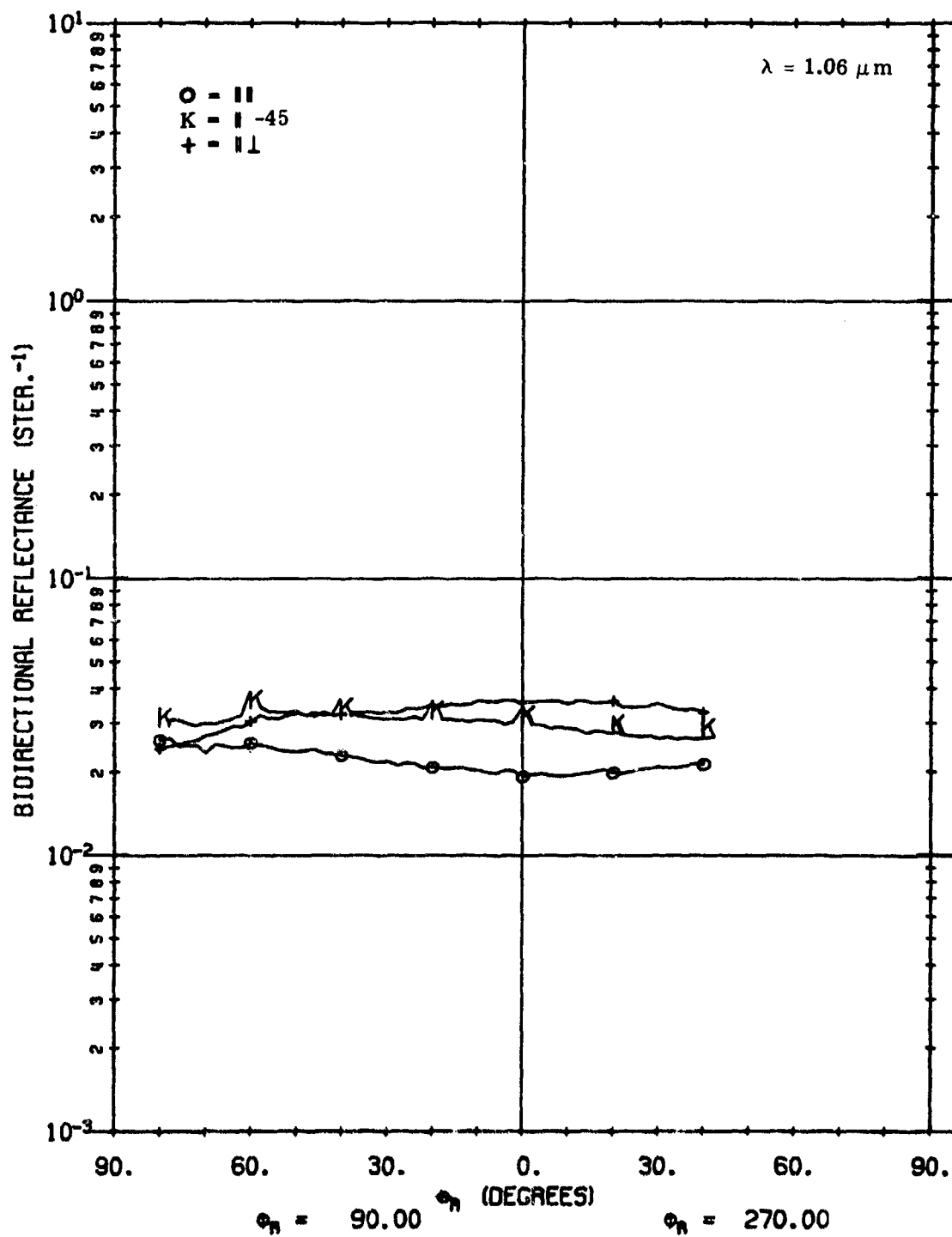


FIGURE 28. MEASURED ρ' FOR A02018-002. $\theta_i = 40^\circ$, $\phi_i = 180^\circ$, $\phi_r = 90^\circ, 270^\circ$.

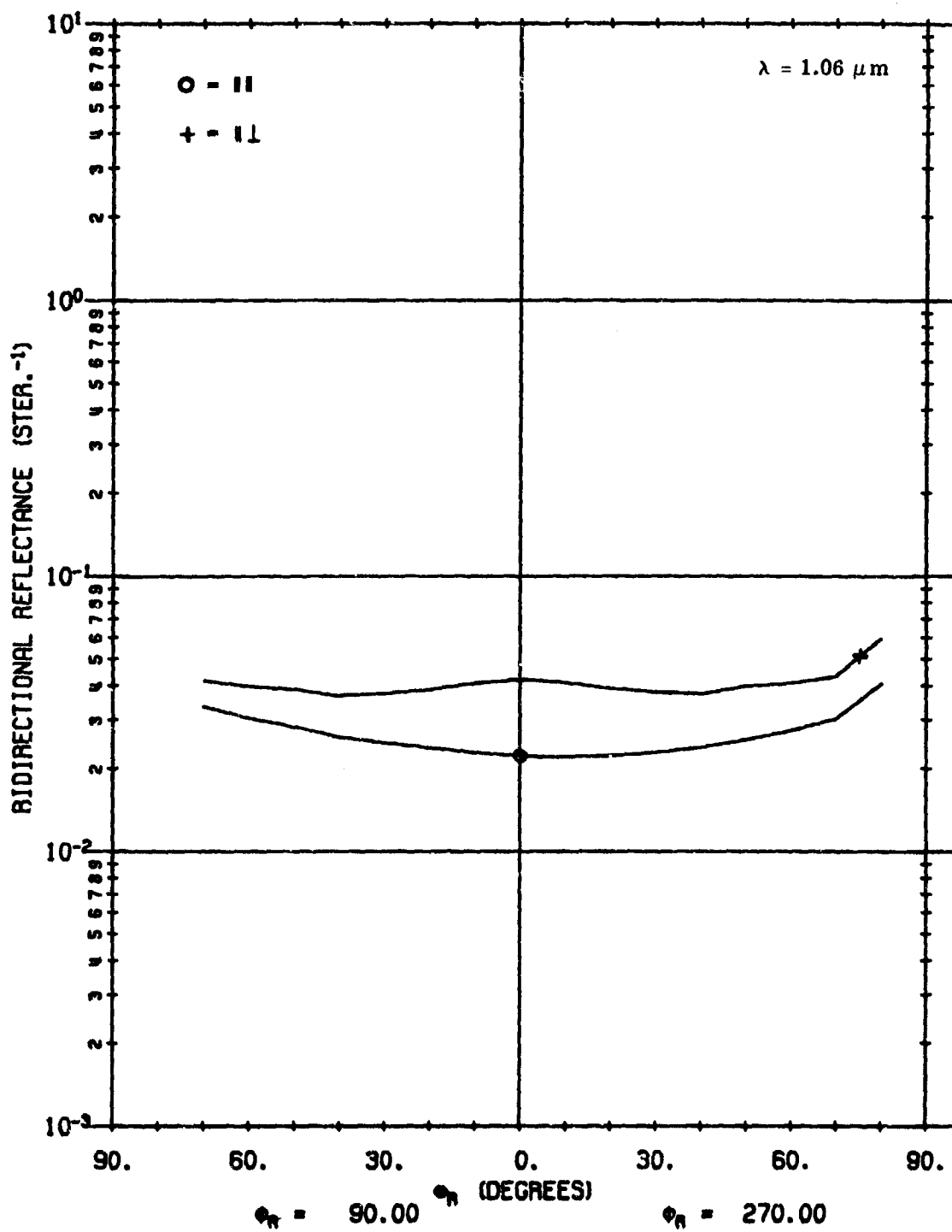


FIGURE 29. CALCULATED ρ' FOR A02018-002 USING LAMBERTIAN VOLUME MODEL.
 $\theta_i = 40^\circ$, $\phi_i = 180^\circ$, $\phi_r = 90^\circ, 270^\circ$.

covered in this report, the variation is considered to be zero. Therefore, for these surfaces, polarization angle is essentially a function only of source-receiver positions.

As additional validation for the model, predicted polarization angles are compared with polarization angles extracted from the measured data. Figures 30 through 33 show plots obtained for the 0° , 180° ; 90° , 270° ; 30° , 210° ; and 60° , 240° azimuth planes. Measured data represent material A02018-001. In all cases, agreement between measurements and calculations is excellent, with the average disparity not more than 10%. In particular, the dramatic agreement between measurements and model in the 30° , 210° and 60° , 240° azimuth planes constitutes powerful verification of the model and affirms its usefulness in arbitrary source-receiver positions.

6.4. PERCENT POLARIZATION FOR SAMPLE MATERIALS A02018-001 AND A02018-002

Percent polarization (P) validates the ratio of surface-to-volume contributions to reflectance. Percent polarization depends on both polarized reflectance and angle of polarization, both validated in earlier sections of this report. In this section, we compare model predictions with percent polarization values extracted from measured data.

Figures 34 and 35 illustrate degree of polarization for scans of material A02018-002, for perpendicular and parallel sources, respectively. The validity of the model is supported by the close correlation between the behavior of values extracted from measured data and those calculated with the model.

Additional confirmation of the model is provided in Figs. 36 through 38 where percent polarization plots are given for material A02018-001 in the 0° , 180° and 90° , 270° azimuth angle planes.

6.5. REFLECTANCE FOR SAMPLE MATERIAL A02100

Here the material was a soil specimen. The fixed-bistatic scan (see Fig. 39) indicates a strong angular dependence in both the like-polarized and the cross-polarized components and no specularity. Moreover, the angular dependence in the fixed-bistatic scan looks very much like the $\frac{1}{\cos \theta_i + \cos \theta_r}$ dependence in the non-Lambertian volume model. However, in the θ_r scans with θ_i held fixed, the angular dependence is no longer typical (see Figs. 40, 43, and 46).

Since there is no apparent specularity in the measurement data, the model was run so as to consider only Lambertian or non-Lambertian components, with no specular component. Our validation was done with a perpendicular-polarized source for $\theta_i = 0^\circ$, 20° , and 40° , respectively, and θ_r scanned in-plane. For each θ_i , the measurement graph is given first, followed by the graphs of the non-Lambertian model and the Lambertian model. Note that in selecting ρ_x value for the Lambertian model, we must take an average of the cross-polarized part of the fixed-bistatic. Therefore, this value is slightly higher than the ρ_y used in the non-Lambertian model. (Section 7 describes how to select parameters.)

For the $\theta_i = 0^\circ$ case, note that the measured data (see Fig. 40) lacks the characteristic angular dependence of the non-Lambertian model (see Fig. 41)—in fact, the graph falls off below the Lambertian graph (see Fig. 42).

For the $\theta_i = 20^\circ$ case, the measured data (see Fig. 43) shows an upturn at higher θ_r values, which is more consistent with the non-Lambertian model. In fact, the non-Lambertian model prediction (see Fig. 44) shows much closer agreement than in the $\theta_i = 0^\circ$ case. The Lambertian calculation (see Fig. 45) once again appears to be taking a rough average. The situation for $\theta_i = 40^\circ$ (see Figs. 46–48) is very similar to that for $\theta_i = 20^\circ$.

Behavior of the fixed-bistatic measurement data indicates that the non-Lambertian component should dominate. However, at small values of θ_i the accuracy is not good. It is not absolutely clear where the difficulty lies. One should note, however, that we took the depolarization to be identically equal to 1. Further modeling to determine the depolarization dependence more accurately may well resolve the problem.

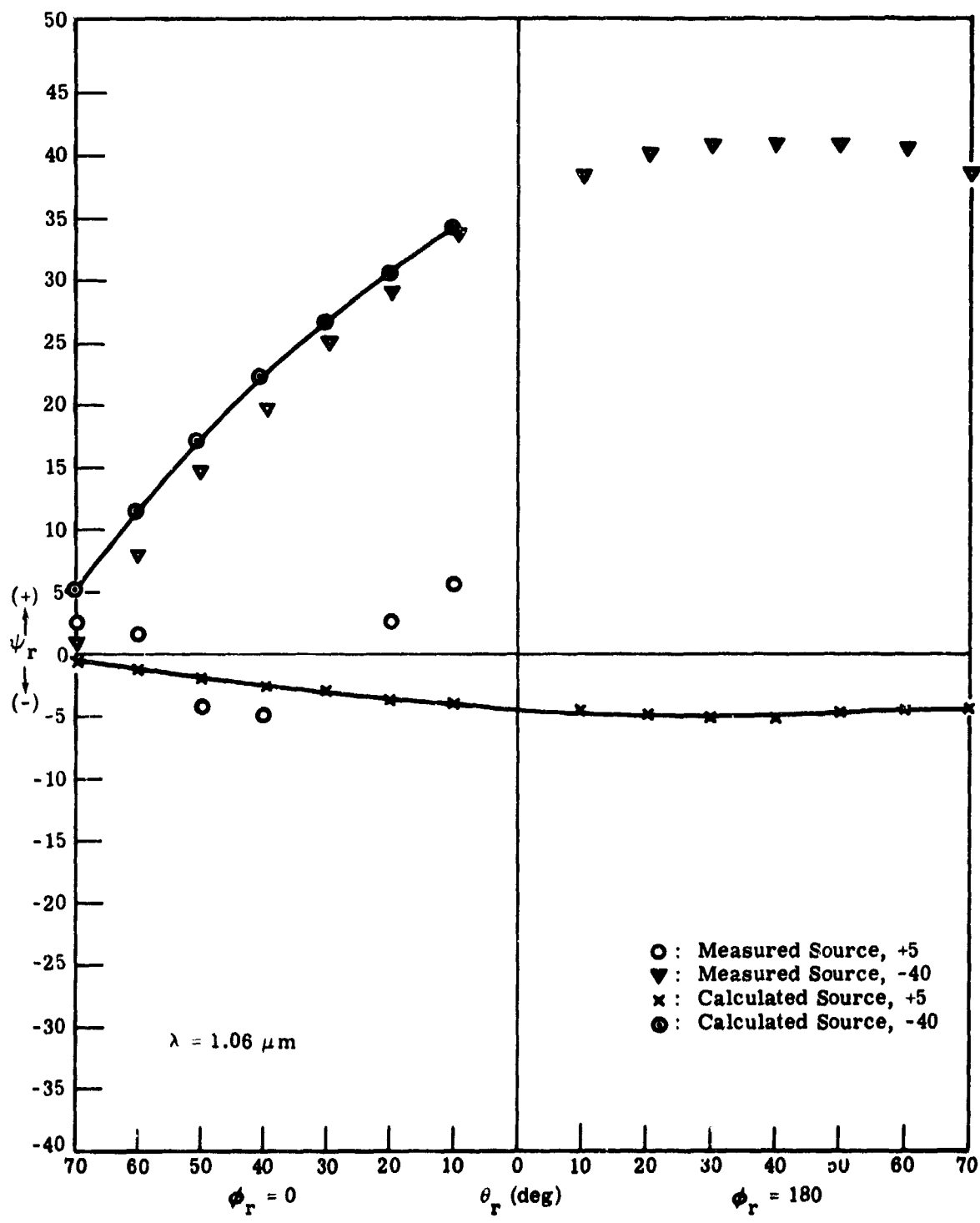


FIGURE 30. VARIATION OF POLARIZATION ANGLE OF REFLECTED RADIANCE AS FUNCTION OF SOURCE-RECEIVER POSITION. $\theta_i = 40^\circ$, $\phi_i = 180^\circ$, $\phi_r = 0^\circ, 180^\circ$.

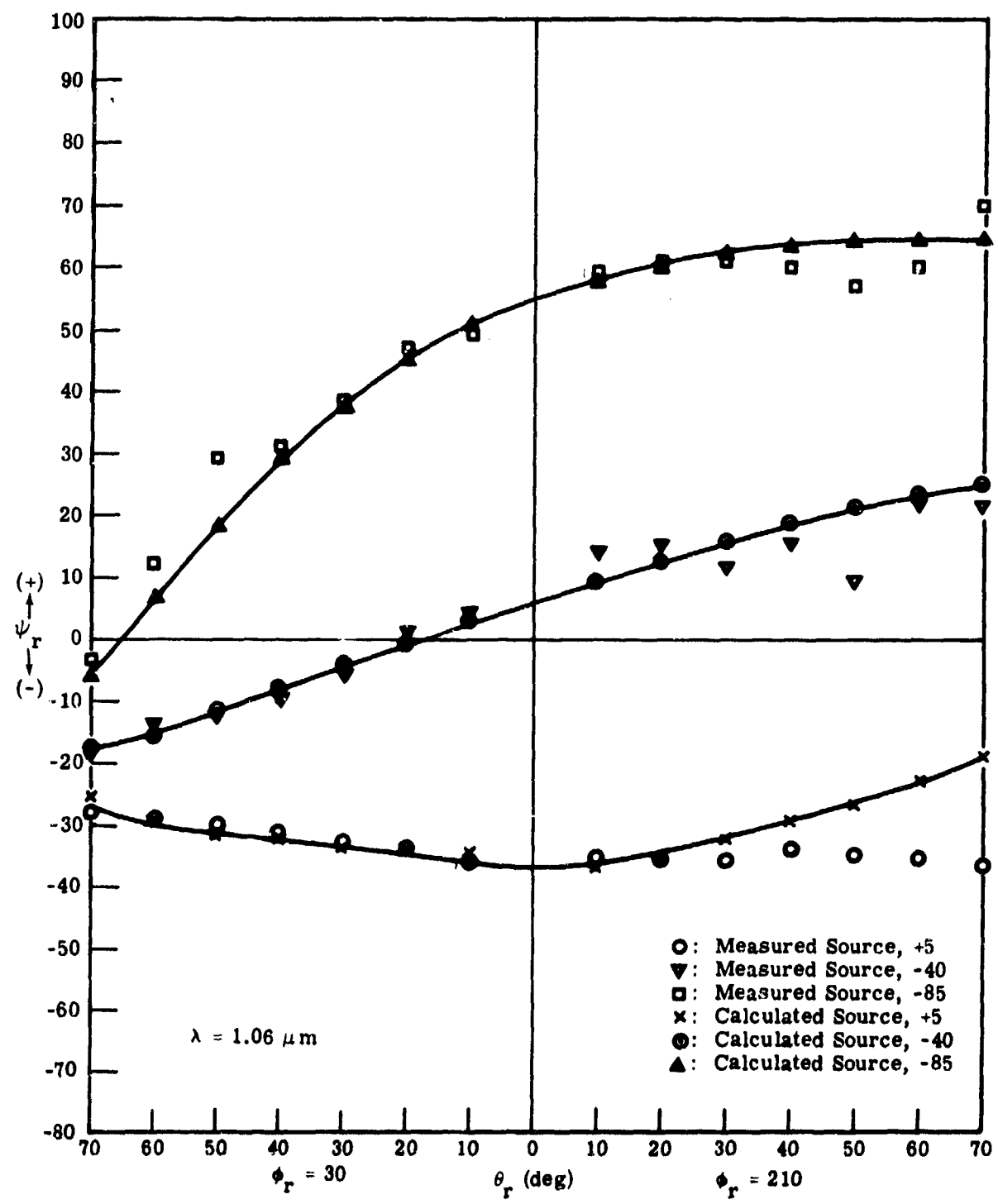


FIGURE 31. VARIATION OF POLARIZATION ANGLE OF REFLECTED RADIANCE AS FUNCTION OF SOURCE-RECEIVER POSITION. $\theta_i = 40^\circ$, $\beta_i = 180^\circ$, $\phi_r = 30^\circ, 210^\circ$.

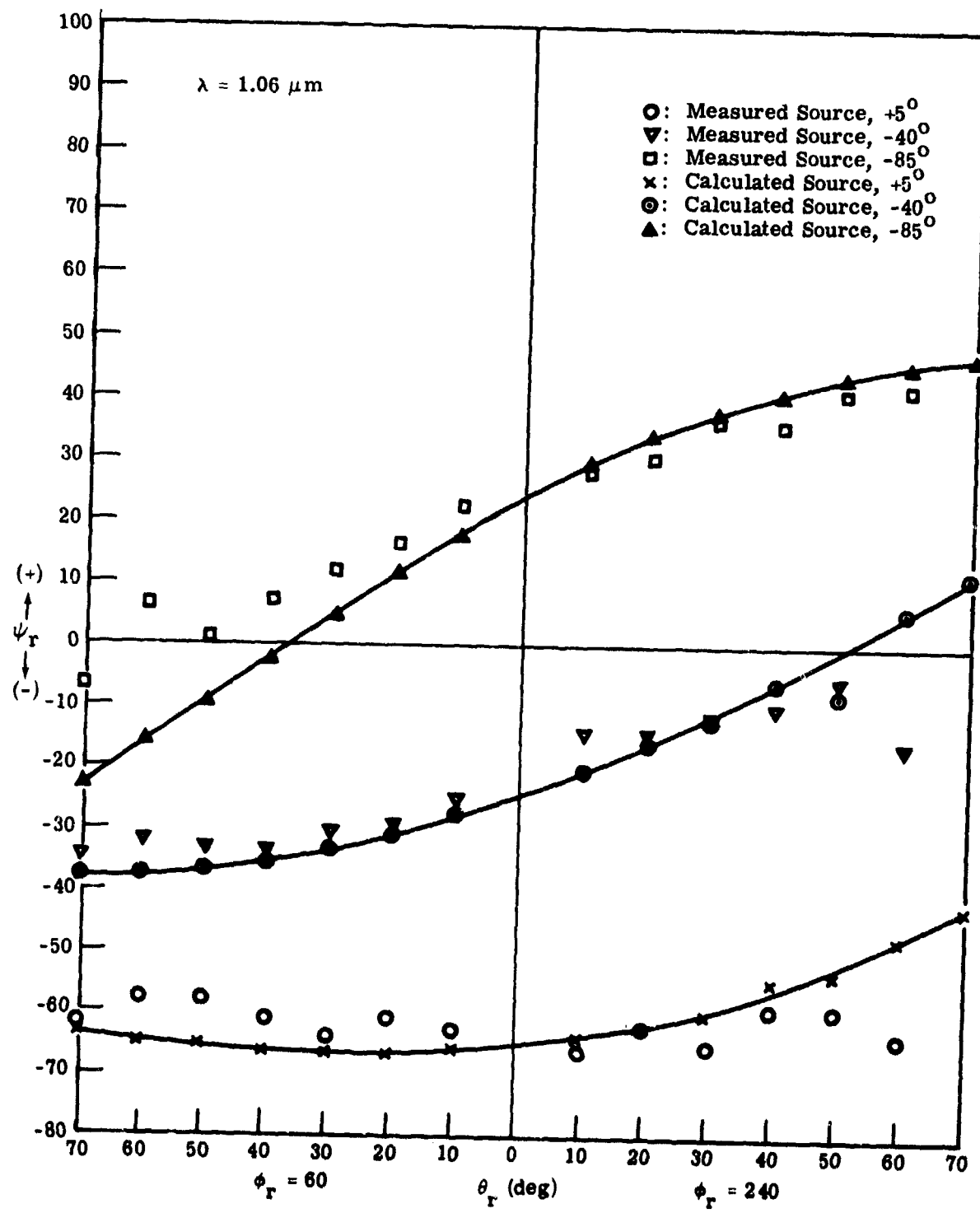


FIGURE 32. VARIATION OF POLARIZATION ANGLE OF REFLECTED RADIANCE AS FUNCTION OF SOURCE-RECEIVER POSITION. $\theta_1 = 40^\circ$, $\phi_1 = 180^\circ$, $\phi_r = 60^\circ, 240^\circ$.

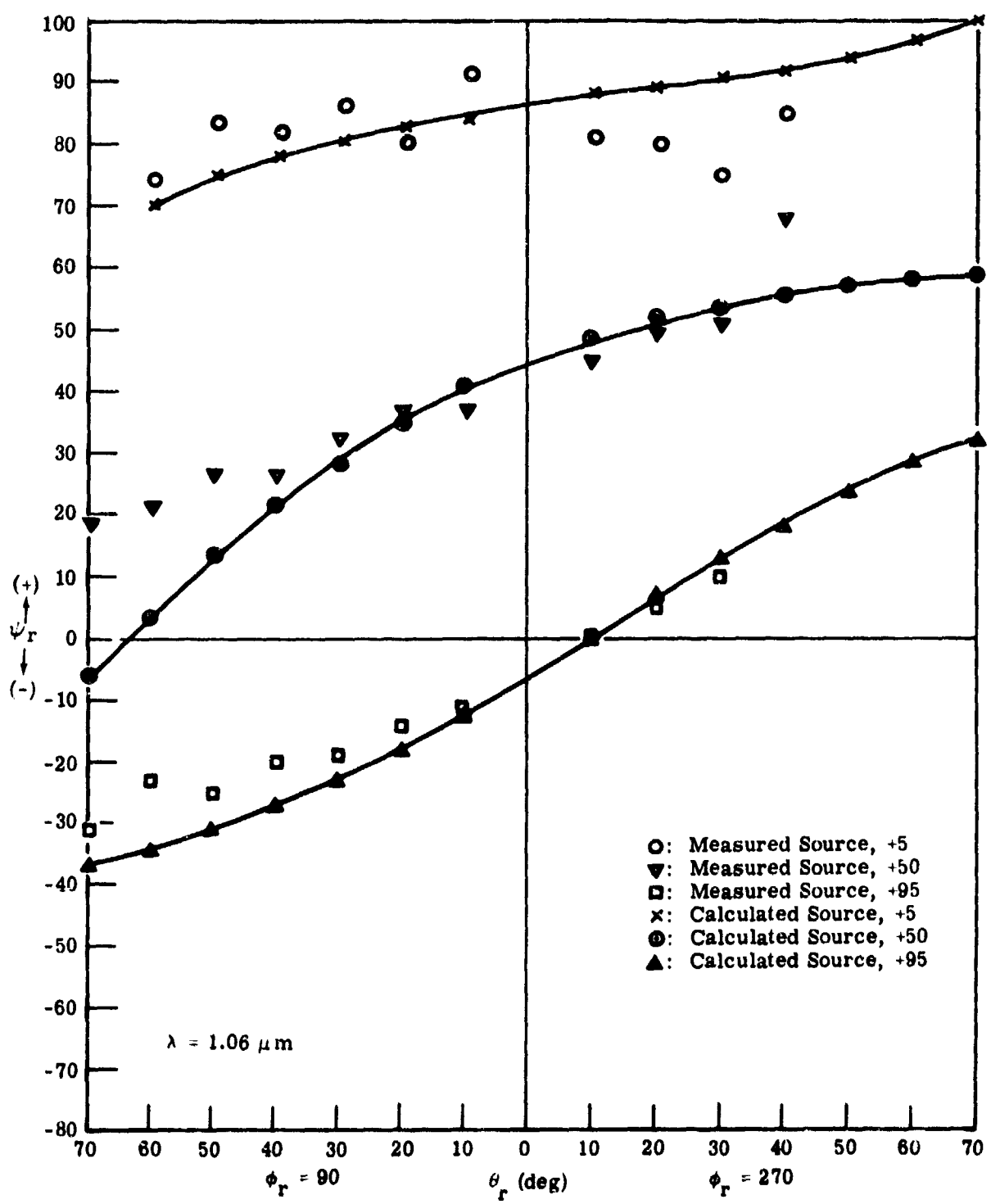


FIGURE 33. VARIATION OF POLARIZATION ANGLE OF REFLECTED RADIANCE AS FUNCTION OF SOURCE-RECEIVER POSITION. $\theta_1 = 40^\circ$, $\phi_1 = 180^\circ$, $\phi_r = 90^\circ, 270^\circ$.

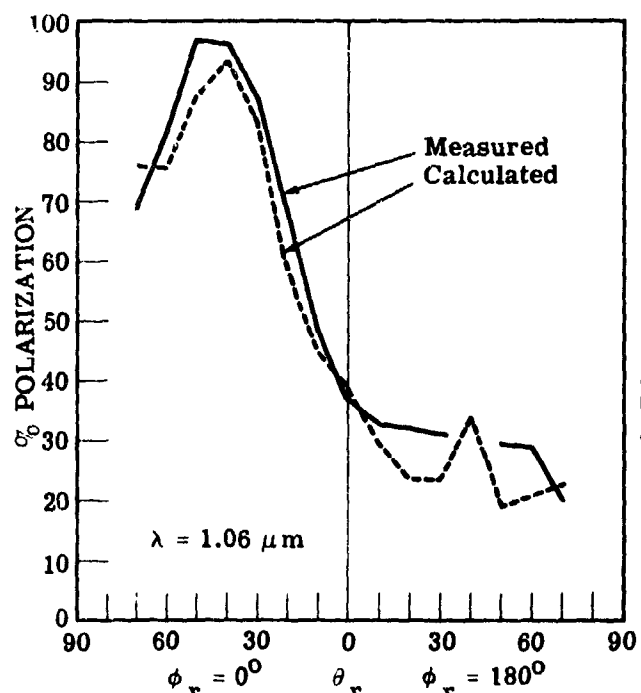


FIGURE 34. PERCENT POLARIZATION VARIATION FOR A02018-002 AS FUNCTION OF SOURCE-RECEIVER POSITION.
 $\theta_i = 40^\circ$, $\phi_i = 180^\circ$, $\phi_r = 0^\circ, 180^\circ$; perpendicular source.

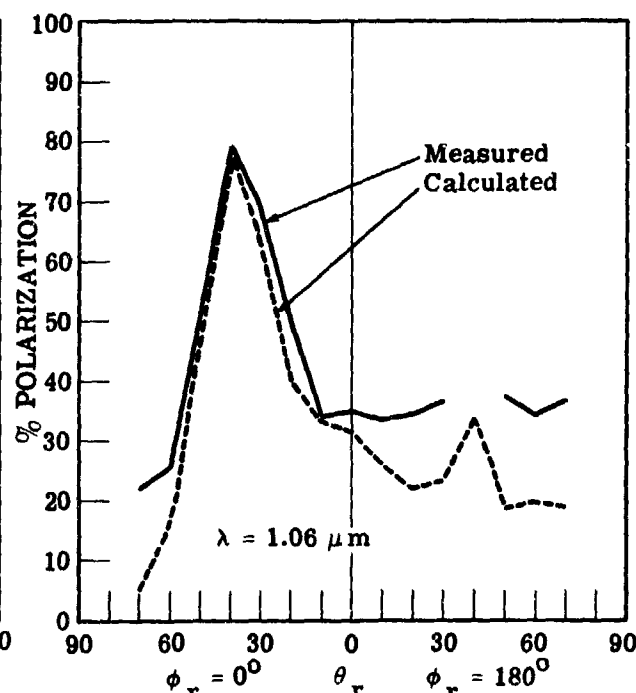


FIGURE 35. PERCENT POLARIZATION VARIATION FOR A02018-002 AS FUNCTION OF SOURCE-RECEIVER POSITION.
 $\theta_i = 40^\circ$, $\phi_i = 180^\circ$, $\phi_r = 0^\circ, 180^\circ$; parallel source.

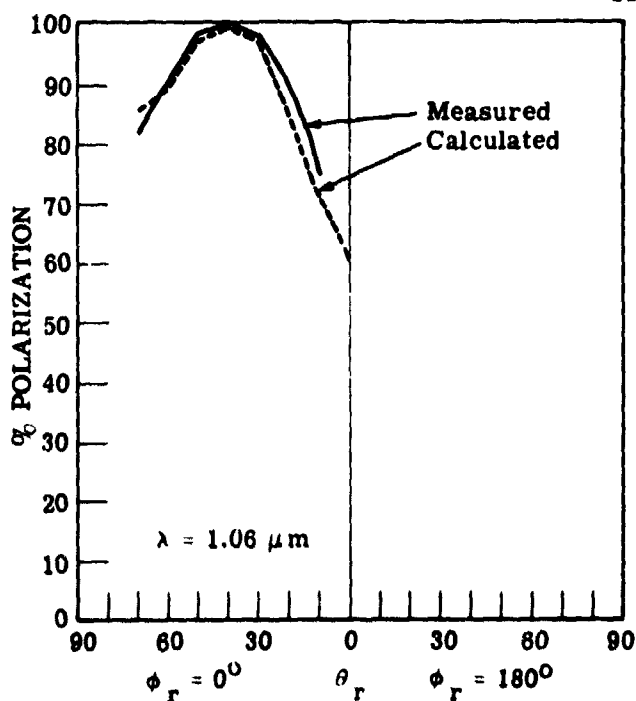


FIGURE 36. PERCENT POLARIZATION VARIATION FOR A02018-001 AS FUNCTION OF SOURCE-RECEIVER POSITION.
 $\theta_i = 40^\circ$, $\phi_i = 180^\circ$, $\phi_r = 0^\circ, 180^\circ$; perpendicular source.

perpendicular source.

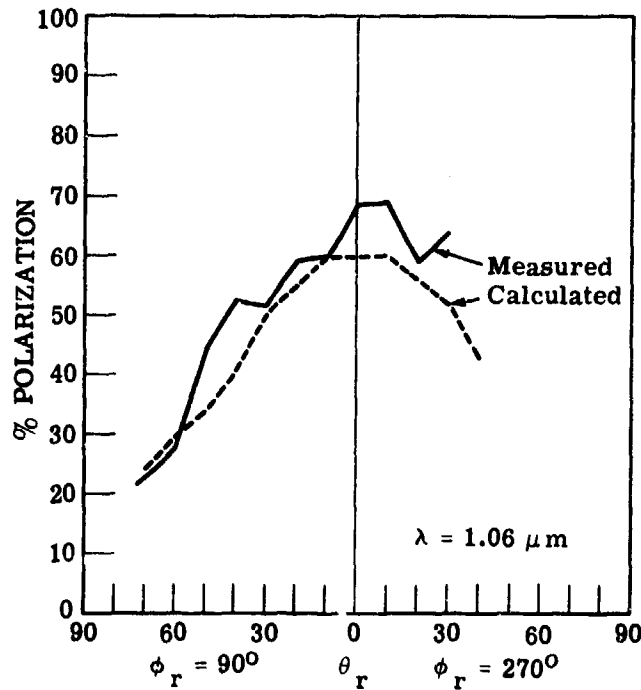


FIGURE 37. PERCENT POLARIZATION VARIATION FOR A02018-001 AS FUNCTION OF SOURCE-RECEIVER POSITION.
 $\theta_i = 40^\circ, \phi_i = 180^\circ, \phi_r = 90^\circ, 270^\circ$.

parallel source.

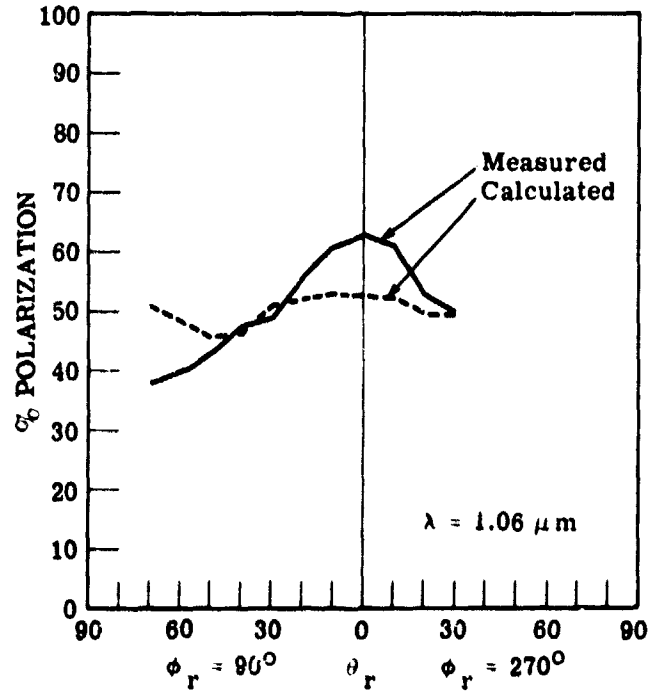


FIGURE 38. PERCENT POLARIZATION VARIATION FOR A02018-001 AS FUNCTION OF SOURCE-RECEIVER POSITION.
 $\theta_i = 40^\circ, \phi_i = 180^\circ, \phi_r = 90^\circ, 270^\circ$.

A02100 101

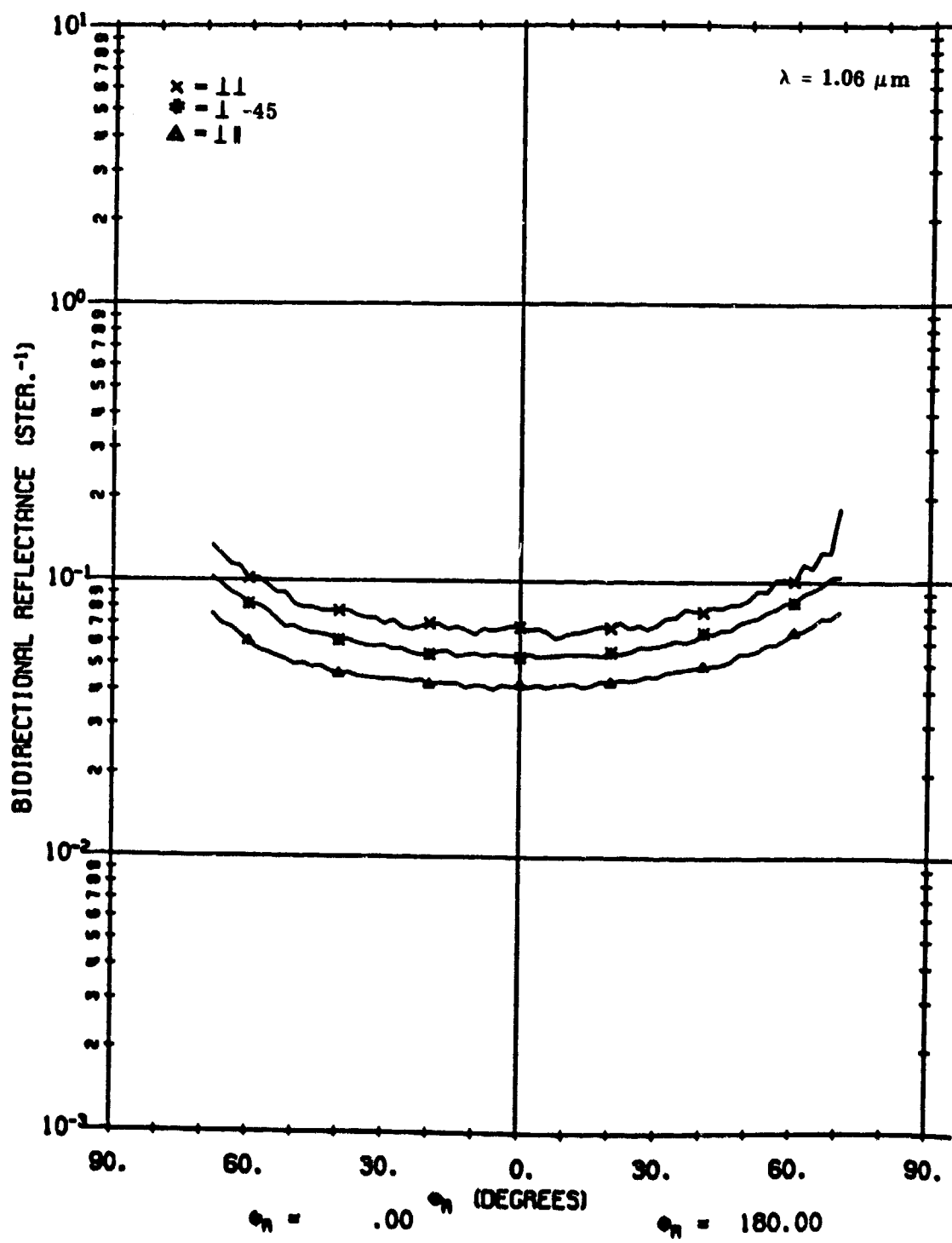


FIGURE 39. FIXED BISTATIC ρ' FOR A02100

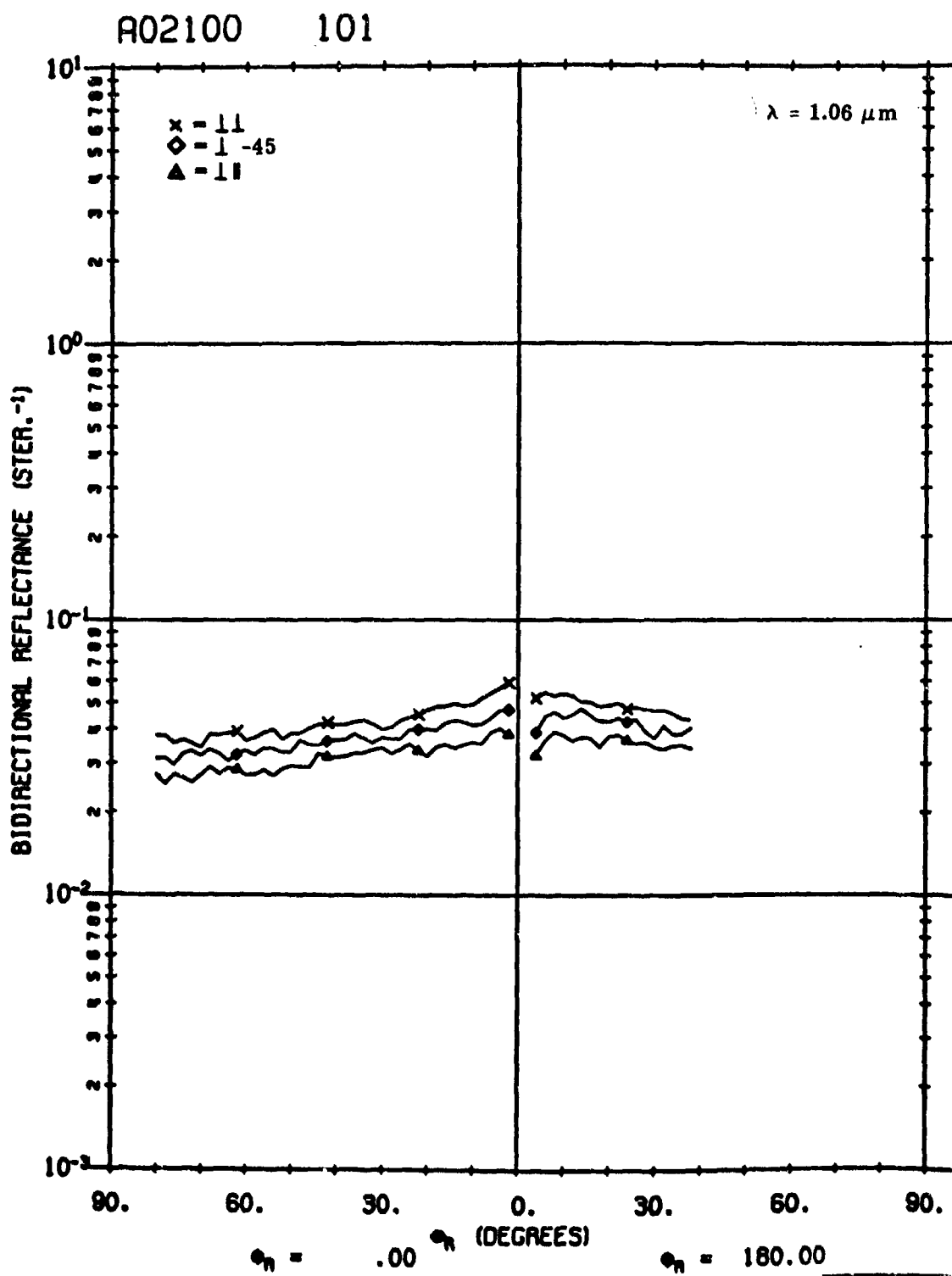


FIGURE 40. MEASURED ρ' FOR A02100. $\theta_i = 0^\circ$, $\phi_i = 0^\circ$, $\phi_r = 0^\circ, 180^\circ$.

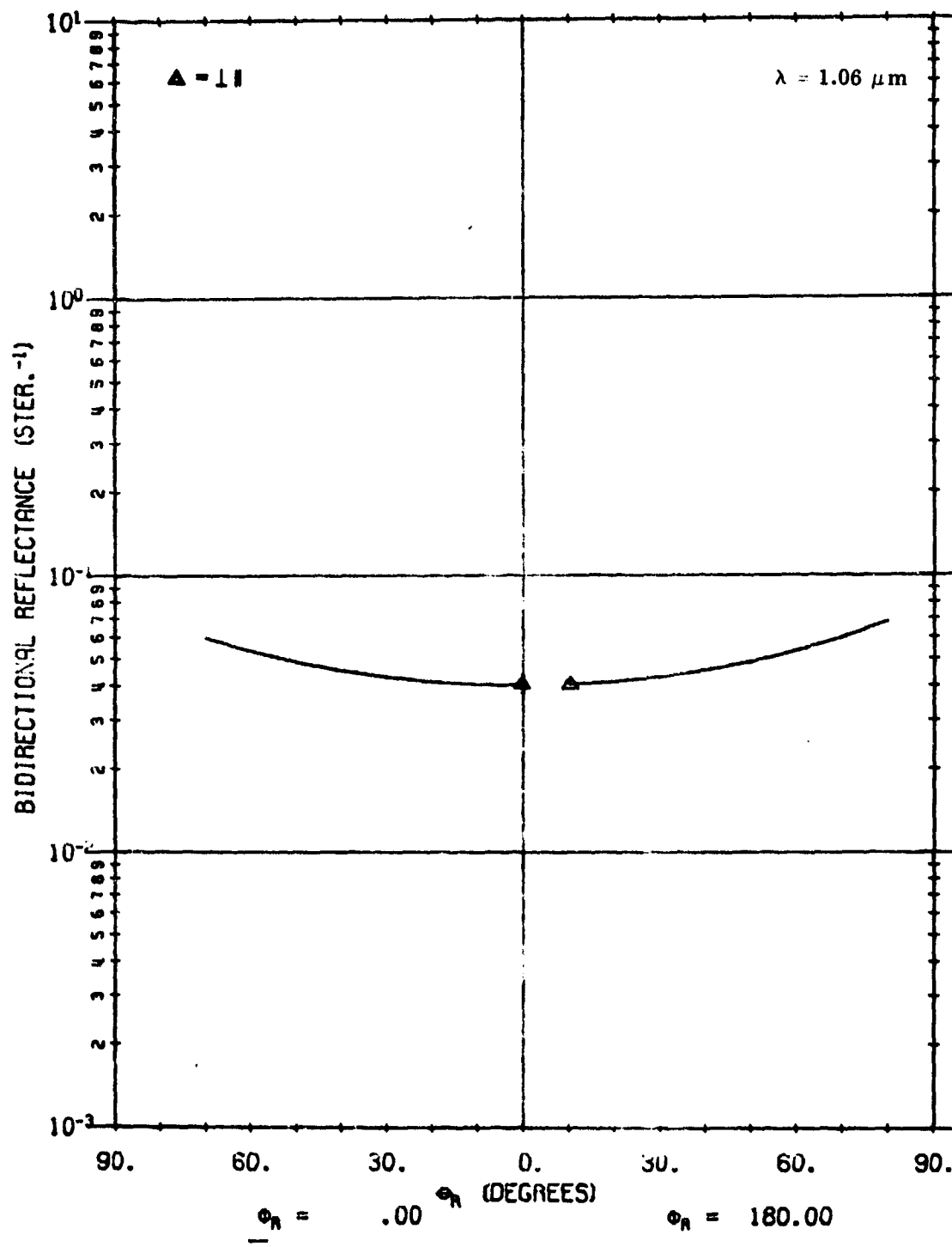


FIGURE 41. CALCULATED ρ' FOR AU2100 USING NON-LAMBERTIAN VOLUME
 MODEL. $\phi_i = 0^\circ, 180^\circ, \phi_r = 0^\circ, 180^\circ$

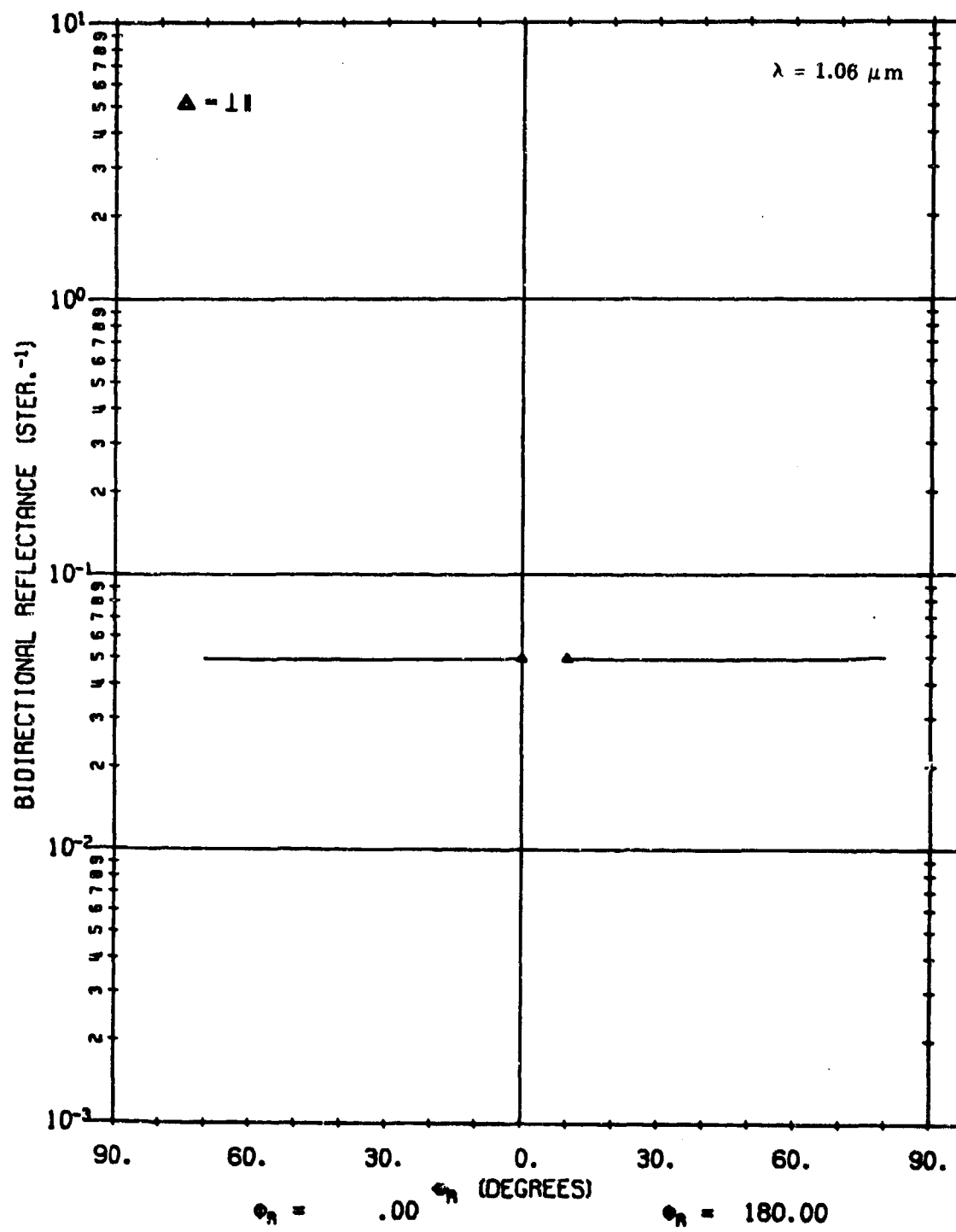


FIGURE 42. CALCULATED ρ' FOR A02100 USING LAMBERTIAN VOLUME MODEL.

$$\theta_i = 0^\circ, \phi_i = 180^\circ, \phi_r = 0^\circ, 180^\circ.$$

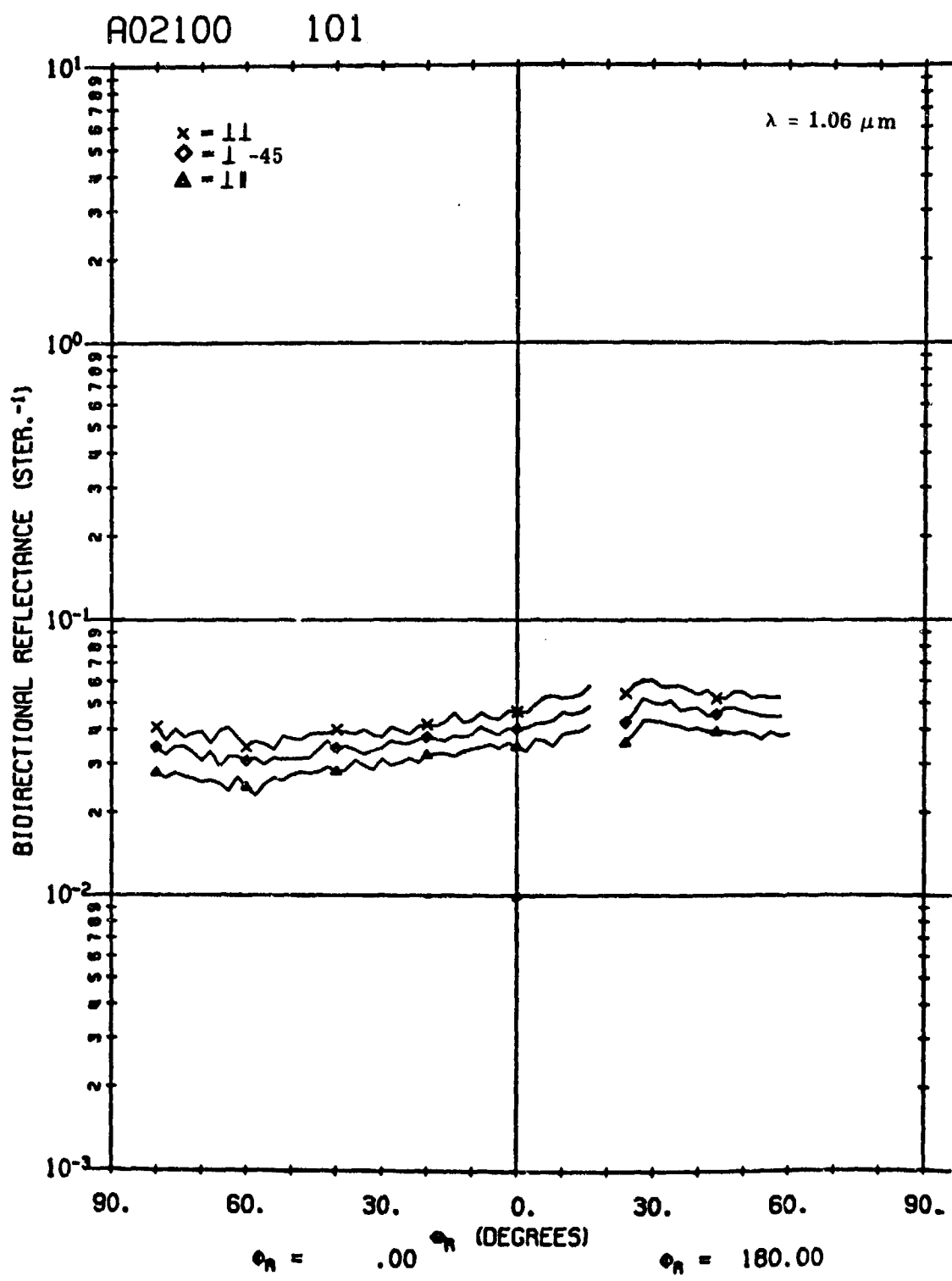


FIGURE 43. MEASURED ρ' FOR A02100 AT $20^\circ, \theta_z = 180^\circ, \theta_h = 0^\circ, 180^\circ$.

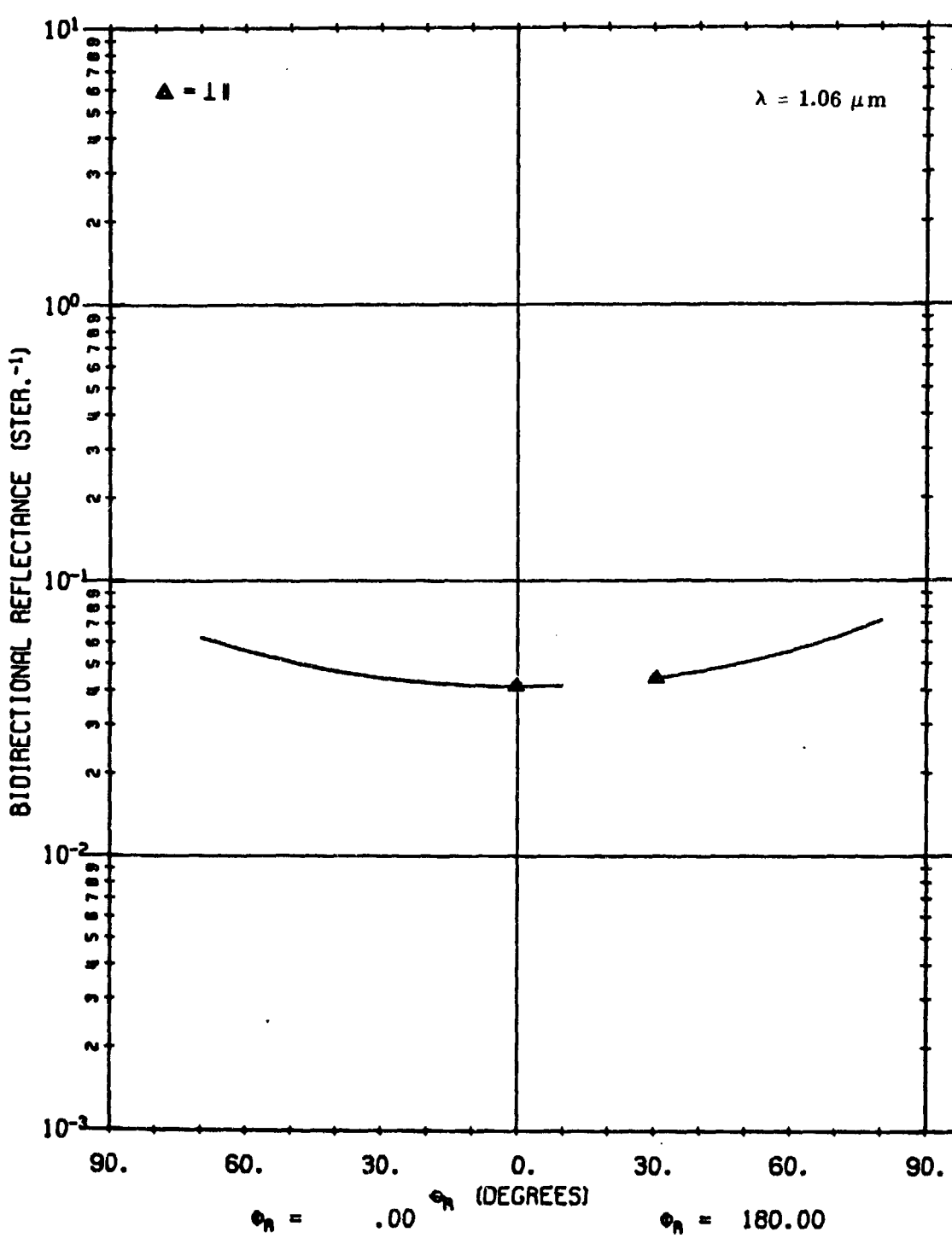


FIGURE 44. CALCULATED ρ' FOR A02100 USING NON-LAMBERTIAN VOLUME
 MODEL. $\theta_i = 20^\circ, \phi_i = 180^\circ, \phi_r = 0^\circ, 180^\circ$.

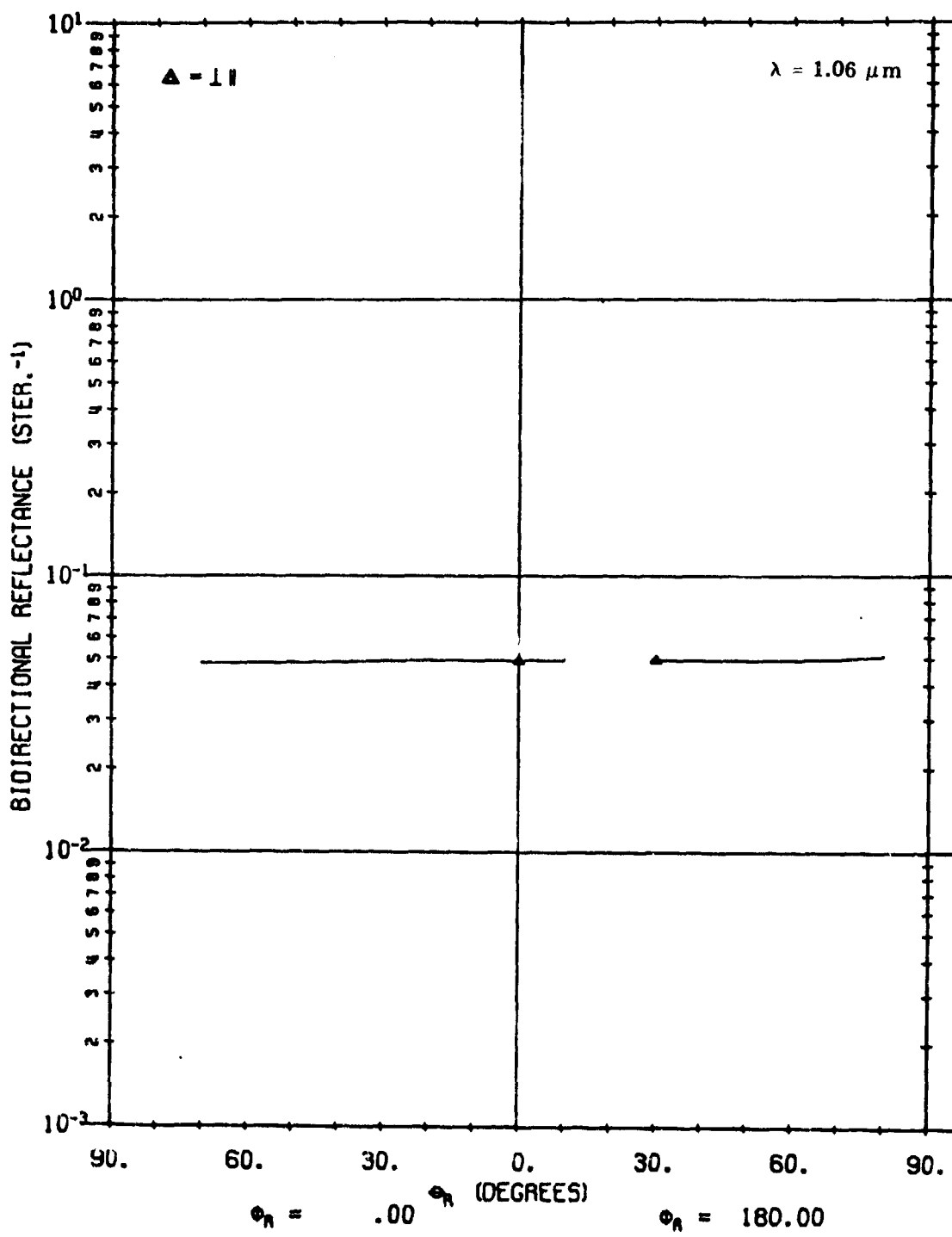


FIGURE 45. CALCULATED ρ' FOR A02100 USING LAMBERTIAN VOLUME MODEL.

$$\theta_i = 20^\circ, \phi_i = 180^\circ, \phi_r = 0^\circ, 180^\circ.$$

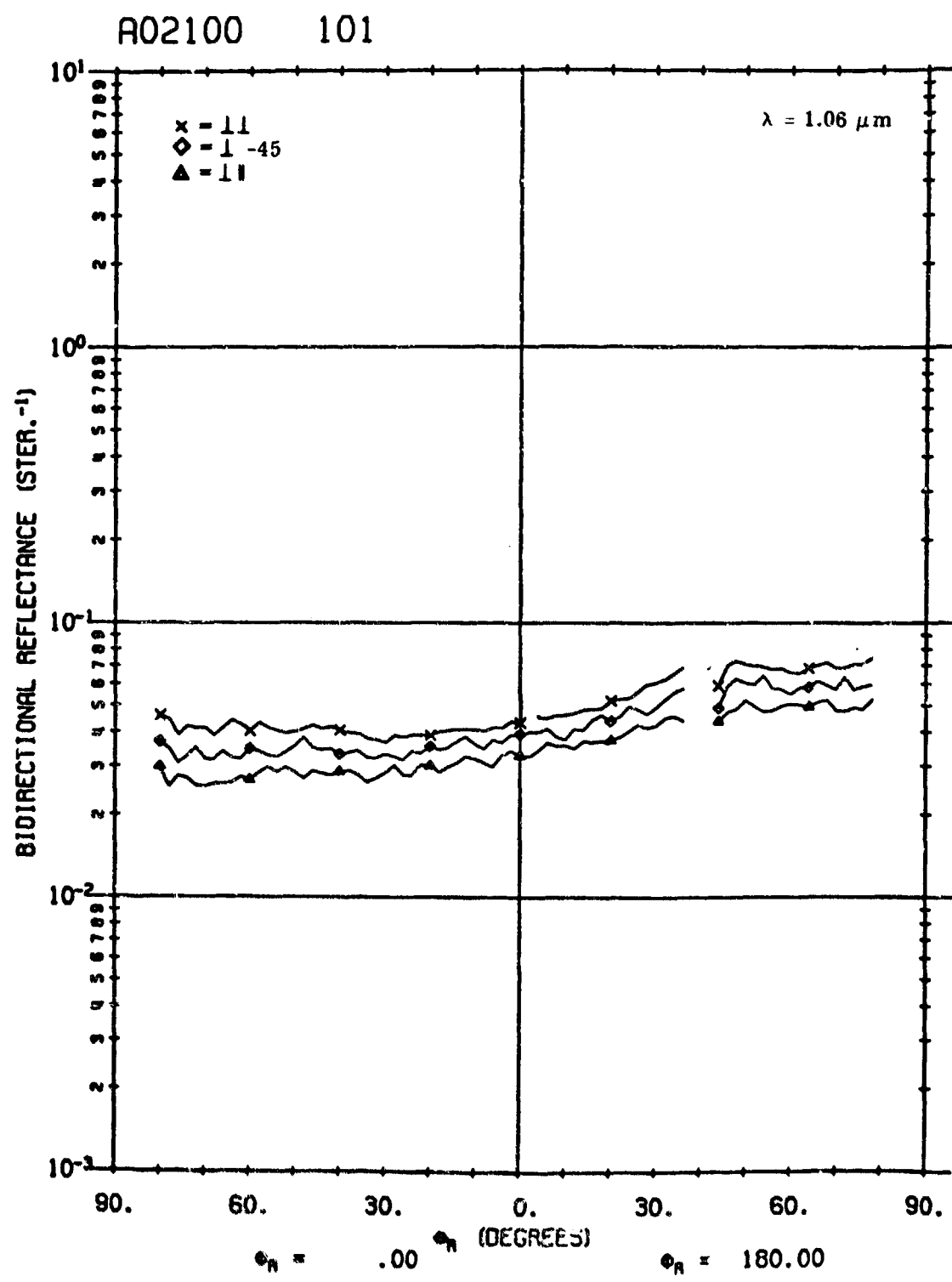


FIGURE 46. MEASURED ρ' FOR A02100. $\theta_i = 40^\circ$, $\phi_i = 180^\circ$, $\phi_r = 0^\circ, 180^\circ$.

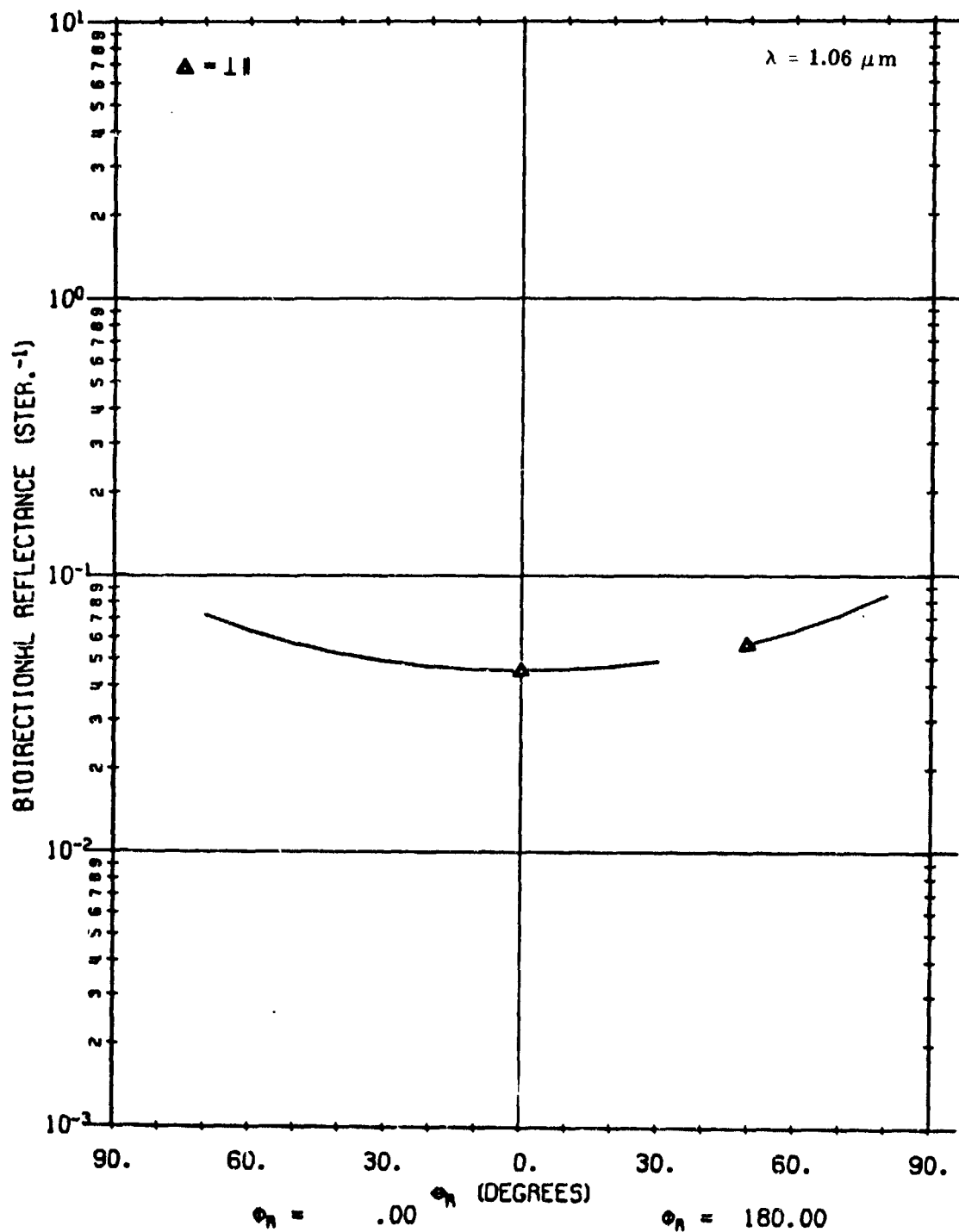


FIGURE 47. CALCULATED ρ' FOR A02100 USING NON-LAMBERTIAN VOLUME
 MODEL. $\psi_i = 40^\circ$, $\phi_i = 180^\circ$, $\phi_r = 0^\circ, 180^\circ$.

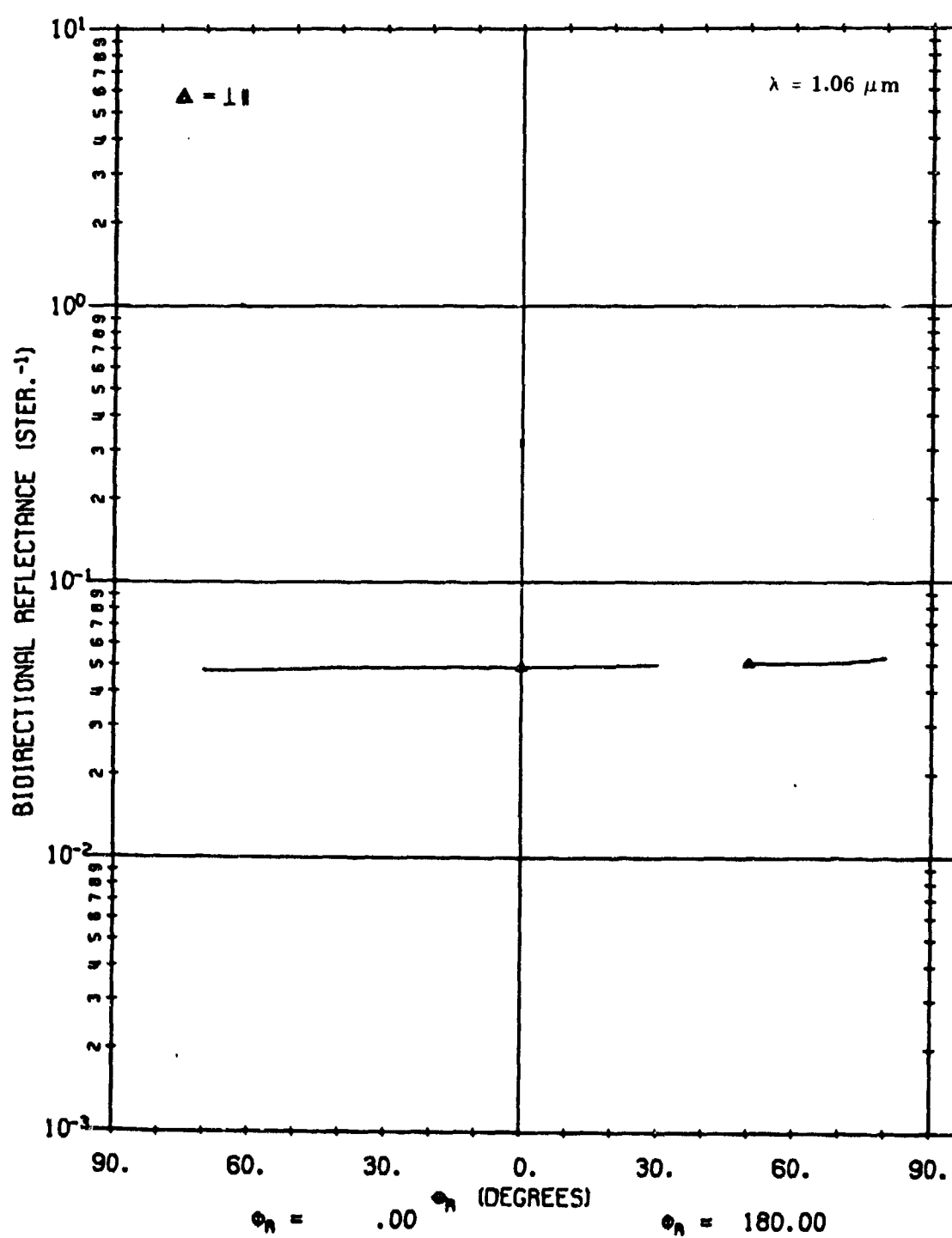


FIGURE 48. CALCULATED ρ' FOR A02100 USING LAMBERTIAN VOLUME MODEL.

$$\theta_i = 40^\circ, \phi_i = 180^\circ, \phi_r = 0^\circ, 180^\circ$$

7 MODEL PARAMETERS

This section briefly describes the model parameters that can be used in the bidirectional reflectance program and explains how their values are derived. The choice of parameters for use in the program depends to some extent on the mode of the model being run. Basically, the model is run in three different modes:

- (1) Surface and Lambertian volume components
- (2) Non-Lambertian volume component (no surface contribution included)
- (3) Surface and non-Lambertian volume components

Therefore, we have grouped the model parameters as follows:

- (1) Polarization parameters
- (2) Surface model parameters
- (3) Lambertian volume model parameters
- (4) Non-Lambertian volume model parameters

7.1. SOURCE POLARIZATION PARAMETERS

The present model has been designed to account for polarization dependence in both surface and volume components.

In the surface component, polarization is accounted for automatically in the Fresnel reflectance coefficients. In the most general case, such polarization can be elliptical and can be decomposed into linear and circular components. To date, only a linearly polarized source and receiver have been used in measurements. However, for some applications, circularly polarized sources or receivers may be of interest. Therefore, in the model, we have provided program subroutines which take into consideration the ellipticity and handedness (i.e., direction of rotation in an elliptically polarized source) of both incident and reflected beam.

For volume components in both Lambertian and non-Lambertian cases, it is assumed that reflectance will be depolarized to some extent. In both cases, in fact, we assume total depolarization. Therefore, although a depolarization factor has been included in the non-Lambertian volume model for future flexibility, we assume $DP(\beta) = 1$.

The source polarization may most generally be defined as partially polarized with the polarized component elliptically polarized. The state of polarization of the source will be defined by its degree of polarization, P , and parameters A , B , ψ , and H to define the elliptical polarization of the polarized component. Here, A and B are the intensities along the semi-major and semi-minor axes, respectively. The angle ψ is the angle between the semi-major axis of the ellipse and the direction normal to the plane of incidence, measured looking into the source beam; ψ is equivalent to α except that $0^\circ \leq \psi \leq 180^\circ$ and $-90^\circ \leq \psi \leq 90^\circ$. The handedness $H = \pm 1$.

The Stokes vectors provide a convenient formalism for defining the polarization state of the reflected radiance. (Reference [5] provides a general discussion of Stokes vectors in this context.)

$$S = \begin{bmatrix} I_p + I_u \\ I_p \cos 2x \cos 2\psi \\ I_p \cos 2x \sin 2\psi \\ I_p \sin 2x \end{bmatrix}$$

where I_p and I_u are the polarized and unpolarized components, respectively, in the reflected radiance. The degree of polarization in the reflected radiance is $P = I_p / (I_p + I_u)$. Angles x and ψ define the polarization state of the reflected radiance: ψ is the angle between the semi-major axis of the ellipse and the direction normal to the plane of reflection; $\tan x = \pm \sqrt{B/A}$ where A and B are the intensities along the semi-major and semi-minor axes of the polarization ellipse and $\tan x < 0$ for left-handed elliptically polarized radiation.

The RHOPRIME program produces the Stokes vector S for unit irradiance in the input beam; the area may also be defined to be unity and then S represents a reflectance Stokes vector. The program also produces the components of the reflected radiance transmitted with a receiver polarization analyzer oriented parallel or perpendicular to the reflectance plane for computing $\rho'_{\psi,\parallel}$ and $\rho'_{\psi,\perp}$.

7.2. SURFACE MODEL PARAMETERS

n and k. These are the real and imaginary parts of the refractive index. As discussed earlier in this report, they are used for the determination of $R(\beta)$, the Fresnel reflectance. Values for n and k are estimated for the paint surfaces in this study. Moreover, the surface is assumed to be essentially nonconducting so that $k = 0$. Based on experience with similar paint samples, n is taken to be 1.65. For a given sample, n and k can be determined accurately by measuring the Brewster angle and calculating n and k as outlined in Section 4 on the surface model. At the present time the program used, RHOPRIME, does not do this.

τ and Ω . These parameters are used in the function which provides a correction to the program to account for shadowing and obscuration effects resulting from the roughness of the surface. Values for τ and Ω have been selected, based on observed characteristics of reflectance properties. They have been established as $\tau = 15$ and $\Omega = 40$.

$\rho'(\hat{n}, \hat{\phi}; \hat{\theta}_i, \hat{\phi}_i) \cos^2 \hat{\theta}_i$. One of the quantities in Eq. (9) from which $\rho'(\hat{\theta}_i, \hat{\phi}_i; \hat{\theta}_r, \hat{\phi}_r)$ is determined is $\rho'(\hat{n}, \hat{\phi}; \hat{\theta}_i, \hat{\phi}_i) \cos^2 \hat{\theta}_i$. As previously discussed, $\rho'(\hat{\theta}_i, \hat{\phi}_i; \hat{\theta}_r, \hat{\phi}_r)$ is obtained from zero bistatic data. Values for $\rho'(\hat{n}, \hat{\phi}; \hat{\theta}_i, \hat{\phi}_i) \cos^2 \hat{\theta}_i$ must be calculated (preferably for increments of two degrees) and made into a table which is one of the model inputs. Values are provided in Tables III-VI for materials A02017-001, A02018-001, A02018-002, and A02100.

7.3. LAMBERTIAN VOLUME MODEL PARAMETERS

$\rho_{\chi 1}$ and $\rho_{\chi 2}$. These are the cross components of polarized radiation used in the model to account for the diffuse contribution, $\rho_{\chi 1} = 2\rho_{\perp\parallel}$ and $\rho_{\chi 2} = 2\rho_{\perp\perp}$, where $\rho_{\perp\parallel}$ and/or $\rho_{\perp\perp}$ is determined by taking the average value of the cross component from the measured data. According to the reciprocity theorem, $\rho_{\chi 1} = \rho_{\chi 2}$ [Ref. 6]. It is important to remember that ρ_{χ} values only used when the volume scatter model is not used. When the volume model is used, $\rho_{\chi 1} = \rho_{\chi 2} = 0$.

7.4. NON-LAMBERTIAN VOLUME MODEL PARAMETERS

ρ_V . This represents the non-Lambertian volume scatter component; it is determined by extracting $\rho'_{\perp\parallel}$ or $\rho'_{\perp\perp}$ at the point which would lie under the peak of the zero bistatic scan if the measured curve were smooth; $\rho_V = 2\rho'_{\perp\parallel} = 2\rho'_{\perp\perp}$ at the peak point. (The fact that a hump sometimes occurs on the measured cross component curve is discussed in the section on Model Validations.)

Here again, it is important to remember that when the Lambertian volume model is used, $\rho_V = 0$ and $\rho_{\chi} \neq 0$. When the non-Lambertian volume model is used, $\rho_V \neq 0$ and $\rho_{\chi} = 0$. Also, ρ_V and ρ_{χ} are never simultaneously nonzero in models which have been validated to date.

$DP(v)$, $f(\beta)$, $g\left(\frac{v}{n}\right)$. Integral parts of SUBROUTINE FUNC, these parameters currently are all set equal to 1. They have been included to provide flexibility for later model modifications.

TABLE III. $\rho'(\theta_n, \phi_n; \hat{\theta}_n, \hat{\phi}_n) \cos^2 \theta_n$ VALUES FOR A02017-001

$\hat{\theta}_n$	$\rho'(\theta_n, \phi_n; \hat{\theta}_n, \hat{\phi}_n) \cos^2 \theta_n$
.9	.14528
2.9	.08415
4.9	.0529
6.9	.03705
8.9	.03077
10.9	.02315
12.9	.01829
14.9	.01786
16.9	.01524
18.9	.01344
20.9	.01169
22.9	.01091
24.9	.01148
26.9	.00984
28.9	.0086
30.9	.00925
32.9	.00908
34.9	.00815
36.9	.00625
38.9	.00649
40.9	.00664
42.9	.00617
44.9	.00531
46.9	.00465
48.9	.00474
50.9	.00406
52.9	.00354
54.9	.00291
56.9	.00323
58.9	.00265
60.9	.00224
62.9	.00217
64.9	.00211
66.9	.00205
68.9	.00196
70.9	.0027

TABLE IV. $\rho'(\theta_n, \phi_n; \theta_n, \phi_n) \cos^2 \theta_n$ VALUES FOR A02018-001

θ_n	$\rho'(\theta_n, \phi_n; \theta_n, \phi_n) \cos^2 \theta_n$
1.1	.5143
3.1	.27294
5.1	.11897
7.1	.05797
9.1	.03291
11.1	.02348
13.1	.02058
15.1	.01614
17.1	.0143
19.1	.0118
21.1	.01191
23.1	.01056
25.1	.01055
27.1	.00924
29.1	.00918
31.1	.00672
33.1	.00708
35.1	.00612
37.1	.00597
39.1	.00578
41.1	.00549
43.1	.00469
45.1	.00459
47.1	.00433
49.1	.00417
51.1	.0046
53.1	.00376
55.1	.00292
57.1	.0023
59.1	.00179
61.1	.00168
63.1	.00132
65.1	.0013
67.1	.00109

TABLE V. $\rho'(\theta_n, \phi_n; \hat{\theta}_n, \hat{\phi}_n) \cos^2 \theta_n$ VALUES FOR A02018-002

θ_n	$\rho'(\theta_n, \phi_n; \hat{\theta}_n, \hat{\phi}_n) \cos^2 \theta_n$
1.15	.02497
3.15	.02520
5.15	.02388
7.15	.01975
9.15	.02135
11.15	.02177
13.15	.02335
15.15	.02353
17.15	.02300
19.15	.02243
21.15	.02338
23.15	.02022
25.15	.02056
27.15	.01726
29.15	.01885
31.15	.01966
33.15	.01875
35.15	.02089
37.15	.01882
39.15	.01709
41.15	.01785
43.15	.01604
45.15	.01545
47.15	.01295
49.15	.01319
51.15	.01434
53.15	.01180
55.15	.01385
57.15	.01190
59.15	.00922
61.15	.01149
63.15	.00869
65.15	.00954
67.15	.00808
69.15	.01349

TABLE VI. $\rho'(\theta_n, \phi_n; \theta_{\hat{n}}, \phi_{\hat{n}}) \cos^2 \theta_{\hat{n}}$ VALUES FOR A02100

θ_n	$\rho'(\theta_n, \phi_n; \theta_{\hat{n}}, \phi_{\hat{n}}) \cos^2 \theta_{\hat{n}}$
0.1	.21399
2.1	.16918
4.1	.1096
6.1	.08454
8.1	.05494
10.1	.03917
12.1	.03869
14.1	.02547
16.1	.03465
18.1	.02112
20.1	.02753
22.1	.02155
24.1	.02261
26.1	.01906
28.1	.02055
30.1	.01637
32.1	.01799
34.1	.01778
36.1	.01601
38.1	.01559
40.1	.01337
42.1	.01626
44.1	.01101
46.1	.01054
48.1	.00894
50.1	.01003
52.1	.00898
54.1	.00648
56.1	.00815
58.1	.00701
60.1	.00470
62.1	.00552
64.1	.00497
66.1	.00387
68.1	.00343
70.1	.00292

Appendix I
DOCUMENTATION OF BIDIRECTIONAL REFLECTANCE PROGRAM (RHOPRIME)

Program RHOPRIME is the main calling program for subroutines to read and store materials data, perform geometrical calculations, compute bidirectional reflectances for any source/receiver position and polarization, and prepare the output in a convenient format. The calling sequence, purpose, and calculations performed by each subroutine are given below, followed by details on the input data formats.

III.1. DESCRIPTIONS OF SUBROUTINES

SUBROUTINE INDATA. This is the first subroutine called. Material parameters needed for the calculation of bidirectional reflectance are read and stored. Material parameters are

MAT = material specifier

N = n = real part of refractive index

K = k = imaginary part of refractive index

RX1 = ρ_{x1} = diffuse reflectance for \perp polarized source

RX2 = ρ_{x2} = diffuse reflectance for \parallel polarized source

RHOV = ρ_v = volume reflectance

SIGMA } parameters available to calculate $\rho'(\theta_n^s, \phi_n^s; \theta_n^r, \phi_n^r)$ in subroutine FUNC
RPO }

TAU = τ (deg)

OMEGA = Ω (deg) } parameters to calculate a shadowing and obscuration factor to be applied to $\rho'(\cos \Omega / NP)$ in subroutine FUNC
Q1
Q2 }

RCOSBNP = $\rho'(\theta_n^s, \phi_n^s; \theta_n^r, \phi_n^r) \cos^2 \theta_n^r$ } table of zero-degree bistatic bidirectional reflectance data
BNP = θ_n^r (deg) }

TITLE. A title card (optional) is read and used to identify on the printed output the calculations to be performed.

FACET. The source and receiver are located in an earth-fixed, right-handed XYZ coordinate system. The XYZ components of the unit normal vector of the reflecting surface are read (optional). If the facet definition card is not supplied, the facet unit normal vector defaults to (0, 0, 1).

COMPUTATION REQUEST. The specification of source and receiver positions and source polarization for computation of the bidirectional reflectance is read.

ISW = model selector

TS = zenith angle of source (deg)

PS = azimuth angle of source (deg)

TD = zenith angle of receiver (deg)

PD = azimuth angle of receiver (deg)

A = intensity of major axis of polarization ellipse

B = intensity of minor axis of polarization ellipse

PSI = angle of major axis of polarization ellipse from the normal to the plane of incidence

measured CCW looking into the source, $0 \leq \text{PSI} \leq 180$ (deg)

P = polarization of source ($0 \leq P \leq 1.0$)

H = handedness of polarization ellipse (+1.0 or -0.0)

MI = material specifier

SUBROUTINE SCAN. This subroutine defines a sequence of detector positions for a specified source position and polarization.

ISW = model selector

TS = zenith angle of source (deg)

PS = azimuth angle of source (deg)

TDS = start zenith angle of receiver (deg)

TDE = end zenith angle of receiver (deg)

TSTEP = zenith angle scan increment (deg)

PDS = start azimuth angle of receiver (deg)

PDE = end azimuth angle of receiver (deg)

PSTEP = azimuth angle scan increment (deg)

A = intensity of major axis of polarization ellipse

B = intensity of minor axis of polarization ellipse

PSI = angle of major axis of polarization ellipse from the normal to the plane of incidence

measured CCW looking into the source $0 \leq \text{PSI} \leq 180$ (deg)

P = polarization of source ($0 \leq P \leq 1.0$)

H = handedness of polarization ellipse (+1.0 or -0.0)

MI = material specifier

SUBROUTINE GEOM. This subroutine does the necessary geometrical calculations of angles needed for the bidirectional reflectance calculations (see Fig. 49).

OR = (0, 0, 1) is a unit vector along the earth-fixed Z axis

PSI = the angle of the major axis of polarization ellipse from the normal vector of the **OR**,

E plane measured CCW looking into the source, $0 \leq \text{PSI} \leq 180$ (deg)

X = $\frac{D - E}{\sqrt{D^2 + E^2}}$

Y = $\frac{E D - D E}{\sqrt{D^2 + E^2}}$

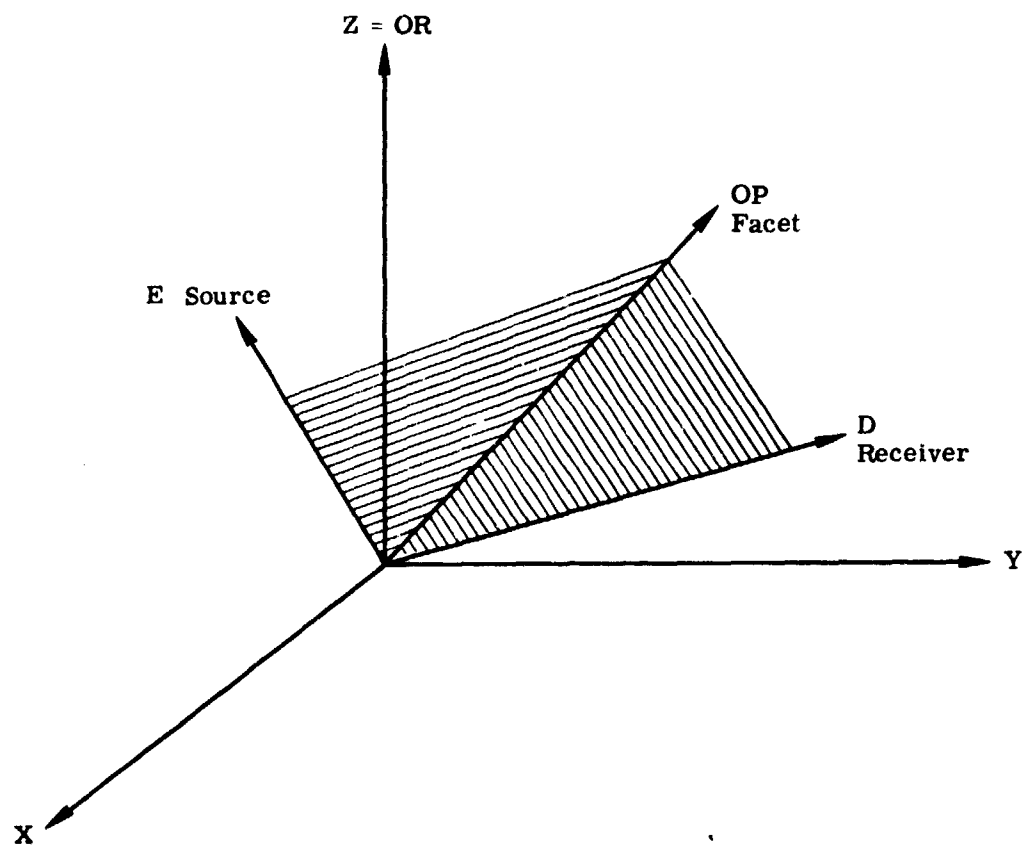


FIGURE 49. BIDIRECTIONAL REFLECTANCE GEOMETRY

$$YA = \frac{OR \times D}{|OR \times D|}$$

$$XA = \frac{E \times D}{|E \times D|}$$

$$U = \frac{D \times E}{|D \times E|}$$

$$XAP = \frac{OP \times E}{|OP \times E|}$$

$$YAP = \frac{OP \times D}{|OP \times D|}$$

$$\text{COSB} = X \cdot D$$

$$\text{COSBDP} = OP \cdot D$$

$$\text{COSBEP} = OP \cdot E$$

$$\text{COSBNP} = OP \cdot X$$

$$\text{PSIPE} = \text{PSI} - \text{SIGN}(-XAP \cdot OR) \text{ARCOS}(XAP \cdot Y)$$

= angle of major axis of polarization ellipse from the normal vector of the OP, E plane

$$\text{PSIDE} = \text{PSI} - \text{SIGN}(Y \cdot D) \text{ARCOS}(U \cdot Y)$$

= angle of major axis of polarization ellipse from the normal vector of the D, E plane

$$\text{WADE} = -\text{SIGN}(-YA \cdot E) \text{ARCOS}(XA \cdot YA)$$

= angle for transforming the output angle of polarization from E, D plane to OR, D plane

EDPHI = $\text{ARCOS}(XAP \cdot YAP)$ = the relative azimuth angle between E and D in the facet coordinate system

DC = $(-\text{SINBEP}, 0, \text{COSBEP})$ = direction of specular ray in the facet coordinate system

D1 = $(\text{SINBDP} \cos \text{EDPHI}, \text{SINBDP} \sin \text{EDPHI}, \text{COSBDP})$ = direction of reflected ray in the facet coordinate system

$$NZ1 = DC \cdot OP$$

$$NZ = NZ1 \cdot DC$$

$$DN = D1 \cdot NZ$$

PHIEN = 0 IF DN > 0	parameter required in FUNCTION FUNC for shadowing and obscuration
= 2 - $\text{ARCOS}(-DN)$ IF DN < 0	

SUBROUTINE GFRM. GFRM does all of the bidirectional reflectance calculations. The subroutine requires:

F = series of switches which can be set (optional) to reduce the number of redundant computations when GFRM is used as part of the multifaceted target model

COSB defined in **SUBROUTINE GEOM**

COSBDP defined in **SUBROUTINE GEOM**

COSBEP defined in **SUBROUTINE GEOM**

COSBNP = defined in SUBROUTINE GEOM

PSIPE = defined in SUBROUTINE GEOM

PSIDE = defined in SUBROUTINE GEOM

WADE = defined in SUBROUTINE GEOM

AP = area of facet (if AP = zero, GFRM returns a bidirectional reflectance Stokes vector;
if AP ≠ 0, GFRM returns a Stokes vector for the reflected radiant intensity for unity
irradiance in the incident beam)

MI = material specifier (available in COMMON)

ISW = model selector (available in COMMON)

W = wavelength specifier (available in COMMON), not used

TABLE = array containing all of the materials properties data read in SUBROUTINE IN-
DATA

GFRM returns the bidirectional reflectance Stokes vector (AP = 0) or radiant intensity Stokes
vector (AP ≠ 0).

I11 = Stokes vector for surface plus Lambertian model with polarized source

I21 = Stokes vector for surface plus Lambertian model with unpolarized source

I13 = Stokes vector for non-Lambertian volume model with polarized source

I23 = Stokes vector for non-Lambertian volume model with unpolarized source

I14 = Stokes vector for combined model with polarized source

I24 = Stokes vector for combined model with unpolarized source

FUNCTION GETDAT returns the appropriate material parameters for bidirectional re-
flectance calculations, namely N, K, RX1, RX2, RHOV, RCOSBNP, DP0, DP90, F, G.

FUNCTION FUNC provides the optional capability for deriving RCOSBNP analytically (if
SIGMA ≠ 0) and for deriving a shadowing and obscuration correction factor (optional) to the
RCOSBNP used in the specular model. In addition, the depolarization factors DP0(B) and
DP90(B), as well as F(B) and G(BNP) needed in the volume model, are defined analytically.

FUNCTION FUNC currently yields

DP0(B) = 1.0

DP90(B) = 1.0

F(B) = 1.0

G(BNP) = 1.0

$$RCOSBNP = (\text{COSBNP})^2 \text{RPO} \left[Q1 e^{-\frac{1}{2} \frac{\text{BNP}^2}{\text{SIGMA}^2}} - \frac{1}{2} \frac{\text{BNP}^2}{\text{SIGMA}^2} \right] \cdot Q2 \text{RHOV}$$

for BNP < SIGMA

$$= (\text{COSBNP})^2 \text{RPO} \left[Q1 e^{-\frac{\text{BNP}}{\text{SIGMA}}} \right] \cdot Q2 \text{RHOV}$$

for BNP > SIGMA

The shadowing and obscuration factor applied to RCOSBNP (measured values read during the input phase of RHOPRIME or defined analytically in FUNC) is

$$\frac{1 + \frac{BNP}{OMEGA} e^{\frac{-2B}{TAU}}}{1 + \frac{BNP}{OMEGA}} \cdot \frac{1}{1 + \frac{PHIEN}{OMEGA} \cdot \frac{BEP}{OMEGA}}$$

(a) SURFACE-PLUS-LAMBERTIAN MODEL CALCULATION

$$RO = \frac{(N+1)^2 + K^2}{(N-1)^2 + K^2} \cdot \frac{(V2 - COSB)^2 + V3}{(V2 + COSB)^2 + V3}$$

= normalized reflectance for \perp polarized incidence

$$R90 = \frac{(V2COSB + COS^2 B - 1)^2 + V3COS^2 B}{(V2COSB - COS^2 B + 1)^2 + V3COS^2 B} \cdot RO$$

= normalized reflectance for \parallel polarized incidence

where

$$V2 = \sqrt{\frac{4N^2K^2 + (N^2 - K^2 - 1 + COS^2 B)^2 + (N^2 - K^2 - 1 + COS^2 B)}{2}}$$

$$V3 = \sqrt{\frac{4N^2K^2 + (N^2 - K^2 - 1 - COS^2 B)^2 - (N^2 - K^2 - 1 + COS^2 B)}{2}}$$

If $H = 0$ the calculation is made for a plane polarized source (polarization angle PSI). The calculation ignores the induced elliptical polarization for $K \neq 0$.

$$PSIED = ATAN \left[\sqrt{\frac{R90}{0}} \cdot TAN PSIDE \cdot SIGN (COSATAN(N) - COSB) \right]$$

polarization angle with respect to D, E reference plane, after reflection

C = 1 if AP = 0, then a bidirectional reflectance Stokes vector is computed

C = AP · COSBEP · COSBDP if AP $\neq 0$, then a reflected radiant intensity Stokes vector is computed

$$III(1) = C \left[\frac{RCOSBNP}{COSBEP COSBDP} (R0 \cdot COS^2 PSIDE + R90 \cdot SIN^2 PSIDE) \right. \\ \left. + (RX1 \cdot COS^2 PSIPE + RX2 \cdot SIN^2 PSIPE) \right]$$

$$III(2) = C \left[\frac{RCOSBNP}{COSBEP COSBDP} (R0 \cdot COS^2 PSIDE + R90 \cdot SIN^2 PSIDE) COS2 (PSIED-WADE) \right]$$

$$III(3) = C \left[\frac{RCOSBNP}{COSBEP COSBDP} (R0 \cdot COS^2 PSIDE + R90 \cdot SIN^2 PSIDE) SIN2 (PSIED-WADE) \right]$$

$$I21(1) = C \left[\frac{RCOSBNP}{COSBEP COSBDP} \frac{1}{2} (R0 + R90) + \frac{1}{2} (RX1 + RX2) \right]$$

$$I21(2) = C \left[\frac{RCOSBNP}{COSBEP COSBDP} \frac{1}{2} (R0 - R90) \cos 2 (-WADE) \right]$$

$$I21(3) = C \left[\frac{RCOSBNP}{COSBEP COSBDP} \frac{1}{2} (R0 - R90) \sin 2 (-WADE) \right]$$

If $H = \pm 1$ the calculation includes the phase difference and ellipticity induced by reflection for $K \neq 0$ and is an exact treatment of the Fresnel equations.

SUBROUTINE ELIPS1 (AA, AB, PSIDE, H; AA1, AA2, D) defines the following input elliptical polarization parameters: the amplitudes perpendicular (AA1) and parallel (AA2) to the D, E plane and the relative phase $D = \phi_{\parallel} - \phi_{\perp}$ of the amplitudes of the major (AA) and minor (AB) axes of polarization ellipse; the orientation of the ellipse with respect to the D, E plane; PSIDE; and the handedness, H.

$DR = \phi_{\parallel} - \phi_{\perp}$ induced by reflection

FOR $K = 0$, $DR = 0$ if $\cos B < \cos \text{ARTAN}(N)$
 $= -\pi$ if $\cos B > \cos \text{ARTAN}(N)$

FOR $K \neq 0$, $DR = -\pi + \text{ATAN} \left(-\frac{2\sqrt{V3}(1 - \cos^2 B)\cos B}{(1 - \cos^2 B)^2 - \cos^2 B(V_2^2 + V_3)} \right)$
if () < 0

$DR = -\text{ATAN} \left(-\frac{2\sqrt{V3}(1 - \cos^2 B)\cos B}{(1 - \cos^2 B)^2 - \cos^2 B(V_2^2 + V_3)} \right)$
if () > 0

The intensities A1R and A2R, and the relative phase of the parallel and perpendicular components of the reflected radiance induced by the reflections, are

$$A1R = A1 \cdot R0$$

$$A2R = A2 \cdot R0$$

$$DR = DR + D$$

SUBROUTINE ELIPS2 (AA1, AA2, DR, AAR, ABR, PSIED, HR) defines the elliptically polarized reflected radiance as amplitudes AAR and ABR of the major and minor axes, the angle of the ellipse relative to the D, E plane, PSIED, and the handedness, HR. PSIDE = PSIED-WADE is the angle that the polarization ellipse of the reflected radiance makes with the normal vector to the OR, D plane.

$\text{CHI} = HR \cdot \text{ATAN}(ABR/AAR)$ is the parameter used to define the ellipticity of the reflected radiance.

C = 1 if AP = 0

C = AP · COSBEP · COSBDP if AP ≠ 0

$$I11(1) = C \left[\frac{AR + BR}{A + B} \frac{RCOSBNP}{COSBEP COSBDP} + (RX1 \cos^2(\text{PSIPE}) + RX2 \sin^2(\text{PSIPE})) \right]$$

$$I11(2) = C \left[\frac{AR + BR}{A + B} \frac{RCOSBNP}{COSBEP COSBDP} \cos(2\text{PSIDE}) \cos(2\text{CHI}) \right]$$

$$I11(3) = C \left[\frac{AR + BR}{A + B} \frac{RCOSBNP}{COSBEP COSBDP} \sin(2\text{PSIDE}) \cos(2\text{CHI}) \right]$$

$$I11(4) = C \left[\frac{AR + BR}{A + B} \frac{RCOSBNP}{COSBEP COSBDP} \sin(2\text{CHI}) \right]$$

$$I21(1) = C \left[\frac{RCOSBNP}{COSBEP COSBDP} \frac{1}{2} (R0 + R90) + \frac{1}{2} (RX1 + RX2) \right]$$

$$I21(2) = C \left[\frac{RCOSBNP}{COSBEP COSBDP} \frac{1}{2} (R0 - R90) \cos(-2\text{WADE}) \right]$$

$$I21(3) = C \left[\frac{RCOSBNP}{COSBEP COSBDP} \frac{1}{2} (R0 - R90) \sin(-2\text{WADE}) \right]$$

$$I21(4) = 0$$

(b) VOLUME MODEL CALCULATION

The angular-dependent, volume reflectance model, Stokes vector is given by

$$I13(1) = C \frac{1}{DP90(1+DP0)} \frac{2RH0V \cdot F \cdot G}{COSBEP+COSBDP} [\cos^2 \text{PSIDE} \cdot DP90(1+DP0) + \sin^2 \text{PSIDE} \cdot DP90(1+DP0)]$$

$$I13(2) = C \frac{1}{DP90(1+DP0)} \frac{2RH0V \cdot F \cdot G}{COSBEP+COSBDP} [\cos^2 \text{PSIDE} \cdot DP90(1+DP0) + \sin^2 \text{PSIDE} \cdot DP0(1-DP90)] \cos^2 2AD$$

$$I13(3) = C \frac{1}{DP90(1+DP0)} \frac{2RH0V \cdot F \cdot G}{COSBEP+COSBDP} [\cos^2 \text{PSIDE} \cdot DP90(1+DP90) + \sin^2 \text{PSIDE} \cdot DP0(1+DP90)] \sin^2 2AD$$

$$I23(1) = C \frac{1}{DP90(1+DP0)} \frac{2RH0V \cdot F \cdot G}{COSBEP+COSBDP} \frac{1}{2} [DP90(1+DP0) - DP0(1+DP90)]$$

$$I23(2) = C \frac{1}{DP90(1+DP0)} \frac{2RH0V \cdot F \cdot G}{COSBEP+COSBDP} \frac{1}{2} [DP90 - DP0] \cos(-2\text{WADE})$$

$$I23(3) = C \frac{1}{DP90(1+DP0)} \frac{2RH0V \cdot F \cdot G}{COSBEP+COSBDP} \frac{1}{2} [DP90 - DP0] \sin(-2\text{WADE})$$

where

$$C = 1 \text{ for } AP = 0$$

$$C = AP \cdot COSBEP \cdot COSBDP \text{ for } AP \neq 0$$

The angle of polarization of the reflected radiance, AED, from the normal vector of the D, E plane is

$$AED = ATAN \left[\sqrt{\frac{DP0(1 - DP90)}{DP90(1 - DP0)}} \cdot TAN(PSIDE) \cdot \text{SIGN}(\cos ATAN(N) - \cos B) \right]$$

and the angle of polarization referred to the OR, D plane is

$$AD = AED - WADE$$

SUBROUTINE OUTPUT. This subroutine prints the Stokes vectors for the bidirectional reflectance ($AP = 0$) or reflected radiant intensity for unit incident irradiance ($AP \neq 0$) for the surface model, the volume models, and for the combined specular and volume model. Stokes vectors are printed for a completely polarized source, for a completely unpolarized beam, and also for a partially polarized beam (polarization defined by the input parameter P).

In addition, several calculations are made with the Stokes vectors. For a bidirectional reflectance (or radiant intensity) Stokes vector, the bidirectional reflectance (or radiant intensity) for a receiver polarized \perp or \parallel to the OR, D plane is

$$\text{receiver } \perp = \frac{A + B}{2}$$

$$\text{receiver } \parallel = \frac{A - B}{2}$$

where the Stokes vector is of the form:

$$\begin{bmatrix} A \\ B \\ C \\ D \end{bmatrix}$$

The angle of the major axis of the reflected radiance and the percent polarization of the reflected radiance are also given; they are

$$AL = \pm \frac{1}{2} ATAN \left| \frac{C}{B} \right| \quad -90^\circ \leq AL \leq 90^\circ \quad (\text{looking into the source, } AL > 0 \text{ is a CCW angle}; \\ AL < 0 \text{ is a CW angle})$$

$$\% P = \frac{\sqrt{B^2 + C^2 + D^2}}{A} \times 100\%$$

The output includes TS, PS, TD, PD, P, as well as the input and output values of A, B, PSI, H from the surface model calculation (if the input H = 0, the input and output values of A, B, H default to 1, 0, and 0).

SUBROUTINE ELIPS1 (A, B, PSI, H; A1, A2, DELTA). The basic equations which relate two specifications of an elliptically polarized beam (A, B, PSI, H) and (A1, B1, DELTA) are

$$\tan \alpha = A1 \cdot A2 \quad 0^\circ \leq \alpha \leq \pi/2$$

$$\tan \lambda = \pm B/A \text{ for } \frac{rt}{lt} = \pi/4 \leq \lambda \leq \pi/4$$

$$\tan 2\psi = \tan 2\alpha \cos \delta$$

$$\sin 2\lambda = \sin 2\alpha \sin \delta$$

from which we obtain

$$\sin^2 2\alpha = \frac{\sin^2 2\lambda + \tan^2 2\psi}{1 + \tan^2 2\psi}$$

or equivalently

$$\cos 2\alpha = \cos 2\lambda \cos 2\psi$$

Subroutine ELIPS1 determines A1, A2, DELTA from A, B, PSI, H

$$\text{LAMBDA} = \sqrt{A^2 + B^2}$$

If $B = 0$, $A1 = \text{LAMBDA} \cos \text{PSI}$

$A2 = \text{LAMBDA} \sin \text{PSI}$

$\text{DELTA} = 0$ when $0 \leq \text{PSI} \leq \pi/2$

$\text{DELTA} = \pi$ when $\pi/2 < \text{PSI} \leq \pi$

Otherwise:

$$\text{CHI} = H \cdot \text{ATAN}(B/A)$$

$$\text{TI} = |\text{COS } 2\text{CHI} \text{ COS } 2\text{PSI}|$$

$$\text{ALPHA} = 1/2 \text{ ARCCOS}(-\text{TI}) \text{ if } \pi/4 < \text{PSI} < 3\pi/4$$

$$= 1/2 \text{ ARCCOS}(\text{TI}) \text{ if } \text{PSI} < \pi/4 \text{ or } > 3\pi/4$$

If $\text{ALPHA} = 0$, $A1 = \text{LAMBDA}$, $A2 = 0$, $\text{DELTA} = 0$

If $\text{ALPHA} = \pi/4$, $A1 = A2 = \text{LAMBDA}/\sqrt{2}$, $\text{DELTA} = 2\text{CHI}$ if $\text{PSI} = \pi/4$,

$= H/\sqrt{2} \text{ CHI}$ if $\text{PSI} = 3\pi/4$,

If $\text{ALPHA} = \pi/2$, $A1 = 0$, $A2 = \text{LAMBDA}$, $\text{DELTA} = 0$

Otherwise

$$\text{TI} = \text{SIN } 2\text{CHI} \text{ SIN } 2\text{ALPHA}$$

$$\text{MU} = \text{ARSIN } \text{TI}$$

$$A1 = \text{LAMBDA} \cos \text{ALPHA}$$

$$A2 = \text{LAMBDA} \sin \text{ALPHA}$$

$$\text{COSD} = \text{TAN } 2\text{PSI} / \text{TAN } 2\text{ALPHA}$$

If $\text{COSD} > 0$ $\text{DELTA} = H \cdot \text{MU}$

If $\text{COSD} < 0$ $\text{DELTA} = H \cdot (\pi - \text{MU})$

SUBROUTINE ELIPS2 (A1, A2, DELTA; A, B, PSI, H). Subroutine ELIPS2 determines A, B, PSI, H from A1, A2, DELTA.

$$\text{LAMBDA} = \sqrt{A1^2 + A2^2}$$

If $A1 = 0$ or $A2 = 0$, then $A = \text{LAMBDA}$, $B = 0$, $H = 1$, and

$\text{PSI} = 0$ if $A2 = 0$

$\text{PSI} = \pi/2$ if $A1 = 0$

If $A1 = A2$, then $\text{CHI} = 1/2|\text{DELTA}|$, $A = \text{LAMBDA} \cos \text{CHI}$, $B = \text{LAMBDA} \sin \text{CHI}$, and

$H = 1$ if $\text{DELTA} > 0$

$= -1$ if $\text{DELTA} < 0$

$\text{PSI} = \pi/4$ if $\text{CHI} < \pi/4$

$= 3\pi/4$ if $\text{CHI} > \pi/4$

If $\text{DELTA} = \pm\pi$, $A = \text{LAMBDA}$, $B = 0$, $H = 1$, $\text{PSI} = \pi - \text{ATAN } A2/A1$

If $\text{DELTA} = 0$, $A = \text{LAMBDA}$, $B = 0$, $H = 1$, $\text{PSI} = \text{ATAN } A2/A1$

If $\text{DELTA} = \pm\pi/2$, $H = +1$ if $\text{DELTA} > 0$

-1 if $\text{DELTA} < 0$

If $A1 > A2$, $A = A1$, $B = A2$, $\text{PSI} = 0$

If $A1 < A2$, $A = A2$, $B = A1$, $\text{PSI} = \pi/2$

Otherwise

If $A1 > A2$, $\text{ALPHA} = \text{ATAN } A2/A1$

$\text{CHI} = 1/2 \text{ ARSIN} |\text{SIN2ALPHA SINDELTA}|$

$\text{LAMBDA} = |\text{TAN2ALPHA COSDELTA}|$

$A = \text{LAMBDA} \cos \text{CHI}$

$B = \text{LAMBDA} \sin \text{CHI}$

$H = \pm$ if $\text{DELTA} > 0$

Part 1: $0 < |\text{DELTA}| < \pi/2$; $\text{PSI} = 1/2 \text{ ATANLAMDA}$

Part 2: $\pi/2 < |\text{DELTA}| < \pi$; $\text{PSI} = \pi - 1/2 \text{ ATANLAMDA}$

and

If $A1 < A2$, $0 < |\text{DELTA}| < \pi/2$; $\text{PSI} = \pi/2 - 1/2 \text{ ATANLAMDA}$

$\pi/2 < |\text{DELTA}| < \pi$; $\text{PSI} = \pi/2 + 1/2 \text{ ATANLAMDA}$

III.2. INPUT DATA FORMATS

The input to the RHOPRIME program is segmented into logical blocks. Each block is initiated by a block header and terminated by an end card. Blocks may be in any order, but a data block is assumed to precede any computation request blocks or scan request blocks. If a block header specifies an invalid block types, all input up to and including the next end card is ignored.

DATA TABLES BLOCK. The data tables block specifies all physical characteristics of the materials to be studied. The block header is one card with the following format:

<u>Columns</u>	<u>Description</u>
1-4	'TABL'
5-19	ignored
20-25	maximum material index to be expected
26-80	ignored

The data tables block is itself segmented into material blocks each characterizing one material to be studied. Each material block is initiated by a material header and terminated by an end card. The material header is two cards with the following format:

Card 1

<u>Columns</u>	<u>Description</u>
1-4	'MATR'
5-8	ignored
9-10	material index
11-20	n
21-30	k
31-40	$\rho_{\chi 1}$
41-50	$\rho_{\chi 2}$
51-60	ρ_v
61-70	SIGMA [if SIGMA ≠ 0, RCOSBNP is computed]
71-80	RP0

Card 2

<u>Columns</u>	<u>Description</u>
1-10	ignored
11-20	τ
21-30	Ω
31-40	Q1
41-50	Q2
51-80	blank

Following a material header, there may be a set of ρ' data. If present, the ρ' is a function of θ_n and the θ_n 's must be in ascending order. The format is

<u>Columns</u>	<u>Description</u>
1-4	blank or 'ANGL'
5-10	ignored
11-20	θ_n (deg)
21-30	$\rho'(\theta_n, \phi_n; \theta_n, \phi_n) \cos^2 \theta_n$
31-80	ignored

WARNING: Each material block must be terminated by an end card. The entire data tables block must also be terminated by an end card.

COMPUTATION REQUEST BLOCK. The computation requests block contains all information needed to perform desired computations. The block header is one card with the following format:

<u>Columns</u>	<u>Description</u>
1-4	'COMP'
5-19	ignored
20-25	model selector
26-80	ignored

The model selector, ISW, is:

- 1 — if specular and diffuse models are desired
- 3 — if volume model is desired
- 7 — if combined model is desired

Following the block header, computation requests are processed sequentially until an end card is encountered. The format of a computation request is:

<u>Columns</u>	<u>Description</u>
1-4	blank
5-9	ignored
10-16	source zenith (deg)
17	ignored
18-24	source azimuth (deg)
25	ignored
26-32	detector zenith (deg)
33	ignored
34-40	detector azimuth (deg)
41	ignored
42-48	polarization major axis length
49	ignored
50-56	polarization minor axis length
57	ignored
58-64	angle of source polarization (deg)
65	ignored
66-72	source percent polarization + 100
73	ignored
74-76	handedness of polarization (if ≠ 0, elliptical polarization is assumed)
77	ignored
78-80	material index

SCAN REQUEST BLOCK. If a scan of the detector zenith and/or azimuth is desired, a scan request block may be used. The block header is one card with the following format:

<u>Columns</u>	<u>Description</u>
1-4	'SCAN'
5-19	ignored
20-25	model selector
26-80	ignored

One card follows the block header giving all required parameters. The format of this card is:

<u>Columns</u>	<u>Description</u>
1-6	source zenith (deg)
7-12	source azimuth (deg)
13-18	initial detector zenith (deg)
19-24	final detector zenith (deg)
25-30	zenith increment (deg)
31-36	initial detector azimuth (deg)
37-42	final detector azimuth (deg)
43-48	azimuth increment (deg)
49-54	polarization major axis length
55-60	polarization minor axis length
61-66	angle of source polarization (deg)
67-72	source percent polarization + 100
73-76	handedness of polarization
77-80	material index

TITLE SPECIFICATION BLOCK. A title may be printed at the top of each page of long form output using the title specification block. The block header is one card in the following format:

<u>Columns</u>	<u>Description</u>
1-4	'TITLE'
5-19	ignored
20-25	blank
26-80	ignored

One card following the block header specifies the title. The format of this card is:

<u>Columns</u>	<u>Description</u>
1-60	title
61-80	ignored

FACET DEFINITION BLOCK. If default facet definition is not desired, the facet may be redefined using the facet definition block. The block header is one card in the following format:

<u>Columns</u>	<u>Description</u>
1-4	'FACE'
5-19	ignored
20-25	blank
26-80	ignored

One card following the block header defines the facet. The format of this card is:

<u>Columns</u>	<u>Description</u>
1-4	blank
5-9	ignored
10-16	facet area (default = 0)
17	ignored
18-24	facet normal - x (default = 0)
25	ignored
26-32	facet normal - y (default = 0)
33	ignored
34-40	facet normal - z (default = 1)
41-80	blank

END BLOCK. The end block terminates the program. The format of the block header is the same as that of the end card.

<u>Columns</u>	<u>Description</u>
1-4	'END'
5-80	blank

This block does not need an end card.

Appendix II
INSTRUCTIONS FOR USE OF PROGRAM
WITH SAMPLE COMPUTER OUTPUT

The program documentation in Appendix I, together with the sample computations included in this appendix should enable the user to (1) modify this program to accommodate the requirements of his own computer and (2) verify output from his modified program by comparison with the samples given herein.

Note that the input parameter values shown in Table VII are the ones with which the program has been run.

Sample outputs presented in this appendix include

- (1) a listing of the input information (Table VII)
- (2) the computed output of the program (long form) (Table VIII)
- (3) a short form of the computed output, containing only that information necessary to feed into a computer program for the purpose of obtaining plots of the data (Table IX)

The three tables mentioned above appear at the end of this appendix. All of the sample information is keyed and labelled so that elements may be identified easily. However, the further descriptive detail below may be helpful in studying the samples given.

RHOPRIME Input Listing

The following items appear across the top of Table VII. One line 2:

n = real part of index of refraction

k = imaginary part of index of refraction

$\rho_{\chi 1} = \text{cross component } (2\rho_{\parallel 1})$ } used for surface model

$\rho_{\chi 2} = \text{cross component } (2\rho_{\perp 1})$ }

$\rho_V = \text{volume component used for volume model}$

SIGMA = generating function parameter

RPO = generating function parameter

And on line 3:

τ = shadowing and obscuration parameter

Ω = shadowing and obscuration parameter

Q1 = generating function parameter

Q2 = generating function parameter

Following these items in Table VII is the $\rho'(\theta_{\hat{n}}, \phi_{\hat{n}}; \theta_{\hat{n}}, \phi_{\hat{n}}) \cos^2 \theta_{\hat{n}}$ tabulation which, in this case, was extracted from measured data and determined from the zero bistatic scan. Alternatively, such a tabulation can be generated by use of a generating function specified in the SUBROUTINE FUNC.

Note in the sample input information of Table VII that values are provided for ρ_{x1} , and ρ_{x2} and also for ρ_V . In practice, ρ_{x1} , and ρ_{x2} will be used or ρ_V will be used; all three values will never be nonzero simultaneously.

If the table is supplied as part of the input, the parameters SIGMA and RPO are set to 0 and Q1 = Q2 = 1.

The $\rho'(\theta_r^{\hat{n}}, \phi_r^{\hat{n}}; \theta_i^{\hat{n}}, \phi_i^{\hat{n}}) \cos^2 \theta_r^{\hat{n}}$ tabulation is followed by scan request information telling the computer what source-receiver combinations are to be computed and what model is to be selected:

$\theta_i^{\hat{n}}$ - θ for source

$\phi_i^{\hat{n}}$ - ϕ for source

$\theta_{r1}^{\hat{n}}$ - initial θ for receiver

$\theta_{r2}^{\hat{n}}$ - maximum θ for receiver

$\theta_{r3}^{\hat{n}}$ - size of angular step for $\theta_r^{\hat{n}}$ scan

$\phi_{r1}^{\hat{n}}$ - ϕ for receiver

$\phi_{r2}^{\hat{n}}$ - ϕ for receiver (value for second scan)

$\phi_{r3}^{\hat{n}}$ - size of angular step for $\phi_r^{\hat{n}}$

A - semi-major axis of polarization ellipse (normalized to 1.0)

B - semi-minor axis of polarization ellipse (B = 0 implies linear polarization)

PSI - angle of source polarization

P - percent polarization (1.0 - 100%)

MI - material index

ISW - 7 for combined model. (When volume model is used, set $\rho_{x1} = \rho_{x2} = 0$.)

Note that in addition to these input parameters, others must be added in the SUBROUTINE FUNC:

DP0, DP90 - depolarizations for perpendicular and parallel components of incident beam

f, g - volume model parameters.

For the materials in the sample listing, values for DP0, DP90, f, and g have been set equal to 1.0.

Computer Output (Long Form)

As exemplified by Table VIII, each page of the computed output corresponds to one source-receiver configuration. Items at the upper left are self-explanatory. However it should be borne in mind that MAJOR refers to the semi-major elliptical axis (a), which is taken to be 1.0. Since MINOR, which refers to the semi-minor axis (b), is 0, the MAJOR-MINOR combination implies linear polarization with polarization angle PSI for the incident beam. HANDED = 0 whenever the polarization is linear only.

The entries in the three main columns are reflectances. From the top, the first four entries in each column are the surface model elements of the Stokes vector which describes the polarization state of the beam as it leaves the target:

A = total reflectance

B = reflectance with receiver polarization angle = 0 (perpendicular polarization)

C = reflectance with receiver polarization angle = 45°

D = reflectance with receiver circularly polarized

The second four entries, still in the surface model block, are

$\frac{A+B}{2}$ = reflectance recorded from receiver with analyzer set for perpendicular polarization

$\frac{A-B}{2}$ = reflectance recorded from receiver with analyzer set for parallel polarization

AL = angle of polarization for reflected beam

P = percent polarization of reflected beam

Thus far the first two blocks of four entries have been discussed. The foregoing, as previously stated, apply to the surface plus Lambertian volume model.

The third and fourth blocks apply to the non-Lambertian volume model and are to be interpreted in exactly the same manner as above.

The fifth and sixth blocks consist of the sum of the surface + volume models and are printed out for convenience.

Note that in the volume model output and in the summed output, item D (circularly-polarized component) is not present.

Computer Output (Short Form)

The short form of the computer output consists of the information in the last four entries of the summed output (surface + volume), $\frac{A+B}{2}$, $\frac{A-B}{2}$, AL, P (see Table IX). Moreover, the data are compressed so that, whereas the long form has only one source-receiver configuration per page, the short form contains a complete scan in one block.

One scan consists of four item numbers. Preceding each of the first two item numbers in each scan are

Wavelength (1.06 μm)

θ_i (0°)

ϕ_i (180°)

ϕ_r (0° or 180°)

The first item number in each scan contains $\frac{A+B}{2}$. Each output entry is preceded by the θ_r scan angle—i.e., 0.0, 0.0268 means that the reflectance at θ_r = 0 is 0.0268. The second item number contains $\frac{A-B}{2}$. The third item number contains the polarization angle, AL, at each receiver angle. The fourth item number contains the percent polarization.

The scans are in the same overall order as those in the long form of the output

TAN. 37 DB=0

TABLE VII. REOPRIME INPUT LISTING

$$= \left[\rho_{11} \left(\frac{e^{\phi}}{n}, \frac{\phi}{n}; \frac{e^{\phi}}{n}, \frac{\phi}{n} \right) - \rho_{11} \left(\frac{e^{\phi}}{n}, \frac{\phi}{n}; \frac{e^{-\phi}}{n}, \frac{-\phi}{n} \right) \right] \cos^2 \theta_n$$

Reflectances for Zero Bi static Scan

7-
MSI

TABLE VIII. LONG FORM OUTPUT

REFLECTANCE	TRANSMISSION	Wavelength	PHOTON	POLARIZATION	PARTIAL POLARIZATION
SURFACE	TRANSMISSION	180.00	180.00	0.29667E-01-A	0.29667E-01
DETECTION	TRANSMISSION	180.00	180.00	0.29216E-01-B	0.29216E-01
PERCENT POLAR.	TRANSMISSION	1.00	1.00	-0.51516E-02-C	-0.51516E-02
MAJUR	TRANSMISSION	1.00	1.00	0.0	0.0
MINIR	TRANSMISSION	1.00	1.00	0.0	0.0
PSI	TRANSMISSION	1.00	1.00	0.0	0.0
MANDF	TRANSMISSION	0.	0.	0.0	0.0
SURFACE	POLARIZED	0.29667E-01-A	0.29667E-01	0.29667E-01	0.29667E-01
DETECTION	POLARIZED	0.29216E-01-B	0.29216E-01	0.29216E-01	0.29216E-01
PERCENT POLAR.	POLARIZED	-0.51516E-02-C	-0.51516E-02	-0.51516E-02	-0.51516E-02
MAJUR	POLARIZED	0.0	0.0	0.0	0.0
MINIR	POLARIZED	0.0	0.0	0.0	0.0
PSI	POLARIZED	0.0	0.0	0.0	0.0
MANDF	POLARIZED	0.0	0.0	0.0	0.0
Surface	POLARIZED	0.29216E-01-B	0.29216E-01	0.29216E-01	0.29216E-01
Plus	POLARIZED	-0.51516E-02-C	-0.51516E-02	-0.51516E-02	-0.51516E-02
Lambertian	POLARIZED	0.0	0.0	0.0	0.0
Bertian	POLARIZED	0.29443E-01	0.29443E-01	0.29443E-01	0.29443E-01
Volume	POLARIZED	0.22555E-03	0.22555E-03	0.22555E-03	0.22555E-03
Model	POLARIZED	-0.50001E-01-AL	-0.50001E-01-AL	-0.50001E-01-AL	-0.50001E-01-AL
Non-Lambertian	POLARIZED	0.10443E-01-A	0.10443E-01	0.10443E-01	0.10443E-01
Volume	POLARIZED	0.0	0.0	0.0	0.0
Model	POLARIZED	0.52216E-01	0.52216E-01	0.52216E-01	0.52216E-01
Non-Lambertian	POLARIZED	0.0	0.0	0.0	0.0
Volume	POLARIZED	0.52216E-01	0.52216E-01	0.52216E-01	0.52216E-01
Model	POLARIZED	0.99999E-09-AL	0.99999E-09-AL	0.99999E-09-AL	0.99999E-09-AL
Surface	POLARIZED	0.13410E-01-A	0.13410E-01	0.13410E-01	0.13410E-01
Plus	POLARIZED	0.29216E-01-B	0.29216E-01	0.29216E-01	0.29216E-01
Volume	POLARIZED	-0.51516E-02-C	-0.51516E-02	-0.51516E-02	-0.51516E-02
Models	POLARIZED	0.0	0.0	0.0	0.0
Non-Lambertian	POLARIZED	0.13410E-01-A	0.13410E-01	0.13410E-01	0.13410E-01
Volume	POLARIZED	0.29216E-01-B	0.29216E-01	0.29216E-01	0.29216E-01
Models	POLARIZED	-0.50001E-01-AL	-0.50001E-01-AL	-0.50001E-01-AL	-0.50001E-01-AL
Non-Lambertian	POLARIZED	0.0	0.0	0.0	0.0
Volume	POLARIZED	0.52216E-01	0.52216E-01	0.52216E-01	0.52216E-01
Models	POLARIZED	0.99999E-09-AL	0.99999E-09-AL	0.99999E-09-AL	0.99999E-09-AL

TABLE IX. SHORT FORM OUTPUT

Item No.	$\frac{A+B}{2}$	$\frac{A-B}{2}$	A	θ_i	ϕ_i	ϕ_T
1	1021004015001	9001	1	-		
2			9	1.06	0.0 180.00	0.0 0
3			9	30.000.0671	30.000.0642	40.000.0651
4			9	80.076.1580		
5	First	9001	9	1.06	0.0 180.00	0.0 0
6	Set of		9	30.000.0450	30.000.0430	40.000.0454
7	4-Item		9	80.000.0534	80.000.0517	80.000.0526
8	Numbers	3(ALL)	9			
9			9			
10			9			
11		J(P)	9			
12			9			
13			9			
14			9			
15			9			
16	Second	9001	9	1.06	0.0 180.00	180.0
17	Set of	9001	9	30.000.0642	30.000.0642	40.000.0642
18	4-Item		9	80.076.1580		
19	Numbers	9001	9	1.06	0.0 180.00	180.0
20			9	30.000.0430	30.000.0430	40.000.0434
21			9	80.076.0597	80.076.0597	80.076.0623
22			9			
23			9			
24			9			
25			9			
26			9			
27			9			
28			9			
29			9			
30			9			
31			9			
32			9			
33			9			
34			9			
35			9			
36			9			
37			9			
38			9			
39			9			
40			9			

Appendix III
RHOPRIME PROGRAM LISTING

```

1      PMPRIME AS OF 02.20.73
2      DMFNRION K(500),MP(3),F(3),D(3),MP(5),LABEL(15),TABLE(500)
3      EQUIVALENCE (TABLE,K)
4      INTEGER COUN,F,TABLES//TABLE//,COMP//COMP//,END//END//,SCAN//SCAN//
5      INTEGER TITLE//TITLE//,FACE//FACE//,
6      REAL T21(4),T23(3),T15(31,T24(3),T14(3)
7      COMMON MI,IRW,N,TABLE,IPI,III,IP3,IP4,IP5
8      COMMON /CMPT/PS1,PD1,BETA,BFTAB,RPO,COSTNF,SIGMA,PHIEN,REP,TS
9      DATA MP/0.0E0,0.1E0,1.0E0,AP/0.0E0,PR/0.0E0,0.1E0/
10     C*****
11     C      FORMATS
12     C
13     C*****FORMATS*****
14     100 FORMAT(A4,15X,16)
15     110 FORMAT(A4,5Y,8(F7.2,1Y),F3.0,1X,13)
16     120 FORMAT('1NORMAL TERMINATION')
17     140 FORMAT('1','***** END-OF-FILE ENCOUNTRED')
18     150 FORMAT('1','***** TABLE READ ERROR -- CONDITION CODE =',F3.0)
19     170 FORMAT('1','***** WARNING EOF IN COMPUTATION REQUESTS')
20     180 FORMAT('1','***** INVALID CARD TYPE')
21     190 FORMAT('1','***** EOF IN SCAN DATA.')
22     200 FORMAT(15B4)
23     C*****
24     C      DATA BLOCK READ-IN PHASE
25     C
26     C*****DATA BLOCK READ-IN PHASE*****
27     1000 READ(2,100,END=800)CODE,NMAT
28     C*****
29     C      MATERIAL TABLES
30     C*****
31     1010 IF(CODE .NE. TABLES)GO TO 1020
32     CALL TDATA(NMAT,PC)
33     IF(PC .GT. 0.0)GO TO 8010
34     GO TO 1000
35
36     C*****
37     C      COMPUTATION REQUEST
38     C*****
39     1020 IF(CODE .NE. PUMP)GO TO 1040
40     RESTGN 1030 TO MDE
41     ISW = NMAT
42     1030 READ(2,110,END=8030)(OLF,TS,PS,TU,HD,A,R,PST,D,H,MI
43     IF(CODE .EQ. END)GO TO 8070
44     IF(H .GT. 0.0)H = 1.0
45     IF(H .LT. 0.0)H = -1.0
46     IF(H .EQ. 0.0)A = 1.0
47     IF(H .EQ. 0.0)D = 0.0
48     GO TO 2000
49
50     C*****
51     C      DEFECTIVE SCAN REQUEST
52     C*****
53     1040 IF(CODE .NE. SCANT)GO TO 1060
54     ISW = NMAT
55     RESTGN 1050 TO MDE
56     1050 CALL SCANTC,TS,PS,TU,HD,P,A,R,PST,H)
57     IF(CC .GT. 0.0)GO TO 8060
58     GO TO 2000
59
60     C*****
61     C      TITLE SPECIFICATION

```

```

60      C*****
61      1060  IF(CODE .NE. TITLE)GO TO 1070
62          READ(2,200)LABEL
63          CALL AUYINT(LABEL,0,0,0,0,0,0,0,0,0,0,0,0,0,0,1)
64          IF(DP(S1) .EQ. 1.0160) GO TO 1090
65          JP(1) = 0.0
66          JP(2) = 0.0
67          JP(3) = 1.0
68          GO TO 1090
69      C*****
70      C      FACET DEFINITION
71      C*****
72      1070  IF(CODE .NE. FACET)GO TO 1080
73          READ(2,110)CODE,AP,DP
74          GO TO 1090
75      C*****
76      C      PROGRAM TERMINATION
77      C*****
78      1080  IF(CODE .NE. END)GO TO 8040
79          WRITE(5,120)
80          CALL SYSTEM
81      C*****
82      C      READ END CARD
83      C*****
84      1090  READ(2,100,END=8001)CNUF
85          IF(CODE .NE. END)GO TO 1090
86          GO TO 1060
87      C***** **** ***** **** ***** **** ***** **** ***** **** ***** ****
88      C
89      C      COMPUTATION PHASE
90      C
91      C***** **** ***** **** ***** **** ***** **** ***** **** ***** ****
92      2000  PS11 = PST/57.29577
93          TS1 = TS/57.29577
94          RS1 = RS/57.29577
95          T11 = TD/57.29577
96          R11 = RD/57.29577
97          E(1) = SIN(TS1)*COS(RS1)
98          E(2) = SIN(TS1)*SIN(RS1)
99          E(3) = COS(TS1)
100         U(1) = SIN(TU1)*COS(RH1)
101         U(2) = SIN(TU1)*SIN(RH1)
102         U(3) = COS(TU1)
103         CALL GEMYC(E,U,P,RS11,PSTUF,PSTHF,PUSD,COSHDP,CUSHFP,
104             ,CSHFP,WAUF)
105         CALL GEMYC(CSHR,PUSDRH,U1,AEP,PUSDRP,CNSRC,PSCIP,EPSIPE,WAUF,AP,
106             ,A,AP,H,RK,H,MR,PSTU)
107         RS10 = PSTJ*57.29577
108      C***** **** ***** **** ***** **** ***** **** ***** **** ***** ****
109      C
110      C      OUTPUT PHASE
111      C
112      C***** **** ***** **** ***** **** ***** **** ***** **** ***** ****
113      C*****
114      C      END OF RUN
115      C*****
116      CALL OUTPIT(TS,PS,TN,PU,H,A,AP,R,RK,HC1,RS10,H,RK,L4FL,AP)
117      GO TO M00F,FIN30,10501
118      C*****
119      C      SHIFT END

```

```

120      *****
121      5000 IF(CC .GT. 2.0)GO TO 8050
122      CALL AUX17(LABEL,0,0,0,0,0,0,0,0,0,0,0,0,0,0,0,3)
123      IF(CC .EQ. 1.0)GO TO 2000
124      CC = 0.0
125      GO TO 1000
126      ****
127      C
128      C      ERROR HANDLING PHASE
129      C
130      ****
131      8000 WRITE(0,1401
132      STOP R000
133      8010 WRITE(0,1501)CC
134      STOP R010
135      8030 WRITE(0,1701
136      STOP R030
137      8040 WRITE(0,1801
138      GO TO 1090
139      8050 WRITE(0,1901
140      STOP R050
141      END
142      SUBROUTINE INDATA(NMAT,CC)
143      DIMENSION TABLE(5001),KTAB(5001)
144      EQUVALENCE (TABLE,KTAB)
145      REAL N,K
146      INTEGER NPS,CODE,FNU//END 1/,ANGLE//ANGLE//,BLANK//'
147      DATA MATR//IMATR//
148      COMMON /I,I9N,N,TABLE,I21,I11,I23,I13,I24,I14
149      *****
150      C      FORMATS
151      *****
152      100  FORMAT(A4,4X,T2,7F10.3)
153      110  FORMAT(A4,5Y,2E10.3)
154      120  FORMAT(/'***** WARNING -- ANGLES OUT OF ORDER. 1/')
155      130  FORMAT(10Y,7E10.3)
156      CC = 0.0
157      NPS = NMAT+2
158      *****
159      C      READ MATERIAL HEADER
160      *****
161      1000 READ(2,100,END=8000)CODE,MAT,N,K,RX1,RX2,PHOV,STGMA,RPU
162      IF(CODE .EQ. END)RETURN
163      IF(CODE .NE. MAT)GO TO 8010
164      READ(2,130,END=80001)TAU,OMEGA,Q1,Q2
165      IF(MAT .GT. NMAT)GO TO 8020
166      BFTAO = -5.0
167      *****
168      C      STORE MATERIAL CONSTANTS
169      *****
170      KTAB(MAT) = NPS
171      TABLE(NPS+1) = N
172      TABLE(NPS+2) = K
173      TABLE(NPS+3) = RX1
174      TABLE(NPS+4) = RX2
175      TABLE(NPS+5) = PHOV
176      TABLE(NPS+6) = TAU//0.0174533
177      TABLE(NPS+7) = OMEGA//0.0174533
178      TABLE(NPS+8) = Q1//0.0174533
179      TABLE(NPS+9) = Q2//0.0174533

```

```

180      TABLE(WRS+10) = J1
181      TABLE(WRS+11) = J2
182      *****
183      C      READ AND STORE FACTORABLE TABLE IF GIVEN
184      *****
185          K1 = WRS+12
186          NA = 0
187      1010  READ(P,110,FND=RN000)CODE,BETA,RCUR
188          IF(CODE .EQ. FND) GO TO 1020
189          IF(CODE .NE. ANGL .AND. CODE .NE. BLANK) GO TO R030
190          IF(BETA .LE. BETAT0) WRITE(0,120)*AT
191          BETAU = BETA
192          BETA = BETA*0.01/4535
193          TABLE(K1) = COST(BETA)
194          TABLE(K1+1) = RCUR
195          K1 = K1+2
196          NA = NA+1
197          GO TO 1010
198      *****
199      C      SET NUMBER OF BETA'S
200      *****
201      1020  KTAU(WRS) = NA
202          WRS = WRS+NA+NA+12
203          GO TO 1000
204      *****
205      C      ERDNK HANDLING
206      *****
207          0000  CF = 1.0
208          RETURN
209          0010  CF = 2.0
210          RETURN
211          0020  CF = 3.0
212          RETURN
213          0030  CF = 4.0
214          RETURN
215          END
216          SUBROUTINE ERDNK(TS,HQ,TL,HD,P,A,B,PST,H)
217          COMMON/W1,ISW,/,TABLE,I21,I11,I25,I13,I24,I14
218          DATA TABLE/5001
219          REAL T61(4),I11(4),T23(3),I15(3),T24(3),I14(3)
220          INTEGER C7DF,FND,I7DU /
221          DATA FENTER/0.0/
222      *****
223      C      FORMATS
224      *****
225      100  FORMAT(L12F5.2,E4.0,T4)
226      110  FORMAT(A4)
227      *****
228      C      READ ERDNK PARAMETERS
229      *****
230          CF = 0.0
231          IF(FENTER .GT. 0.0) GO TO 2300
232          CF = 1.0
233          READ(F,100,FND=90001TS,PS,TDS,TDE,TSTEP,HD,PR,PSIFP,A,BS,RI,D,HR,
234          ,MT
235          IF(TDF = TDE) TS=0,1000,1010
236          TS = 0.0
237          TDE = 85.0
238          TD = TDE-TSTEP
239          IF(PDF=PDQ) 1020,1020,1030

```

```

240      1020  PDS = 0.0
241      PDE = 180.0
242      PSTEP = 180.0
243      1030  IF(PSTEP .LT. 5.0)P9TEP = 5.0
244      IF(TSTEP .LT. 2.0)T9TEP = 2.0
245      IF(H .GT. 0.0)H = 1.0
246      IF(H .LT. 0.0)H = -1.0
247      IF(H .EQ. 0.0)A = 1.0
248      IF(H .EQ. 0.0)B = 0.0
249      PD = PD9
250      1040  READ(2,110,END=9000)CODE
251      IF(CODE .NE. END)GO TO 1040
252      C*****
253      C   INCREMENT THETA
254      C*****
255      2000  TD = TD+T9TEP
256      IF(TD .LE. TDE)RETURN
257      C*****
258      C   INCREMENT PHI
259      C*****
260      PD = PD+PSTEP
261      IF(PD .GE. PDE)GO TO 3000
262      TD = TD9
263      CF = 1.0
264      RETURN
265      C*****
266      C   SCAN COMPLETE
267      C*****
268      3000  CC = 2.0
269      ENTER = 0.0
270      RETURN
271      C*****
272      C   ERROR HANDLING
273      C*****
274      9000  CC = 3.0
275      ENTER = 0.0
276      RETURN
277      END
278      SUBROUTINE GETDAT(R,COSB)
279      DIMENSION TABLE(500),KTAB(500),P(10)
280      EQUVALNCE (TABLE,KTAB)
281      INTGFR WRS
282      COMMON /I1,I2A,N,TABLE,I21,I11,I23,I13,I24,I14
283      COMMON /CMPT/PS,PD,RETA,BF14B,RP0,COSTNF,SIGMA,PHTEN,REP,TS
284      C***** ****
285      C
286      C   THIS SUBROUTINE RETRIEVES DATA FROM TABLE
287      C   INPUT:
288      C       COSB = COS(BETA)
289      C       COSINE = COS(BETA-N,P)
290      C
291      C   OUTPUT:
292      C       P(1) = N
293      C       P(2) = K
294      C       P(3) = RHO-CHI,1
295      C       P(4) = RHO-CHI,2
296      C       P(5) = RHO-V
297      C       P(6) = RHO(BETA=N,P)
298      C       P(7) = DP-PFRP
299      C       P(8) = DP-PAR

```



```

360      C*****
361      C    FORMATS
362      C*****
363      100  FORMAT(' ***** FACET NOT VISIBLE.')
364      C
365      IF(PST .GE. 1.5707963)PSI = PSI-3.1415927
366      IT = 0
367      C*****
368      C
369      C*****
370      X(1) = D(1)+E(1)
371      X(2) = D(2)+E(2)
372      X(3) = D(3)+E(3)
373      T1 = VNDRV(X,X)
374      C*****
375      C
376      C*****
377      IF(ABS(F(3)-1.0) .GT. 0.0001)GO TO 1000
378      Y(1) = COS(PS+1.570791)
379      Y(2) = SIN(PS+1.570791)
380      Y(3) = 0.0
381      GO TO 1010
382      1000 CALL CR089(DH,E,Y)
383      T1 = VNDRV(Y,Y)
384      C*****
385      C
386      C*****
387      1010 IF(ABS(D(3)-1.0) .GT. 0.0001)GO TO 1020
388      YA(1) = COS(PD+1.57079)
389      YA(2) = SIN(PD+1.57079)
390      YA(3) = 0.0
391      GO TO 1030
392      1020 CALL CR089(DH,D,YA)
393      T1 = VNDRV(YA,YA)
394      C*****
395      C
396      C*****
397      1030 IF(ABS(F(1)-D(1)) .GT. 0.0001 .OR. ABS(F(2)-D(2)) .GT. 0.0001)
398      1  GO TO 1040
399      UF(1) = Y(1)
400      UF(2) = Y(2)
401      UF(3) = Y(3)
402      XA(1) = YA(1)
403      XA(2) = YA(2)
404      XA(3) = YA(3)
405      IT = 1
406      GO TO 1050
407      1040 CALL CR089(F,D,XA)
408      T1 = VNDRV(YA,XA)
409      UF(1) = -XA(1)
410      UF(2) = -XA(2)
411      UF(3) = -XA(3)
412      C*****
413      C
414      C*****
415      1050 IF(ABS(DP(1)-F(1)) .GT. 0.0001 .OR. ABS(DP(2)-F(2)) .GT. 0.0001)
416      1  GO TO 1060
417      XAP(1) = Y(1)
418      XAP(2) = Y(2)
419      XAP(3) = Y(3)

```

```

420      G7 TU 1070
421      1060 CALL CRROSS(UP,L,XAP)
422      T1 = VNDRH(YAP,XAP)
423      C*****
424      C
425      C*****
426      1070 IF(ABS(UP(1)-D(1)) .GT. 0.0001 .OR. ABS(UP(2)-D(2)) .GT. 0.0001)
427      ! GU 10 1080
428      YAP(1) = YAF(1)
429      YAP(2) = YAF(2)
430      YAP(3) = YAF(3)
431      G7 TU 1090
432      1080 CALL CRROSS(UP,D,YAP)
433      T1 = VNDRH(YAP,YAP)
434      C*****
435      C
436      C*****
437      1090 CNSR = RCT(X,D)
438      CNSRD = RCT(UP,D)
439      CNSREP = RCT(D,E)
440      CNSRNP = RCT(D,X)
441      CNSR2 = CNSR*CNSR
442      PSIPE = PSI-ARCOS(FUN(XAP,Y))+SIGN(-DUT(XAP,UP))
443      PSIPE = PSI-ARCOS(FUN(Y,D))+SIGN(DUT(Y,D))
444      IF(T1 .LT. 1)GU 10 1100
445      IF(ABS(F(1)-UP(1)) .GT. 0.0001 .OR. ABS(F(2)-UP(2))
446      ! .GT. 0.0001)GU 10 1100
447      WADF = UP-PSI
448      IF(WADF .GE. 3.14159)WADF = WADF-3.14159
449      IF(WADF .LT. 0.0)WADF = WADF+3.14159
450      GU TU 1110
451      YAF(1) = -YA(1)
452      YAF(2) = -YA(2)
453      YAF(3) = -YA(3)
454      WADF = -ARCOS(FUN(XA,YA))+SIGN(DUT(YA,F))
455      C*****
456      C
457      C*****
458      1110 BNP = ARCS(C15BD)
459      BNP = ARCS(C15BD)
460      IF(BLP .GT. 1.57079 .OR. BNP .GT. 1.57079)WRITE(V,100)
461      BNPFI = ARCS(FUN(XA,YA))
462      PHIFN = 0.0
463      IF(ABS(Y(1)-UP(1)) .LT. 0.0001 .AND. ABS(Y(2)-UP(2)) .LT. 0.0001)
464      ! RETURN
465      IF(ABS(D(1)-UP(1)) .LT. 0.0001 .AND. ABS(D(2)-UP(2)) .LT. 0.0001)
466      ! RETURN
467      IF(ABS(F(1)-UP(1)) .LT. 0.0001 .AND. ABS(F(2)-UP(2)) .LT. 0.0001)
468      ! RETURN
469      C
470      UP(1) = -SIN(BLP)
471      UP(2) = 0.0
472      UP(3) = CNSREP
473      C
474      J1(1) = STY(FUN)+COS(FUN)
475      J1(2) = STY(FUN)*SIN(FUN)
476      J1(3) = CNSRDP
477      C
478      CALL CRROSS(BC,UP,NZ1)
479      T1 = VNDRH(NZ1,NZ1)

```

```

480 CALL CRSSR(NZ1,DC,N7)
481 T1 = VNDRM(NZ,N7)
482 DN = DUT(D1,N7)
483 IF(DN .LT. 0.0) PHTEN = 1.57079-ARCOS(-DN)
484 RETURN
485 END
486 SUBROUTINE GFRM(CNSR,CUSBPP,CUSREP,CUSBNP,CNSA2,PRIME,PRIDE,
487           WADE,AP,A,AR,B,BR,H,MR,PSID1
488           DIMENSION TABLE(500),KTAB(500),R(10),ST(5)
489           LOGICAL M0D1,M0D2,M0D3,M0D4
490           EQUIVALENCE (M0D1,M0D2,I1),(M0D3,I3),(M0D4,I4),(R(1),N),(R(2),K),
491           ,(R(3),HY1),(R(4),RX2),(R(5),RHUV),(R(6),RHD),
492           ,(R(7),DP0),(R(8),DP90),(R(9),FF),(R(10),G)
493           INTFGR SHFTR
494           RFAL I21(4),I11(4),I23(3),I13(3),I24(3),I12,I22,N,K
495           COMMUN MI,ISW,W,TABLE,I21,I11,I23,I13,I24,I14
496           DATA MASK/200000001/
497           EXTERNAL SIGN
498 C*****C
499 C
500 C     CHOOSE MODEL AND RETRIEVE DATA
501 C
502 C*****C
503 I1 = LANDMASK,ISW)
504 I3 = LANDMASK,SHFTR(TSW,1))
505 I4 = LANDMASK,SHFTR(TSW,2))
506 CALL GETDAT(R,CNSR),
507 DN 1000 I * 1.5
508 IP1(I1) = 0.0
509 I11(I1) = 0.0
510 IP3(I1) = 0.0
511 I13(I1) = 0.0
512 IP4(I1) = 0.0
513 1000 I14(I1) = 0.0
514 C*****C
515 C
516 C     SPECULAR AND DIFFUSE MODEL (M0D1 & M0D2)
517 C
518 C*****C
519 IF(.NOT. M0D1 .AND. .NOT. M0D2) GO TO 3000
520 C*****
521 C     COMPUTE FRESNEL COEFFICIENTS
522 C*****
523 V1 = DIVIDE(((N+1.0)*(N+1.0)+K*K),((N-1.0)*(N-1.0)+K*K))
524 U = N*N-K*K-1.0+C7SR2
525 P = SQR((N.0+N*K*K+0.0))
526 V2 = SQRT(P*(P+U)*U*.5)
527 V3 = ABS((P-U)*0.5)
528 C
529 R0 = V1*((V2-C7SR)+(V2-C7SR)+V3)/((V2+C7SR)*(V2+C7SR)+V3))
530 C
531 V4 = V2+C7SR
532 R00 = R0*((V4+C7SR2-1.0)*V2+V3*C7SR2)/((V4+C7SR2+1.0)*V2+
533           V3*C7SR2))
534 IP1(4) = 0.0
535 I11(4) = 0.0
536 IF(H .NE. 0) GO TO 2000
537 AP = 0.0
538 BR = 0.0
539 PRIN = 0.0

```

```

540      HR = 0.0
541  C*****
542  C      PLANE POLARIZED MODEL
543  C*****
544      T1 = ABS(PSTDF)-1.570746)
545      T2 = ABS(4YS(PSTDF)-4.712389)
546      IF(T1 .LT. 0.001 .AND. T2 .GT. 0.001)PSTER = ATAN(SQRT(DIVIDE
547      (R90,R0)) *TAN(PSTER)*SIGN(COS(ATAN(N))-COSB))
548      IF(T1 .LE. 0.001 ,UP., T2 .LE., 0.001)PSTER = PSTDF*SIGN(COS(ATAN
549      (N))-COSB)
550      AP11 = PSTER-WADE
551      T1 = AP11+AP11
552      ST(1) = COS(T1)
553      ST(2) = STN(T1)
554      T1 = -WADE-NAUF
555      V1 = (R0-R90)*0.5
556      ST(3) = (R0+R90)*0.5
557      ST(4) = V1*COS(T1)
558      ST(5) = V1*SIN(T1)
559  C
560      IF(AP .GT. 0.0)GJ TO 1010
561      V1 = RHO/(COSREP*COSRDP)
562      V4 = 1.0
563      GO TO 1020
564  C
565  1010  V1 = RHO*AP
566      V4 = FURBEP*COSRDP*AP
567  C*****
568  C      COMPUTE STJKS VER10K
569  C*****
570  C
571  C      UNPOLARIZED SOURCE
572  C
573  1020  IP2 = (R*V1+R*V2)+V4*0.5
574      IP1(1) = V1*ST(3)+IP2
575      IP1(2) = V1*ST(4)
576      IP1(3) = V1*ST(5)
577  C
578  C      POLARIZED SOURCE
579  C
580      I12 = (R*X1+R*Y1*(PSTDF)**2+R*Z1*(PSTDF)**2)**V4
581  C
582      V1 = (COSREP*V1**2+COSRDP*SIN(PSTDF)**2*RHO)*V1
583      I11(1) = V1*I11C
584      I11(2) = V1*I11S
585      I11(3) = V1*I11P
586      GO TO 3000
587  C*****
588  C      ELLIPTICAL MODEL
589  C*****
590  2000  IF(PSTDF .LT. -3.141593)PSTDF = PSTDF-3.141593
591  IF(PSTDF .LT. 0.01PI*100 = PI*100+S.141593
592  IF(PSTDF .LT. 0.01PI*100 = PI*100+S.141593
593  AA = R0*PI*100
594  AB = R0*PI*100
595  CALL FLTRP1(AB,AD,PCINE,4,AA1,AA2)
596  AA = AA1*AA1
597  AB = AB2*AB2
598  C
599  IF(ABS(R0*93-1.0) .LT. 0.001)LO = -3.141593

```

```

600      IF(ABS(FURB) .LT. 0.001)DR = 0.0
601      C
602      IF(K .NE. 0.01GN TO 2040
603          BFTAB = C7S(ATAN(N))
604          IF(COSB=BFTAB)2010,2020,2030
605          DR = 0.0
606          GN TU 2060
607          2020  DR = -1.570796
608          GN TU 2060
609          2030  DR = -3.141593
610          GN TU 2060
611      C
612          2040  T3 = 2.0*90RT(V3)*(1.0-COSB2)*COSR
613          T4 = (1.0-COSR2)*COSR2*(V2*V2+V3)
614          IF(ABS(T4) .GT. 0.00001)GN TO 2050
615          DR = -1.570796
616          GN TU 2060
617      C
618          2050  T1 = T3/T4
619          IF(T1 .LT. 0.0)DR = -3.141593+ATAN(-T1)
620          IF(T1 .GE. 0.0)DR = -ATAN(T1)
621      C
622          2060  DR = DR+D
623          ATR = A1*P0
624          APR = A2*P0
625          AA1P = 90RT(A1R)
626          AA2P = 90RT(A2R)
627          CALL FLTP92(AA1P,AAP,DR,AAP,PSTD0,HR)
628      C
629          AP = AAP+AAP/(A+B)
630          BP = ABR+AAR/(A+B)
631          IF(PSTD0 .GE. 3.141593)PSTD0 = PSTD0-3.141593
632          PRIN = PSTD0-WANE
633          IF(PSTD0 .GE. 3.141593)PRIN = PSTD0-3.141593
634          IF(PSTD0 .LE. 0.0)PSTD0 = PRIN+3.141593
635          T1 = PSTD0+PRIN
636          T2 = 1.570796
637          IF(ABS(AAP) .GT. 0.0001)T2 = HR*ATAN(AAP/AAP)
638          T2 = T2+T2
639      C
640          IF(AP .GT. 0.0)GU TU 2070
641          V1 = RHN/(C7SRBP+FURBMP)
642          V2 = 1.0
643          GN TU 2080
644      C
645          2070  V1 = RHN*AP
646          V2 = FURBFP+C7SRBP*AP
647      C*****
648      C      COMPLETE STICKER VECTOR
649      C*****
650      C
651      C
652      C      UNPOLARIZED SOURCE
653      C
654          2080  IZ2 = FRY1+HYZ2)*V2+0.5
655          IZ1(1) = V1*(R0+H90)*0.5+T2
656          IZ1(2) = V1*(R0-H90)*0.5*COS(-WADF-WANE)
657          IZ1(3) = V1*(R0-H90)*0.5*SIN(-WADF-WANE)
658      C
659      C      POLARIZED SOURCE

```

```

660      C
661      I12    = (RY1*COS(PRIPE)**2+RX2*STN(PRIPE)**2)*V2
662      C
663      V3    = V1*(AR+RR)
664      I11(1) = V3+I12
665      I11(2) = V3*COS(T1)*COS(T2)
666      I11(3) = V3*STN(T1)*COS(T2)
667      I11(4) = V3*STN(T2)
668      ****
669      C
670      C      VOLTMF MODEL (M003)
671      C
672      ****
673 3000 IF(.NOT. M031G0 TU 4000
674      V1 = 1.0
675      IF(AP .GT. 0.0)V1 = COSREP*FORBOP*AP
676      V1 = 2.0*V1*RHOV*FF*G/(COSREP+COSPUP)
677      AFD = 0.0
678      T1 = ABS(ABS(PSTDFF)-1.570796)
679      T2 = ABS(ABS(PSTDFF)-4.712389)
680      IF(T1 .GE. 0.001 .AND. T2 .GE. 0.001)GO TU 3010
681      AFD = PI/2E
682      GO TU 3030
683      C
684 5010 IF(DPH0 .GT. 0.001 .AND. DPH .LT. 0.999)GO TU 3020
685      AFD = 1.57079
686      GO TU 3030
687 5020 V2 = RUT(CP0 *(1.0-DRY0)/(DPH0*(1.0-DRY0)))*TAN(PSIDE)*SIGN
688      ' (COSATAN(N))-RUB1
689      AFD = ATAN(V2)
690      C
691 5030 AN = AFD-WAD
692      C1 = RUB(PSTDFF)
693      C1 = C1*C1*DPH0
694      S1 = RIN(PSTDFF)
695      S1 = S1*S1*DPH0
696      V1 = V1/(C1.0+DRY0*DPH0)
697      ****
698      C      COMPUTE STOCKER VECTOR
699      ****
700      C
701      C      POLARIZED SOURCE
702      C
703      I13(1) = V1*(C1*(1.0+DRY0)+S1*(C1.0+DRY0))
704      I13(2) = V1*(C1*(1.0-DRY0)+S1*(C1.0-DRY0))*RUB(AU+AD)
705      I13(3) = V1*(C1*(1.0-DRY0)+S1*(C1.0-DRY0))*SIN(AU+AD)
706      C
707      C      UNPOLARIZED SOURCE
708      C
709      V1    = V1*0.5
710      I23(1) = V1*(DRH0*(1.0+DRH0)+DRH0*(1.0+DRH0))
711      I23(2) = V1*(DRH0-DRH0)*RUB(-WAD-WAD)
712      I23(3) = V1*(DRH0-DRH0)*SIN(-WAD-WAD)
713      ****
714      C
715      C      TOTREFACE M031 (M004)
716      C
717      ****
718 4000 IF(.NOT. M031HFTUH)
719      KFTUH

```

```

720      END
721      SUBROUTINE OUTPUT(TS,PS,TD,PD,P,AA,AR,BR,BR,PSI,P9ID,M,MR,LABEL,
722                           AP)
723      DIMENSION AF(3),B(3),C(3),AER(3,3),AFP(3,3),AL(3,3),PP(3,3)
724      DIMEN4ION LABEL(15),D(1),TABLE(500)
725      LOGICAL MUD1,MUD2,MUD3,MUD4
726      RFAL T21(4),I11(4),T23(3),I13(3),T24(3),I14(3)
727      INTGFR SHFTR
728      COMMUN MI,I9W,W,TABLE,I21,I11,I23,I13,I24,I14
729      EQUIVALENCE (MUD1,MUD2,T1),(MUD3,T3),(MUD4,T4)
730      DATA MASK/Z00000001/,ZERO/0.0/,ONE/1.0/
731      *****
732      C FORMATS
733      *****
734      100  FORMAT(T1,10X,'REFLECTANCE',2X,4L1,2X,15A4//21X,'THFTA',6X,'PHI',
735           1 13X,'POLARIZED',13X,'UNPOLARIZED',12X,'PARTIAL PUL.')
736      110  FORMAT(T1,10X,'INTENSTY',2X,4L1,2X,15A4//21X,'THFTA',6X,'PHI',
737           1 13X,'POLARIZED',13X,'UNPOLARIZED',12X,'PARTIAL PUL.')
738      120  FORMAT(11Y,'SNURCE',2(4X,F6.2),3(10X,F13.5)/11X,'DETECTOR',2X,
739           1 F6.2,4X,F6.2,3(10X,F13.5)/11X,'PERCENT POLAR.',4X,F6.2,3(10X,
740           2 E13.5)/37X,3(10X,F13.5))
741      130  FORMAT(2SY,'IN',8Y,'INT',11X,'MAJOR',1X,2(4X,F6.2),3(10X,F13.5)/
742           1 11X,'MINOR',1X,2(4X,F6.2),3(10X,E13.5)/11X,'PSI',3X,2(4X,F6.2),
743           2 ,3(10Y,F13.5)/11X,'HANDFL',2(4X,F5.0),2X,3(10X,E13.5)//)
744      140  FORMAT(2(37Y,3(10Y,F13.5))/4(57X,3(10X,E13.5))//)
745      PA = ABS(P)
746      IT = 1
747      I1 = LAND(MASK,TSW)
748      I3 = LAND(MASK,SHFTR(TSW,1))
749      I4 = LAND(MASK,SHFTR(TSW,2))
750      IF(.NOT. MUD1 .AND. .NOT. MUD2) GO TO 2000
751      A(1) = PA*I11(1)+(1.0-PA)*I21(1)
752      B(1) = PA*I11(2)+(1.0-PA)*I21(2)
753      C(1) = PA*I11(3)+(1.0-PA)*I21(3)
754      D(1) = PA*I11(4)+(1.0-PA)*I21(4)
755      AFS(1,1) = (I11(1)+T21(2))/2.0
756      AFS(2,1) = (I21(1)+T21(2))/2.0
757      AFS(3,1) = (A(1)+B(1))/2.0
758      AFP(1,1) = (I11(1)-T21(2))/2.0
759      AFP(2,1) = (I21(1)-T21(2))/2.0
760      AFP(3,1) = (A(1)-B(1))/2.0
761      AI(1,1) = 0.99999E0
762      IF(T21(2) .NE. 0.0 .OR. I11(3) .NE. 0.0)
763      1 AL(1,1) = ATAN2(T21(3),I11(2))+2P.6488
764      AI(2,1) = 0.99999E0
765      IF(T21(2) .NE. 0.0 .OR. I21(3) .NE. 0.0)
766      1 AL(2,1) = ATAN2(T21(3),I21(2))+2P.6488
767      AI(3,1) = 0.99999E0
768      IF(A(1) .NE. 0.0 .OR. B(1) .NE. 0.0)
769      1 AL(3,1) = ATAN2(B(1),A(1))+2P.6488
770      1 PP(1,1) = SQRT((I21(2)*T21(2)+I11(3)*T21(3)+I11(4)*T21(4))/2
771      1 T21(1)+100.0
772      1 PP(2,1) = SQRT((I21(2)*T21(2)+I21(3)*T21(3)+I21(4)*T21(4))/2
773      1 T21(1)+100.0
774      1 PP(3,1) = SQRT((B(1)*B(1)+C(1)*C(1)+D(1)*D(1))/4+100.0
775      2000  IF(.NOT. MUD3) GO TO 3000
776      A(2) = PA*I13(1)+(1.0-PA)*I23(1)
777      B(2) = PA*I13(2)+(1.0-PA)*I23(2)
778      C(2) = PA*I13(3)+(1.0-PA)*I23(3)
779      AFS(1,2) = (I13(1)+T23(2))/2.0

```

```

780      AFS(2,2) = (I23(1)+T23(2))/2.0
781      AFS(3,2) = (A(2)+B(2))/2.0
782      AFP(1,2) = (I13(1)-T13(2))/2.0
783      AFP(2,2) = (I23(1)-T23(2))/2.0
784      AFP(3,2) = (A(2)-B(2))/2.0
785      AI(1,2) = 0.99999E9
786      IF(T13(2) .NE. 0.0 .OR. I13(3) .NE. 0.0)
787      1 AL(1,2) = ATAN2(T13(3),I13(2))*2R.64R8
788      AL(2,2) = 0.99999E9
789      IF(I23(2) .NE. 0.0 .OR. I23(3) .NE. 0.0)
790      1 AL(2,2) = ATAN2(I23(3),I23(2))*2R.64R8
791      AL(3,2) = 0.99999E9
792      IF(B(2) .NE. 0.0 .OR. C(2) .NE. 0.0)
793      1 AL(3,2) = ATAN2(C(2),B(2))*2R.64R8
794      PP(1,2)=SQR(T13(2)*I13(2)+T13(3)*I13(3))/I13(1)*100.0
795      PP(2,2)=SQR(T23(2)*I23(2)+T23(3)*I23(3))/I23(1)*100.0
796      PP(3,2)=SQR(B(2)*B(2)+C(2)*C(2))/A(2)*100.0
797      3N00  IF(.NOT. 4J041GN TU 4N00
798      I14(1) = T11(1)+I13(1)
799      I24(1) = T21(1)+I23(1)
800      I14(2) = T11(2)+I13(2)
801      I24(2) = T21(2)+I23(2)
802      I14(3) = T11(3)+I13(3)
803      I24(3) = T21(3)+I23(3)
804      A(3) = PA*I14(1)+(1.0-PA)*I24(1)
805      B(3) = PA*I14(2)+(1.0-PA)*I24(2)
806      C(3) = PA*I14(3)+(1.0-PA)*I24(3)
807      AFS(1,3)= (T14(1)+I14(2))/2.0
808      AFS(2,3)= (T24(1)+I24(2))/2.0
809      AFS(3,3)= (A(3)+B(3))/2.0
810      AFP(1,3)= (I14(1)-T14(2))/2.0
811      AFP(2,3)= (I24(1)-T24(2))/2.0
812      AFP(3,3)= (A(3)-B(3))/2.0
813      AI(1,3) = 0.99999E9
814      IF(T14(2) .NE. 0.0 .OR. I14(3) .NE. 0.0)
815      1 AL(1,3) = ATAN2(T14(3),I14(2))*2R.64R8
816      AI(2,3) = 0.99999E9
817      IF(T24(2) .NE. 0.0 .OR. I24(3) .NE. 0.0)
818      1 AL(2,3) = ATAN2(T24(3),I24(2))*2R.64R8
819      AI(3,3) = 0.99999E9
820      IF(B(3) .NE. 0.0 .OR. C(3) .NE. 0.0)
821      1 AL(3,3)= ATAN2(C(3),B(3))*2R.64R8
822      PP(1,3)=SQR(T14(2)*I14(2)+T14(3)*I14(3))/I14(1)*100.0
823      PP(2,3)=SQR(T24(2)*I24(2)+T24(3)*I24(3))/I24(1)*100.0
824      PP(3,3)=SQR(B(3)*B(3)+C(3)*C(3))/A(3)*100.0
825      CALI 4U817(LAREL,TU,AFS(1,3),AE(1,3),AI(1,3),HP(1,3),2)
826      4N00  IF(AP .LE. 0.0)WHITF(3,100)T1,MNU1,MNU2,MNU3,MNU4,LABFL
827      IF(AP .GT. 0.0)WHITF(3,110)T1,MNU1,MNU2,MNU3,MNU4,LABFL
828      IF(.NOT. 4J01 .AND. .NOT. MNU2)GJ TU 4O20
829      #PITE(3,120)T9,P5,I11(1),T21(1),A(1),TU,MN,T31(2),I21(2),B(1),PA,
830      1 T11(3),I21(3),C(1),I11(4),T21(4),J511
831      #PITE(3,130)AA,BH,(AE(3,T,1),I21(3),B(3),HP,(AFH(3,T,1),T21(3)),PA),
832      1 P5T0,(AL(3,T,1),T21(3),M,M0,(PP(3,T,1),I21(3))
833      IF(.NOT. 4J01 .AND. .NOT. MNU2)TU 4N10
834      #PITE(3,140)I13(1),T23(1),A(2),T13(2),I23(2),B(2),I13(3),T23(3),
835      1 C(2),(AE(3,T,2),I21(3),(AFH(3,T,2),T21(3)),(AL(3,T,2),T21(3)),
836      2 (HP(3,T,2),I21(3))
837      4N10  IF(.NOT. 4J041GN)
838      #PITE(3,150)I14(1),T24(1),A(3),T14(2),I24(2),B(3),I14(3),T24(3),
839      1 C(3),(AE(3,T,3),I21(3),(AFH(3,T,3),T21(3)),(AL(3,T,3),T21(3)),

```

```

840      7      (PP(T,3),I=1,5)
841      RETURN
842 4020  IF(.NOT., M053) GO TO 4030
843      WRITE(5,120) TS,PS,I13(1),T23(1),A(2),TD,PD,T13(2),T23(2),R(2),PA,
844      1      T13(3),IP3(3),C(2)
845      WRITE(3,130) ONE,ZFRD,(AFS(I,2),T=1,3),ZFRD,ZERU,(AEP(T,2),I=1,3),
846      1      PST,ZERU,(AL(1,2),T=1,3),ZFRD,ZERU,(PP(I,2),T=1,3)
847      IF(.NOT., M054) RETURN
848      WRITE(5,140) I14(1),T24(1),A(3),T14(2),T24(2),R(3),I14(3),T24(3),
849      1      C(3),(AE9(T,3),I=1,3),(AFP(I,3),T=1,3),(AL(I,3),T=1,3),
850      2      (PP(T,3),I=1,3)
851      RETURN
852 4030  IF(.NOT., M054) RETURN
853      WRITE(3,120) TS,PS,I14(1),T24(1),A(3),TD,PD,T14(2),T24(2),R(3),PA,
854      1      T14(3),IP4(3),C(3)
855      WRITE(3,130) ONE,ZFRD,(AFS(I,3),T=1,3),ZFRD,ZERU,(AEP(T,3),I=1,3),
856      1      PSI,ZFRD,(AL(T,3),I=1,3),ZERU,ZFRD,(PP(T,3),I=1,3)
857      RETURN
858      END
859      SUBROUTINE AUXIN(TITLE,Y1,Y1,Y2,Y3,Y4,ICODE)
860      COMMON /CHPT/PS1,PD1,RETA,BF1AB,KPU,CNSINF,SIGMA,PHTEN,REP,TS
861      DMENSION TTT1E31,Y(5,46)
862      DATA WL/1.0/
863      ****
864      C
865      C FORMATS
866      C
867      ****
868 100   FORMAT(A4,A4,A1,'5001',1/Y,'0101')
869 110   FORMAT(9X,'9001',T5,27X,I3,2X,3F6.2,6X,F6.1)
870 120   FORMAT(20Y,5(F6.2,F6.4)/(20Y,5(F6.2,F6.4)))
871 130   FORMAT(20Y,5(F6.2,F6.1)/(20Y,5(F6.2,F6.1)))
872 140   FORMAT(20Y,5(F6.2,F6.2)/(20Y,5(F6.2,F6.2)))
873      ****
874      C
875      C SUBROUTINE CUNITD
876      C
877      ****
878      GO TURNO,2000,3000),ICODE
879      STOP 1111
880      ****
881      C
882      C HEADER
883      C
884      ****
885 1000  IC = 0
886      ID = 0
887      WRITE(4,100) TITLE
888      RETURN
889      ****
890      C
891      C STURE
892      C
893      ****
894 2000  IP = YP+1
895      X(1,IP) = Y1
896      X(2,IP) = Y1
897      X(3,IP) = Y2
898      X(4,IP) = Y3
899      X(5,IP) = Y4

```

```

900      IF(TP .GE. 45)GO TO 3000
901      RETURN
902      C***** ****
903      C
904      C      WRITE UNIT
905      C
906      C***** ****
907      3000  CONTINUE
908      C*****
909      C      REFLECTANCES
910      C*****
911      PD = PD1*57.29577
912      PS = PS1*57.29577
913      DN 3010 I=2,3
914      IS = TS+1
915      WRITE(4,110)IS,TP,WI,TS,PS,PD
916      WRITE(4,120)(Y(1,J),X(1,J)),J=1,TP)
917      3010  CONTINUE
918      C*****
919      C      ANGLE OF POLARIZATION
920      C*****
921      IS = TS+1
922      WRITE(4,110)IS,TP
923      WRITE(4,130)(X(1,I),X(4,I)),I=1,TP)
924      C*****
925      C      PERCENT POLARIZATION
926      C*****
927      IS = TS+1
928      WRITE(4,110)IS,TP
929      WRITE(4,140)(Y(1,I),X(5,I)),I=1,TP)
930      IP = 0
931      RETURN
932      END
933      SUBROUTINE FLTHS1(A,B,PSI,M,A1,A2,UFLTA)
934      REAL LAMBDA,MH
935      IF(PST .LT. 0.0 .OR. PST .LT. 3.141593)GO TO 8000
936      LAMBDA = SQRT(A*A+B*B)
937      C*****
938      C      DETERMINE PHASE
939      C*****
940      IF(H .LT. 0.01GO TO 1000
941      A1 = ABS(COS(PST))**1.01AMDA
942      A2 = ABS(SIN(PST))**1.01AMDA
943      UFLTA = 0.0
944      IF(PST .LT. 1.570796)DELTA = 3.141593
945      RETURN
946      C*****
947      C      ELLIPTICAL PHASE
948      C*****
949      1000  CHI = H*ATAN(H/A)
950      T1 = ABS(COS(PST*(2.0*PI)))*(COS((2.0*PI*H)))
951      IF(PST .LT. 0.785398 .AND. PST .LT. 2.356195)ALPHA = .5*ARCOS(-T1)
952      IF(PST .LT. 0.785398 .OR. PST .LT. 2.356195)ALPHA = .5*ARCSIN(T1)
953      IF(ALPHA .LT. 0.01GO TO 1710
954      A1 = 1.01AMDA
955      A2 = 0.0
956      UFLTA = 0.0
957      RETURN
958      1010  IF(ABS(ALPHA)-0.7853981 .LT. 0.0001)GO TO 1020
959      A1 = 1.01AMDA/1.014714

```

```

960      AP = A1
961      DFLTA = 2.0*CHI
962      IF(ABS(PST-2.356195).LT.0.0001) DFLTA = H*3.141593 + 2.0*PHT
963      RETURN
964      C
965 1020  IF(ABS(ALPHA-1.570796).GT. 0.0001) GO TO 1030
966      A1 = 0.0
967      AP = LAMBDA
968      DFLTA = 0.0
969      RETURN
970      C
971 1030  T1 = ABS(SIN(2.0*CHI)/SIN(2.0*ALPHA))
972      IF(T1 .GT. 1.0) T1 = 1.0
973      MU = ARCSIN(T1)
974      A1 = LAMBDA+COS(ALPHA)
975      AP = LAMBDA*SIN(ALPHA)
976      COSD = TAN(2.0*PST)/TAN(2.0*ALPHA)
977      IF(COSD .GT. 0.0) DELTA = H*MU
978      IF(COSD .LE. 0.0) DELTA = H*(3.141593-MU)
979      RETURN
980      C*****
981      C  ERROR HANDLING
982      C*****
983 8000  WRITE(3,1001)SI
984 100  FORMAT(//'*'**PST ANGLE OUT OF RANGE ==1,F10.5)
985      STOP
986      END
987      SUBROUTINE FLTHS2(A1,A2,DFLTA,A,B,PST,H)
988      REAL LAMBDA,LAMDA
989      IF(DELTA .LT. -3.1415931) DFLTA = DFLTA+6.283185
990      IF(DELTA .GT. 3.1415931) DFLTA = DFLTA-6.283185
991      LAMDA = PI*(A1+A2+AP*A2)
992      C*****
993      C CASE 1 (A1 = 0 JR AP = 0)
994      C*****
995      IF(A1 .NE. 0.0 .AND. A2 .NE. 0.0) GO TO 1010
996      A = LAMDA
997      B = 0.0
998      H = 1.0
999      IF(A1 .EQ. 0.0) PST = 1.570796
1000     IF(A2 .EQ. 0.0) PST = 0.0
1001     RETURN
1002     C*****
1003     C CASE 2 (A1 = 90)
1004     C*****
1005 1010  IF(A1 .NE. 90) GO TO 1020
1006     CHI = 0.5*ARCS(DFLTA)
1007     A = LAMDA+COS(CHI)
1008     B = LAMDA*SIN(CHI)
1009     H = 1.0
1010     IF(DELTA .LT. 0.01H = -1.0
1011     PPI = 0.785398
1012     IF(PPI .GT. 0.785398) PST = 2.356105
1013     RETURN
1014     C*****
1015     C CASE 3 (DELTA = PI OR -PI)
1016     C*****
1017 1020  IF(ABS(ALB(DELTA)-3.141593) .GT. 0.0001) GO TO 1030
1018     A = LAMDA
1019     B = 0.0

```

```

1020      H = 1.0
1021      PSI = 3.141593-ATAN(A2/A1)
1022      RETURN
1023      *****
1024      C CASE 4 (DELTA = 0)
1025      *****
1026      1030 IF(ABS(DELTA) .GT. 0.0001)GO TO 1040
1027      A = LAMDA
1028      B = 0.0
1029      H = 1.0
1030      PSI = ATAN(A2/A1)
1031      RETURN
1032      *****
1033      C CASE 5 (DELTA = PT HALVES OR -PT HALVES)
1034      *****
1035      1040 IF(ABS(ABS(DELTA)-1.570796) .GT. 0.0001)GO TO 1060
1036      H = 1.0
1037      IF(DELTA .LT. 0.0)H = -1.0
1038
1039      C PART 1 (A1 > A2)
1040      C
1041      IF(A1 .LT. A2)GO TO 1050
1042      A = A1
1043      B = A2
1044      PSI = 0.0
1045      RETURN
1046
1047      C PART 2 (A1 < A2)
1048      C
1049      1050 A = A2
1050      B = A1
1051      PSI = 1.570796
1052      RETURN
1053      *****
1054      C CASE 6 (A1 > A2)
1055      *****
1056      1060 ALPHA = ATAN(A2/A1)
1057      CHI = 0.5*ATAN(ARS(STN(2.0*ALPHA)*SIN(DELTA)))
1058      LAMDA = ARS(TAN(2.0*ALPHA)*COS(DELTA))
1059      A = LAMDA*COS(CHI)
1060      B = LAMDA*SIN(CHI)
1061      H = 1.0
1062      IF(DELTA .LT. 0.0)H = -1.0
1063      IF(A1 .LT. A2)GO TO 1080
1064
1065      C PART 1 (0 < DELTA < PT HALVES)
1066      C
1067      IF(ABS(DELTA) .GT. 1.570796)GO TO 1070
1068      PSI = 0.5*ATAN(LAMDA)
1069      RETURN
1070
1071      C PART 2 (DELTA > PT HALVES)
1072      C
1073      1070 PSI = 3.141593-0.5*ATAN(LAMDA)
1074      RETURN
1075      *****
1076      C CASE 7 (A1 < A2)
1077      *****
1078
1079      C PART 1 (0 < DELTA < PT HALVES)

```

```

1080      C
1081      1080 IF(ABS(DELTA) .GT. 1.570796) GO TO 1090
1082      PSI = 1.570796+0.5*ATAN(LAMDA)
1083      RETURN
1084      C
1085      C      PART 2(DELTA > PI HALVES)
1086      C
1087      1090 PSI = 1.570796+0.5*ATAN(LAMDA)
1088      RETURN
1089      END
1090      FUNCTION DOT(A,B)
1091      DIMENSION A(3), B(3)
1092      *****
1093      C      THIS FUNCTION RETURNS THE DOT PRODUCT OF A AND B
1094      *****
1095      DOT = A(1)*B(1) + A(2)*B(2) + A(3)*B(3)
1096      RETURN
1097      END
1098      SUBROUTINE CROSS(A,B,X)
1099      DIMENSION A(3), B(3), X(3)
1100      *****
1101      C      THIS FUNCTION RETURNS THE CROSS PRODUCT OF A AND B IN X
1102      *****
1103      X(1) = A(2)*B(3) - A(3)*B(2)
1104      X(2) = A(3)*B(1) - A(1)*B(3)
1105      X(3) = A(1)*B(2) - A(2)*B(1)
1106      RETURN
1107      END
1108      FUNCTION VNORM(A,X)
1109      DIMENSION A(3),X(3)
1110      *****
1111      C      THIS FUNCTION RETURNS THE NORM OF A AND THE NORMALIZED VECTOR IN X
1112      *****
1113      VNORM = SQRT( A(1)*A(1) + A(2)*A(2) + A(3)*A(3) )
1114      X(1) = A(1) / VNORM
1115      X(2) = A(2) / VNORM
1116      X(3) = A(3) / VNORM
1117      RETURN
1118      END
1119      FUNCTION SIGN(A)
1120      *****
1121      C      THIS FUNCTION RETURNS THE ALGEBRAIC SIGN OF THE ARGUMENT
1122      *****
1123      SIGN = 1.0
1124      IF(A .LT. 0.0) SIGN = -1.0
1125      RETURN
1126      END
1127      FUNCTION DIVIDE(A,B)
1128      DIVIDE = 0.0
1129      IF(ABS(B) .GT. 1.0E-20) DIVIDE=A/B
1130      RETURN
1131      END
END OF FILE

```

```

FUNCTION AS OF 02.20.73
1      SUBROUTINE FUNC(R)
2      COMMON /CMPT/PS,PD,BETA,BETAB,RPO,COSINE,SIGMA,PHTEN,REP,TS
3      DIMENSION R(10)
4      TAU = R(10)
5      OMEGA = R(7)
6      Q1 = R(8)
7      Q2 = R(9)
8      BNP = ARDCOS(COSINE)
9      IF(ABS(SIGMA) .LE. 0.001) GO TO 1000
10     IF(BNP .GE. SIGMA)
11       R(6) = RPO*COSINE*COSINE*(Q1*EXP(-BNP/SIGMA)+Q2*R(5))
12     IF(BNP .LT. SIGMA)
13       R(6) = RPO*COSINE*COSINE*(Q1*EXP(-0.5+0.5*BNP+BNP/(SIGMA*
14                                     SIGMA))+Q2*R(5))
15     1000 R(6) = R(6)
16     R(7) = 1.0
17     R(8) = R(7)
18     R(9) = 1.0
19     R(10) = 1.0
20     RETURN
21   END
22   SUBROUTINE FUNC(R)
23   COMMON /CMPT/PS,PD,BETA,BETAB,RPO,COSTNE,SIGMA,PHTEN,REP,TS
24   DIMENSION R(10)
25   TAU = R(10)
26   OMEGA = R(7)
27   Q1 = R(8)
28   Q2 = R(9)
29   BNP = ARDCOS(CURINE)
30   IF(ABS(SIGMA) .LE. 0.001) GO TO 1000
31   IF(BNP .GE. SIGMA)
32     R(6) = RPO*COSINE*COSTNE*(Q1*EXP(-BNP/SIGMA)+Q2*R(5))
33   IF(BNP .LT. SIGMA)
34     R(6) = RPO*COSINE*COSTNE*(Q1*EXP(-0.5+0.5*BNP+BNP/(SIGMA*
35                                     SIGMA))+Q2*R(5))
36   1000 R(6) = R(6)
37   R(7) = 1.0
38   R(8) = R(7)
39   R(9) = 1.0
40   R(10) = 1.0+EXP(-151.31221*BNP*BNP)
41   RETURN
42   END
43   SUBROUTINE FUNC(R)
44   COMMON /CMPT/PS,PD,BETA,BETAB,RPO,COSTNE,SIGMA,PHTEN,REP,TS
45   DIMENSION R(10)
46   ****
47   C   THIS IS A REPLACEABLE SUBROUTINE USED IN COMPUTE DPO,DPOU,F,AND G.
48   C   INPUTS:
49   C     R(6) = RPO*BNP
50   C     R(7) = DPO
51   C     R(8) = DPOU
52   C     R(9) = F
53   C     R(10) = G
54   C   ****
55   TAU = R(10)
56   OMEGA = R(7)
57   Q1 = R(8)

```

```

118      QP = R(9)
119      BNP = ARCD9(CUSINE)
120      C
121      C      RC09BNP
122      C
123      IF(ABS(SIGMA) .LE. 0.001)GO TO 1000
124      IF(BNP .GE. STGMA)
125      1      R(6) = RP0*CUSINE*COSINE*(Q1*EXP(-BNP/STGMA)+Q2*R(5))
126      1      IF(BNP .LT. STGMA)
127      1      R(6) = RP0*CUSINE*COSINE*(Q1*EXP(-0.5-0.5*BNP*BNP/(SIGMA*
128      2      SIGMA))+Q2*R(5))
129      1000 R(6) = R(6)*(1.0+BNP/UMEGA*EXP(-2.0*RETA/TAU))/(1.0+BNP/UMEGA)
130      1      /(1.0+PHTEN*REP/(UMEGA*UMEGA))
131      C
132      C      DPO
133      C
134      C      R(7) = 1.0
135      C
136      C      DP90
137      C
138      C      R(8) = R(7)
139      C
140      C      F
141      C
142      C      R(9) = 1.0
143      C
144      C      G
145      C
146      C      R(10) = 1.0
147      C      RETURN
148      C      END
149      C      SUBROUTINE FUNC(R)
150      C      COMMON /CMPT/PS,PD,BETA,BETAB,RPO,COSINF,SIGMA,PHTEN,REP,TS
151      C      DMFN917N R(10)
152      C      TAU = R(10)
153      C      UMEGA = R(7)
154      C      U1 = R(8)
155      C      U2 = R(9)
156      C      BNP = ARCD9(PURINE)
157      C      IF(ABS(SIGMA) .LE. 0.001)GO TO 1000
158      C      IF(BNP .GE. STGMA)
159      1      R(6) = RP0*CUSINE*COSINE*(Q1*EXP(-BNP/STGMA)+Q2*R(5))
160      1      IF(BNP .LT. STGMA)
161      1      R(6) = RP0*CUSINE*COSINE*(Q1*EXP(-0.5-0.5*BNP*BNP/(SIGMA*
162      2      SIGMA))+Q2*R(5))
163      1000 R(6) = R(6)*(1.0+BNP/UMEGA*EXP(-2.0*RETA/TAU))/(1.0+BNP/UMEGA)
164      1      /(1.0+PHTEN*REP/(UMEGA*UMEGA))
165      C      R(7) = 1.0
166      C      R(8) = R(7)
167      C      R(9) = 1.0
168      C      R(10) = 1.0+EXP(-151.31221*BNP*BNP)
169      C      RETURN
170      C
171      C
172      C
END OF FILE

```

REFERENCES

1. Target Signature Analysis Center: Data Compilation, Eleventh Supplement, Vol. I, Report No. 32210-41-B, Willow Run Laboratories of the Institute of Science and Technology, The University of Michigan, Ann Arbor, AFAL-TR-72-226, October 1972.
2. Target Signature Analysis Center: Data Compilation, Eleventh Supplement, Vol. II, Report No. 32210-41-B, Willow Run Laboratories of the Institute of Science and Technology, The University of Michigan, Ann Arbor, AFAL-TR-72-226, October 1972.
3. M. Born and E. Wolf, **Principles of Optics**, Pergamon Press, London, 1964.
4. K. E. Torrance and E. M. Sparrow, "Theory for Off-Specular Reflection from Roughened Surfaces," *J. Opt. Soc. Amer.*, Vol. 57, No. 9, September 1967, pp. 1105-1114.
5. W. A. Shurcliff, **Polarized Light**, Harvard University Press, Cambridge, 1962.
6. H. B. Holl, **Reflection of Electromagnetic Radiation**, Vol. I, Report RF-TR-63-4, U.S. Army Missile Command, Redstone Arsenal, Huntsville, Alabama, 15 March 1963.